Analysis of the cAMP-regulated metabolome of skeletal muscle and adipose tissue

Dissertation

zur

Erlangung des Doktorgrades (Dr. rer. nat.)

der

Mathematisch-Naturwissenschaftlichen Fakultät

der

Rheinischen Friedrich-Wilhelms-Universität Bonn

vorgelegt von

Carolin Stefanie Möller

aus

Bingen, Deutschland

Bonn 2024

Angefertigt mit Genehmigung der Mathematisch-Naturwissenschaftlichen Fakultät

der Rheinischen Friedrich-Wilhelms-Universität Bonn

Gutachter/Betreuer: Prof. Dr. Alexander Pfeifer

Gutachterin: Prof. Dr. Christa E. Müller

Tag der Promotion: 16.01.2025

Erscheinungsjahr: 2025

I. Acknowledgements

First and foremost, I would like to thank Prof. Pfeifer, for providing me the opportunity to work in your lab. Your continuous support and guidance shaped my academic and professional development.

I am also highly thankful to Prof. Müller, who not only served as my second supervisor but also guided me through the graduate school GRK 1873.

I would like to extend my thanks to the DFG for funding this project and to Dr. Mies-Klomfass for your support and exceptional organization within the GRK.

My deepest gratitude goes to you, Dr. Thorsten Gnad, for your expertise, cleverness, endurance and humor. You reopened dead ends, taught me resilience and put up with my “Schnodderschnauze”.

I would like to express my appreciation to Prof. Rittweger, Prof. Pesta and the DLR for the opportunity to collaborate on this superb project and extend my horizon.

Thank you, Martin, for your invaluable guidance, support, and expertise with mass spectrometry and metabolomics, which greatly contributed to the success of this project.

To Laura, my colleague, companion, ally and friend-thank you. You filled my days with laughter, made tough ones bearable and good ones even better. This journey tied us together, forever!

I thank Daniel, Danli, Alex, Babsi, Max, Birte, Lena, Elena, my office 006 mates and all members from IPT for your continuous support, fun-filled lunch and ice-cream breaks and countless after-work drinks.

To Lena, Marianna and Julia- you made Bonn a place where I could truly live, love and laugh (a lot). You have made this city my home.

I would like to thank my Pharmily from Mainhattan for providing me with much-needed weekends and annual vacations that allowed me to reset my hard drive. Also I would like to thank my Meenzer Mädcher Nadine and Chantal for keeping me grounded and simply being my friends.

I am deeply thankful for the support from my family. Thank you for your unwavering encouragement and belief in me. You reassured me in my path and provided me a safe space at home.

Lastly, I want to thank Moritz for being my rock. You cheered me up after rough days and recharged my batteries. I could not have done this without your patience, motivation and love.

II. List of Abbreviations

AC	Adenylyl cyclase
ACN	Acetonitrile
AR	Adrenergic receptor
AT	Adipose tissue
BA	Brown adipocyte
BAT	Brown adipose tissue
BCAA	Branched-chain amino acid
BMI	Body mass index
Ca2+	Calcium (free)
cAMP	Cyclic adenosine-mono phosphate
cDNA	Complementary DNA
CNG	Cyclic-nucleotide-gated ion channels
COX	Cyclooxygenase
CREB	cAMP response element binding protein
DHT	Dihydrotestosterone
DLR	Deutsches Institut für Luft- und Raumfahrt
DM	Differentiation medium
DMSO	Dimethylsulfoxide
DNA	Desoxyribonucleic acid
Epac	Exchange protein activated by cAMP
ESI	Electrospray ionization
FA	Fatty acid
FAHFA	Fatty acyl ester of hydroxyl fatty ester
FBS	Fetal bovine serum
FC	Fold change
FDR	False detection rate
FFA	Free fatty acid
FGF21	Fibroblast growth factor 21
FSK	Forskolin
GAPDH	Glyceraldehyde-3-phosphate dehydrogenase
GC	Glucocorticoid
GM	Growth medium
GPCR	G-protein coupled receptor
GPX	Glutathione peroxidase
GSH	Glutathione
HEPES	N-2-Hydroxyethylpiperazine-N-2-Ethane Sulfonic Acid
HILIC	Hydrophilic interaction chromatography
HPLC	High performance liquid chromatography
HS	Horse serum
HSD	11β-Hydroxysteroid-dehydrogenase
hSKM	Human skeletal muscle cells
IBMX	3-isobutyl-1-methyxanthine
IGF-I	Insulin-like growth factor I
IL-6	Interleukine 6
LEA	Linoleoylethanolamide
m/z	mass-to-charge ratio
MALDI	Matrix-assisted laser desorption/ionization

MHC	Myosin heavy chain
MS	Mass spectrometry
NE	Norepinephrine
NAE	N-acylethanolamide
NMR	Nuclear magnetic resonance
NST	Non-shivering thermogenesis
OEA	Oleoylethanolamide
ORA	Overrepresentation analysis
P/S	Penicillin/Streptomycin
PA	Physical activity
PBS	Phosphate buffered saline
PC	Phosphatidylcholine
PCA	Principal component analysis
PDE	Phosphodiesterase
PG	Prostaglandin
PGC1α	Peroxisome proliferator-activated receptor γ coactivator 1α
PKA	cAMP-dependent protein kinase
PUFA	Polyunsaturated fatty acid
QC	Quality control
QEA	Quantitative enrichment analysis
RNA	Ribonucleic acid
ROS	Reactive oxygen species
RP	Reverse phase
Rt	Retention time
S1P	Sphingosine-1-phosphate
SD	Standard deviation
SEM	Standard error of the mean
SFA	Saturated fatty acid
SKM	Skeletal muscle
SR	Sarcoplasmatic reticulum
TAG	Triacylglycerol
TBP	TATA-box-binding protein
TCA cycle	Tricarboxylic acid cycle
TG	Triglyceride
TLR	Toll-like receptor
TOF	Time-of-flight
TRF	Tocotrienol-rich fraction
UCP1	Uncoupling protein 1
UPLC	Ultra high-performance liquid chromatography
VP	Volcano plot analysis
WA	White adipocyte
WAT	White adipose tissue
WT	Wildtype
γ-GCS	γ-glutamylcysteine synthase

Contents

1. Introduction

1.1 Adipose Tissue

In mammals two types of adipose tissue (AT) can be found: white adipose tissue (WAT) and brown adipose tissue (BAT). The two major WAT depots are the subcutaneous and the visceral fat. As the name implies, subcutaneous fat lies underneath the skin, whereas visceral fat surrounds the inner organs. In mice, BAT is mainly located in interscapular regions, whereas in humans, BAT is mainly found in cervical and supraclavicular regions and along the spine (Saely et al., 2012) (Figure 1).

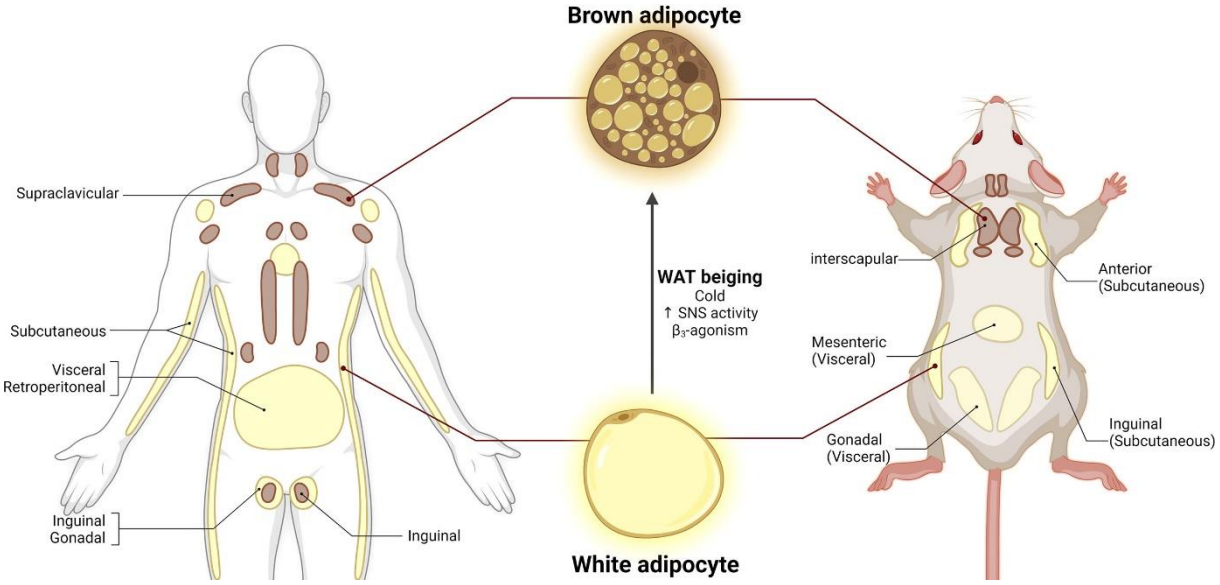

Figure 1: Localisation of WAT and BAT depots in human and mice. Graphical scheme of white and brown adipocyte morphology. Taken over with permission from (Torres Irizarry et al., 2022)

1.1.1. White Adipose Tissue

WAT primarily serves as an energy storage and site of energy metabolism. Moreover, it functions as thermal barrier and mechanic cushion protecting the body from heat loss or mechanical trauma, respectively. Additionally, it is regarded as an endocrine organ which can secrete various factors to influence other organs and therefore whole body metabolism (Wronska and Kmiec, 2012).Leptin and adiponectin are two well established adipokines (Fantuzzi, 2005). Leptin is a protein which is produced and secreted by adipocytes and regulates food intake and bodyweight through hypothalamic pathways (Elmquist, 2001). Adiponectin is also secreted by white adipocytes an influences insulin sensitivity and glucose metabolism by stimulating fatty acid oxidation and decreasing plasma triglycerides (Bełtowski, 2003). WAT contains mainly white adipocytes (WA). Those cells store energy in form of triglycerides (TG) in one large droplet (Figure 1). During periods of nutrient demand, these TG undergo lipolysis, i.e. enzymatic hydrolysis into glycerol and free fatty acids (FFA). The latter are transported to the periphery via blood vessels to supply other organs with energy. Vice versa, under nutrient excess FFA can be

taken up from the blood and reesterified into TG, which then fuse into the large lipid droplet. Apart from adipocytes WAT also contains multipotent stem cells, fibroblasts, pericytes, endothelial cells and infiltrating immune cells like macrophages (Wronska and Kmiec, 2012).

1.1.2. Brown Adipose Tissue

BAT functions as a thermogenic organ that increases energy expenditure and generates heat (Suchacki and Stimson, 2021). BAT is composed of brown adipocytes (BA, 60-70%) but also fibroblasts, endothelial cells or immune cells (Cinti, 2018). BA in contrast to WA store triglycerides in numerous small lipid droplets. They also contain high numbers of mitochondria, which give rise to their characteristic colour. BAT mitochondria express high levels of a protein called “uncoupling protein 1” (UCP1) which allows them to produce heat in a process termed non-shivering thermogenesis (NST). Exposure to cold leads to the activation of sympathetic nerves which release norepinephrine (NE) to stimulate β_3- adrenergic receptors expressed on brown adipocytes. The β_3 receptor is a G_s-protein coupled receptor which stimulates the adenylyl cyclase which generates cyclic AMP (cAMP). This in turn leads to the release of FFA which can activate UCP1 to create a proton leakage in the respiratory chain in the mitochondria: energy is released in form of heat. NST is especially vital for new-borns to sustain their body temperature (Cannon and Nedergaard, 2004). In humans, the amount of active BAT decreases with age to an overall prevalence of around 6% in adults. It is more frequent in women that in men and inversely correlates with a lower body mass index (BMI) (Becher et al., 2021).Even though, the amount and prevalence of BAT can be scarce, it can be induced of recruited by , for example, cold exposure to reduce body fat (Saito, 2013). Since a daily cold exposure to increase BAT amount might not be feasible, the identification of drugs to activate BAT are under great investigation.

1.1.3. Beige Adipose Tissue

In addition to WA and classical BA, a third type of adipocyte has been identified. These so-called beige adipocytes can arise *de novo* from adipose stem/progenitor cells residing in WAT or transdifferentiate from white to brown adipocytes through a process called adipose tissue browning (Bartelt and Heeren, 2014; Zoico et al., 2019). Well-known stimuli for browning are catecholamines released by the sympathetic nervous system (SNS) after cold exposure (Figure 1). Like BA, beige adipocytes also express UCP1, form multilocular lipid droplets and are mitochondria rich (Rui, 2017). Moreover, beige adipocytes influence whole body metabolism and can improve metabolic parameters (Kajimura et al., 2015). Interestingly, also exercise (Stanford et al., 2015) or nutrients like fish oil or corn oil (Sharma and Agnihotri, 2020) can induce browning in WAT and therefore increase energy expenditure.

1.2. Skeletal muscle

Skeletal muscle (SKM) is the largest organ in the human body and makes up to 40% of whole body mass (Hopkins, 2006). Its most obvious and main function is to convert chemical into mechanical energy to produce movement (Frontera and Ochala, 2015). However, SKM also plays a major role in energy metabolism: It stores substrates like amino acids and carbohydrates, produces heat for the maintenance of core body temperature and consumes great amounts of oxygen and energy during physical activity and exercise (Frontera and Ochala, 2015).

SKM contains muscle cells, neurons, blood vessels and connective tissue (Broek et al., 2010). Muscle cells originate from satellite cells which represent the stem cell population in the muscle. They further differentiate into myoblasts which then fuse to multinucleated myotubes. Together, these myotubes form mature myofibers which contain the sarcomeres, the functional units of skeletal muscle. Myofibers are surrounded by the endomysium to create myofiber bundles which are further covered by the perimysium. The epimysium forms the outer fibrous layer and surrounds the complete muscle (Broek et al., 2010) (Figure 2).

In general, muscle fibers are classified into four major types: Type I, type IIa, type IIb and type IIx (Schiaffino and Reggiani, 2011; Rivera-Brown and Frontera, 2012). However, in human SKM, type IIb has so far not been detected (Schiaffino and Reggiani, 2011). The fiber types differ in some characteristics like ATPase and oxidative enzyme activity, contraction or fiber-shortening velocity, and the amount of myosin heavy chain (MHC) isoforms. Type I fiber types are defined as the slow twitching type with an oxidative metabolic profile and expression of MHC Isoform I. They are fatigue-resistant and therefore appear in long duration athletes like marathon runners. Type II fibers are abundant in fast twitching motor units. Type IIa are fast twitching, fatigue-resistant fiber types which express MHC IIa. Type IIb are also fast twitching but fast fatigable. Type IIx have twitch properties comparable to IIa and IIb, and are intermediate in terms of fatigue resistance (Schiaffino and Reggiani, 2011). Those fibers can be found in SKM from weight lifters or sprinters (Rivera-Brown and Frontera, 2012). In any muscle, different fiber types coexist. The proportion of the fiber type can vary according to anatomical site, developmental state but also according to gender or species (Schiaffino and Reggiani, 2011).

To generate force, the coordination of two processes must take place: excitation and contraction. In short, this process begins with a nerve stimulus and ends with the release of calcium from the sarcoplasmatic reticulum (SR), which allows actin and myosin to form cross-bridges (Frontera and Ochala, 2015). Muscle cells are stimulated by the neurotransmitter acetylcholine, which leads to the activation of their receptors and depolarizes the cell. The depolarization is recognized by voltage sensors and transferred into the cell via the transverse tubular. This leads to the opening of ryanodine receptors and the release of calcium from the SR. Calcium in turn binds to troponin C to open myosin-

binding sites on actin. Hydrolisation of myosin bound ATP to ADP allows actin to slide past myosin which activates the contractile apparatus (Kuo and Ehrlich, 2015).

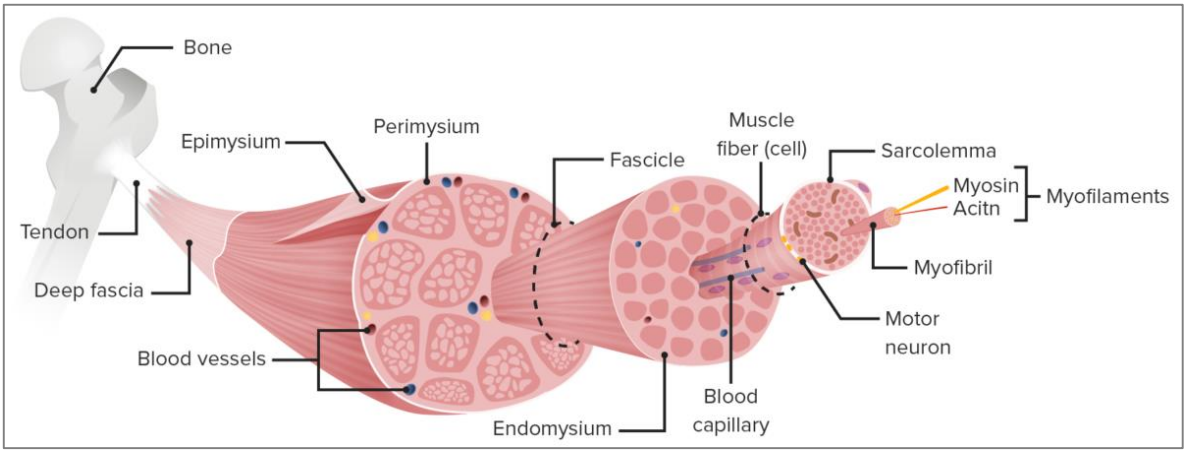

Figure 2: Skeletal muscle structure. Taken over with permission from (Lecturio, 2022).

1.2.1. Soleus muscle

The *soleus* muscle is a calf muscle located at the lower back part of the leg. It originates from the upper tibia and is connected to the heel bone through the Achilles tendon. Together with the larger *gastrocnemius* muscle these calf muscles are sometimes also called the *triceps surae* (Figure 3). The *soleus* muscle is a powerful muscle which is active while walking, running and jumping. It functions to plantar flex the foot. It is mainly composed of slow-twitch, fatigue-resistant muscle fibers and can endure high contractions and workload for a long time (Brett Sears, 2022). Human soleus muscle contains 80% type I fibers (Gollnick et al., 1974). In mice the soleus muscle is mainly composed of type I (37%) and type IIa (39%) fibers (Augusto et al., 2017). Moreover, murine soleus muscle was shown to have the highest similarities with human muscle (Kho et al., 2006). Therefore, soleus muscle serves as an adequate model to study the effects of aging and exercise on SKM metabolism.

During activation, the *soleus* muscle takes up lipids and glucose and uses blood borne fuels and oxygen to fuel its energy demand. Just like BAT, the soleus represents only a small tissue, which could highly influence oxidative metabolism through its activation (Hamilton et al., 2022).

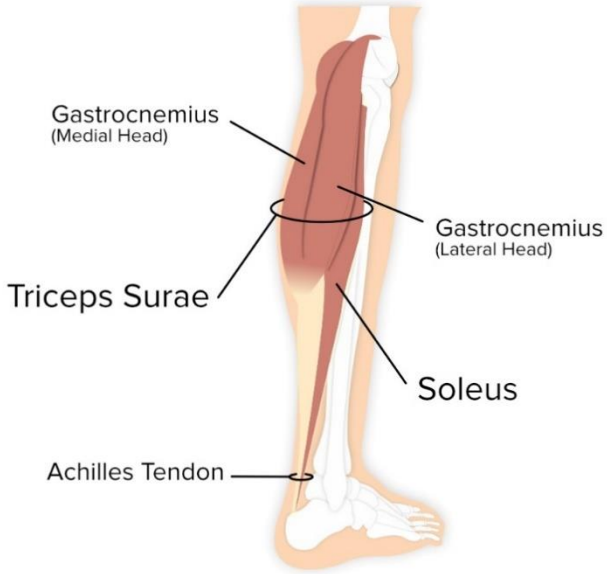

Figure 3: Triceps surea physiology showing the location of gastocnemicus and Soleus muscle in the lower hind limb. Figure adapted from (westcoastsci, 2018a, 2018b)

1.3. Obesity

Obesity originates from an imbalance between energy intake and energy expenditure and results in the accumulation of excessive fat (World Health Organization, 2021). The BMI (weight in kg/height in m^2) is the common parameter to measure obesity. It is a unisex scale which roughly describes the status of overweight and obesity: a BMI greater than or equal to 25 is described as overweight; a BMI greater than or equal to 30 is described as obese. Obesity is often described as pandemic (Roth et al., 2004). It has tripled since 1975 so that in 2016 39% of adults were overweight and 13% were obese (World Health Organization, 2021). The main reasons for overweight are well-known: genetics, malnutrition and physical inactivity (Overweight & Obesity Statistics, 2023). Obesity will eventually increase the risk for many noncommunicable diseases like type 2 diabetes, heart disease, stroke, muscoskeletal disorders and some types of cancers (Abelson and Kennedy, 2004; World Health Organization, 2021) (Figure 4). This increased risk of illness does not only affect the individual wellbeing and quality of life but also the health-care system in terms of capacity and costs (Bray et al., 2016). Therefore, new therapeutics which can ameliorate obesity and improve metabolic health are of utmost concern.

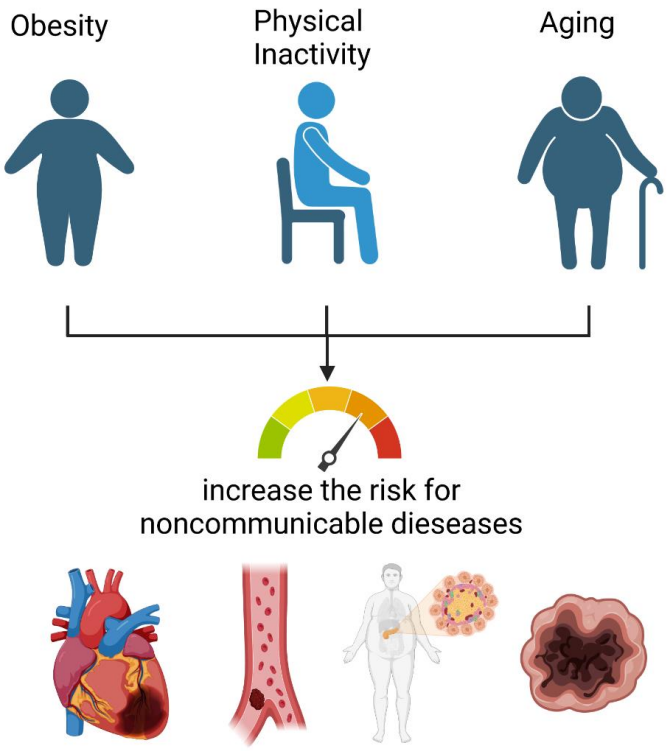

Figure 4:Obesity, PA and Aging lead to an increased risk of noncommunicable diseases

1.4. Physical Activity and Exercise

Regular physical activity (PA) describes all kinds of movements like cycling, sports, walking, hiking and many more. Regular PA leads to obvious improvements like healthy body weight. Furthermore, it reduces the risk for mental disorders, multiple types of cancer, type 2 diabetes, hypertension and coronary heart disease. Especially in the elderly, PA improves mental and cognitive health and reduces the risk of falls (Sigal et al., 2004; World Health Organization, 2022b). Physical inactivity, on the other hand, increases the risk of all-cause mortality. It is the fourth leading risk factor of mortality worldwide and one of the top non-communicable diseases, like heart disease, stroke and diabetes (Figure 4). One in four adults does not meet the criteria for enough PA and as countries develop economically, this inactivity increases further (World Health Organization, 2022b). The WHO suggests that adults "*should do at least 150-300 minutes of moderate-intensity aerobic PA or at least 75-150 minutes of vigorous-intensity aerobic PA throughout the week*" (World Health Organization, 2022b). Luzak et al. report, that only 14% of german adults aged 48-68, meet these WHO PA recommendations and that PA was significantly lower among obese and older (>61 years) adults (Luzak et al., 2017).

During PA or exercise, the muscle cells need energy which can be produced by either anaerobic (glycolytic) or aerobic (oxidative) pathways (Rivera-Brown and Frontera, 2012). Different types of sports require different energy sources. For example, anaerobic sports like short-track racing, tennis

or throwing acquire their energy through ATP-phosphocreatine and glycolysis. Carbohydrates provide energy for short-duration exercises or during the beginning of low-intensity exercise. As a side product during the anaerobic pathway lactic acid can accumulate which impairs force generation and leads to fatigue of the muscle. On the other hand, long-distance swimming and running leads to the activation of the oxidative system located in the mitochondria: Krebs cycle and respiratory chain lead to the formation of large amounts of ATP; much more than the amount produced in the glycolytic pathway. Sources that fuel the oxidative system are glycogen, FA which were broken down in β-oxidation or amino acids which can be converted to glucose (Rivera-Brown and Frontera, 2012).

Exercise highly influences skeletal muscle metabolism. The muscle adaptations depend on the characteristics of the exercise and individual. For example, mild or moderate exercise can increase fatty oxidation 3- to 10- fold, and glucose uptake up to 20-fold compared to resting state (Turcotte and Fisher, 2008). In detail, performing 3 hours of knee extension resistance exercise showed higher levels of FA uptake up to 65% of maximal oxygen uptake (Turcotte and Fisher, 2008). Although acute exercise leads to molecular adaptations, only regular exercise can influence the muscle phenotype and improve exercise performance (Huh, 2018). Amongst others, this can be explained with adaptations in protein content. For examples, a 7-12 week endurance training was shown to increase protein levels of short-chain, medium-chain and very long-chain acyl-CoA dehydrogenases and tricarboxylic acid cycle (TCA) enzyme citrate synthase which are involved in β-oxidation (Turcotte and Fisher, 2008).

Furthermore, exercise influences insulin resistance and can therefore ameliorate type 2 diabetes. Richter et al. detected 2-fold higher levels of insulin stimulated glucose transport in exercised rats and humans compared to the sedentary state (Richter et al., 1982; Richter et al., 1989). Several clinical studies have shown, that regular PA can reduce the cumulative incidence of type 2 diabetes from 68% in the control group to 41% in the exercise group (Sigal et al., 2004).

Research on exercise and PA aims to provide insights into the underlying mechanisms and its impacts on health and well-being. Especially in the context of aging, research on exercise helps to elucidate how PA can contribute to healthy aging, maintaining mobility and reducing the risk of chronic diseases. Understanding the physiological and metabolic effects of exercise helps to establish public health recommendations and clinical guidelines to improve overall well-being.

1.5. Aging

Increasing age is the major risk factor for numerous diseases like cardiovascular diseases, diabetes or depression and the portion of age-related disorders will increase even more in the next decades due to overall improvements in screenings, health-care and new therapeutic approaches. But longevity is not necessarily linked to improved fitness or a better quality of life. The percentage of multimorbid

and handicapped people will increase steadily and lead to a greater demand for geriatric therapies and a greater burden on our health-care systems (World Health Organization, 2022a).

Aging is a complex process which affects all living beings and influences nearly every biological process (Rutledge et al., 2022). It can lead to damages, loss of functions and death in all cells and organs (Valdes et al., 2013). Aging is influenced by signalling pathway and metabolic changes over time, arising from environmental, epigenetic, post-translational, microbial and lifestyle changes. There are obvious physical changes like greying hair or flabby sagging skin. However, the molecular changes underlying these and other aging processes are only partially and poorly understood (Rutledge et al., 2022). Cellular senescence describes a state of permanent growth arrest which leads to the accumulation of dead cells. This will eventually lead to organ-wide disorders and dysfunctions. Especially the accumulation of reactive oxygen species (ROS) and dysregulated energy homeostasis are known molecular drivers for aging (Schosserer et al., 2018). The oxidative stress theory describes aging as a result of the accumulation of ROS which over time damages DNA, protein and lipids of all cells and organs. If the organism is able to rapidly degrade high amounts of ROS, this will improve cellular metabolic stage and can improve longevity (Schosserer et al., 2018).

Aging research aims to understand the molecular changes in biological processes and to find risk factors and markers that lead to a healthier and/or longer life. With Omics technologies these complex changes on molecular and metabolic levels have started to be unravelled. The major goal is to find key regulators for “healthy aging”.

1.5.1. Aging in Skeletal Muscle

Skeletal muscle is strongly affected by aging: with increasing age, muscle mass, function and regenerative capacity decrease. This process is termed sarcopenia. It is a slow process which affects all humans, regardless of physical and mental fitness, but varies among individuals (Larsson et al., 2019). Sarcopenia not only reduces mobility and independent living but also promotes obesity and type 2 diabetes (Cartee et al., 2016). Muscle strength is lost 2-5 times more rapidly than muscle mass (Mitchell et al., 2012): muscle mass declines 0,7-0,8% per year during the seventh and eighth decades of life, while 2-4% of muscle strength can be lost per year. Also lower limb muscle seems to be more affected than upper limb muscle (Distefano and Goodpaster, 2018).

Aging leads to a number of structural and functional changes in skeletal muscle. For example, in soleus muscle of rats, a significant decline in the contractile properties of single soleus fibers are observed during aging (Thompson and Brown, 1999). Furthermore, the composition of muscle fiber types is changed: type II fibers decrease, whereas type I fibers stay rather unaffected (Williams et al., 2002). Moreover, the expression of MyHC IIa decrease significantly and MyHC IIx can only barely be found in

elderly muscle, whereas MyHC I expression increases (Mitchell et al., 2012). These morphological changes might be due to age-related changes in the central and peripheral nervous system. The gradual loss of motoneurons and the degeneration of neuromuscular junctions will eventually lead to a denervation of muscle fibers (Distefano and Goodpaster, 2018). Another vital age effect is the reduced mitochondrial capacity: aging results in a reduced number and density of mitochondria and a reduction in mitochondrial enzymatic activities and increased ROS production, which in turn negatively influences SKM function and bioenergetics. In addition, regenerative capacity is diminished and/or delayed in older muscle due to a reduction of satellite cell number and function (Sousa-Victor et al., 2022). PA can positively influence this phenomenon: endurance and resistance exercise can elevate the number of satellite cells in old animals and subjects, and trained mice show improvements in vascularization. PA also stimulates mitochondrial biogenesis by the increase in peroxisome proliferator-activated receptor γ coactivator 1α (PGC1α), a key regulator of myogenesis (Distefano and Goodpaster, 2018).

Another hallmark of aging is reduced endocrine function: Circulating levels of hormones and cytokines are changed. For example, levels of steroid hormones decrease, especially a decline of testosterone levels could be related to sarcopenia. Chronic inflammation and an increase in proinflammatory cytokines could be another trigger for loss of muscle mass and strength. Especially Interleukin-6 (IL-6) and Insulin-like growth factor I (IGF-I) might influence the risk of disability and immobility (Cappola et al., 2003).

A better understanding of the underlying molecular changes involved in muscle aging is imperative, given the growing number of elderly population to improve prevention and therapy of sarcopenia in the future.

1.5.2. Aging in adipose tissue

In the course of aging, adipose tissue undergoes significant changes in both size and distribution. Older adults tend to accumulate more overall fat, particularly within the intra-abdominal visceral white adipose tissue. At the same time, there is a reduction in brown and beige fat, which contributes to issues with body temperature regulation and energy balance (Ou et al., 2022). Notably, a similar dysregulation of energy homeostasis in adipose tissue can also be observed in obesity. The additional amount of white adipose tissue is mostly characterised by chronic inflammation and lipotoxicity (Schosserer et al., 2018). The chronic state of low grade inflammation is known as metaflammation, or in the context of aging, often described as inflammaging (Fülöp et al., 2019). The combination of a persistent activated immune-system plus the accumulation of senescent cells and epigenetic rearrangements, elevates the risk for further diseases like cardiovascular events, type 2 diabetes or arthritis (Prattichizzo et al., 2018; Mancuso and Bouchard, 2019). Two major drivers of the

inflammatory state are gluco- and lipotoxicity. Under healthy conditions, glucose and dietary lipids are taken up from the blood and processed by the adipose tissue. If this system is overfilled, it can increase ROS production which promotes proinflammatory kinases, NF-κB induction, overexpression and activation of Toll-like receptors (TLRs) and many other responses (Prattichizzo et al., 2018).

With age, the amount of functional BAT decreases which negatively influences whole body energy expenditure (Schosserer et al., 2018; Mancuso and Bouchard, 2019). Not only the amount, but also the activity and capacity for heat production and the rapidity of activation decline with age (Rogers, 2015). Morphologically a whitening of BAT can be observed, which describes a WA infiltration into BAT depots. Potential reasons for the reduced amount and activity of BAT could be an age-related downregulation of adrenergic receptor expression and a pronounced loss of UCP1 expression (Cannon and Nedergaard, 2004). Also decreased levels of positive BAT regulators like growth hormones, estrogens, androgens or thyroid hormone can be observed during aging (Rogers, 2015).

With increasing age human adipose stem cell proliferation and differentiation potential is diminished (Schosserer et al., 2018). Also the adipocytes endocrine function can be reduced leading to an altered secretome: free fatty acids are secreted and the expression of the two adipokines leptin and adiponectin are reduced. This leads to altered insulin sensitivity and fatty acid oxidation and furthermore influences neighbouring (pre-) adipocytes (Mitterberger et al., 2014). Eventually, this alters whole body health and further promotes aging. Especially in BA but also in WA, mitochondria are the key organelles and site of energy turnover. Mitochondrial gene expression and functionality is restricted during aging which can be measured in reduced oxygen consumption and reduced UCP-1 activity (Yamashita et al., 1994; Valle et al., 2008). Yamashita et al. showed that total mitochondria protein content (mg/g tissue) was reduced to 60% in old rats compared to young rats. Also they detected a 70% less thermogenic capacity and activity (GDP binding) in mitochondria from old rats (Yamashita et al., 1994). To date, the reasons for these changes are still under investigation. Since aging in WAT and BAT negatively regulates energy expenditure and whole body metabolism, understanding the underlying molecular processes is a promising approach to identify novel future interventions which can slow down the process of aging in the two tissues (Schosserer et al., 2018).

1.6. cAMP Signaling

Cyclic adenosine 3’-5’ monophosphate (cAMP) is an important second messenger found ubiquitously in nearly every organism and cell type, where it regulates many biological processes like cell growth, differentiation, gene transcription or mitochondrial homeostasis upon others (McKnight, 1991; Lefkimmiatis and Zaccolo, 2014).

cAMP abundance is mainly regulated by G-protein coupled receptors (GPCR) coupled to either $G\alpha_s$ or $G\alpha_i$ proteins. After the stimulation of $G\alpha_s$ coupled GPCRs a transmembrane adenylyl cyclase (AC) is activated which converts ATP to cAMP (Fig. 4). $G\alpha_i$ coupled receptors on the other hand, inhibit ACs and thereby cAMP production. cAMP has three main effector proteins: the cAMP-dependent protein kinase A (PKA), the exchange protein activated by cAMP (Epac) and the cyclic-nucleotide-gated ion channels (CNG) (Lefkimmiatis and Zaccolo, 2014). Moreover, cAMP is not exclusively formed by transmembrane AC, but also by one soluble AC which can be found in different cell compartments like nucleus or mitochondria (Fig. 4) (Tresguerres et al., 2011). cAMP is degraded to AMP by phosphodiesterases (PDE) which terminates the signal (Figure 5).

Overall, cAMP signalling varies highly between species and cell types, depending on the composition of GPCRs, G proteins, ACs and PDEs (Berdeaux and Stewart, 2012).

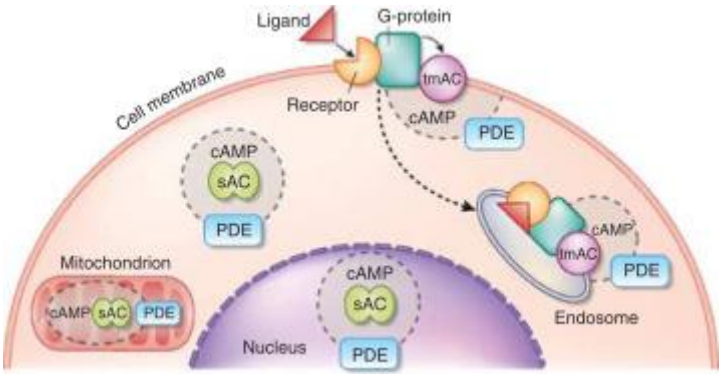

Figure 5: cAMP signaling microdomains. Taken over with permission from (Tresguerres et al., 2011)

To study cAMP regulated pathways and downstream effects, the adenylyl cyclase activator Forskolin (FSK) is often used (Melzig and Alasbahi, 2012). This compound can be isolated from the roots of Plectranthus barbauts. It activates transmembrane ACs in a direct, rapid and reversible manner. (Berdeaux and Stewart, 2012).

1.6.1. cAMP signalling in adipose tissue

In all kind of adipocytes – brown, white, beige – cAMP is a key signalling molecule that regulates function and differentiation, primarily via activation of PKA (Guilherme et al., 2023). For example, hormone-sensitive-lipase and perilipin A are important targets of PKA. PKA-mediated phosphorylation induces translocation of the lipase to the surface of lipid droplets and enhances its catalytic activity facilitating lipolysis. The released FFA activate UCP1 (Figure 6). The cAMP/PKA pathway also regulates UCP1 expression through p38-mitogen-activated protein kinase (Tong and Hotamisligil, 2001; Reverte-Salisa et al., 2019). Moreover, apoptosis of adipocytes is blocked by PKA mediated activation of tyrosin kinase like Src, which in turn activates MAP kinases. cAMP promotes adipogenesis by activating the master transcription factor CREB, which initiates a transcriptional cascade resulting in the expression

of adipogenic genes (Reverte-Salisa et al., 2019). For example, CREB binds to and activates the promotors of C/EBPβ, C/EBPδ and AP2 (Tong and Hotamisligil, 2001). The main function of cAMP in WA is to induce lipolysis to release FA into the blood stream, which can then fuel the energy demand of peripheral organs. In BAT on the other hand, cAMP induction mainly results in the oxidation of FA and the production of NST. Upon cAMP induction, both white and brown adipocytes are able to secrete various protein and metabolites which can in turn modulate metabolism in an auto-, para-, or endocrine manner (Guilherme et al., 2023). Most recently, cAMP has also been shown to regulate brown fat growth via Epac1 (Reverte-Salisa et al., 2024).

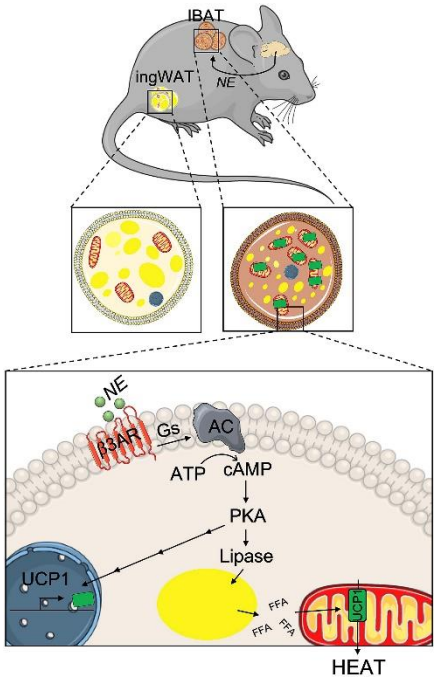

Figure 6: cAMP function in the adipose tissue. Taken over with permission from (Luijten et al., 2019)

1.6.2. cAMP signalling in skeletal muscle

cAMP signalling is vital for full functionality of SKM and can be induced by several ligands, like epinephrine and norepinephrine, adenosine, IL6 or also prostaglandin E_1. Consequently, the associated receptors are also expressed: β_1 and especially β_2-AR are highly expressed in myofibers and are activated during exercise. Myoblasts and myofibers also express Adenosine receptors A_{2A} and A_{2B} which activate CREB and protect the muscle during ischemia (Zheng et al., 2007). Another group of G_s protein-coupled receptors in myoblasts are the prostaglandin receptors EP_1, EP_2 and EP_3, whose activation leads to the fusion of myoblasts (Zalin and Leaver, 1975; Kim and Sainz, 1992; Zheng et al., 2007; Kelly et al., 2009; Berdeaux and Stewart, 2012).

As an acute effect, cAMP regulates contractility, glycogenolysis, calcium signalling and complete recovery after contraction. Rudolf et al showed that the stimulation of murine tibialis anterior skeletal muscle with the β-adrenergic agonist isoproterenol, led to a marked increase in cytosolic cAMP levels accompanied by an increased Ca^{2+} release from the SR (Rudolf et al., 2006). Adrenergic stimulation of skeletal muscle is also known to induce hypertrophy (Kim and Sainz, 1992). Short- and long-term treatment of rat soleus muscle with the β_2-adrenergic agonist clenbuterol showed the attenuation of protein degradation which could in turn attenuate muscle atrophy (Silveira et al., 2014). More long-term effects of cAMP signalling are increased myofiber size and promotion of myocyte differentiation, as well as migration and fusion of myoblasts during muscle repair (Berdeaux and Stewart, 2012).

The induction of cAMP with the adenylylcyclase activator forskolin is widely used to study signalling pathways. Furthermore it serves as a model for in vitro exercise (Carter and Solomon, 2019).

1.7. Adipokines, batokines and myokines

The terms “adipokines”, “batokines” and “myokines” derive from the term “cytokines” and describe factors which are secreted from WAT, BAT or SKM and allow the interaction and communication between different cells and organs (Bełtowski, 2003; Zhang and An, 2007). These factors can be small proteins, metabolites, lipids or microRNAs which are released from cells and act in an auto- or paracrine way.

Villarroya et al. summarize the importance of batokines as follows: *“As BAT dissipates metabolic energy as heat, and actively uses lipids and glucose for oxidation, molecules secreted by activated BAT might be expected to support these functions and coordinate BAT activity with systemic metabolism”* (Villarroya et al., 2017). The first discovered batokine was fibroblast growth factor 21 (FGF21), which can be released by BAT after thermogenic activation to increase glucose uptake in BAT and browning of WAT (Yang and Stanford, 2022). Another small peptide is IL-6 which is a known batokine to signal from BAT to the liver to improve glucose tolerance and insulin sensitivity (Stanford et al., 2013). Mills et al. have furthermore shown that brown and beige adipocytes can ameliorate liver inflammation by the clearance of succinate from the circulation (Mills et al., 2021). Batokines also influence BAT itself: Recently, the purines adenosine and inosine were shown to be released by brown adipocytes and in turn stimulate thermogenic activation and energy expenditure (Gnad et al., 2014; Niemann et al., 2022). Under thermoneutrality, BAT can release the batokine myostatin which acts on skeletal muscle and reduces exercise capacity (Yang and Stanford, 2022).

IL-6 is not only released by BAT but also by SKM after exercise. It is described as an “exercise-factor” which accounts for exercise-induced adaptations in different organs (Pedersen and Febbraio, 2008).

Furthermore, exercise elevates the secretion of the myokine irisin which can induce muscle metabolism and also browning of WAT (Boström et al., 2012; Huh, 2018).

BAT, WAT and SKM are all cytokine-producing organs which can lead to systemic and metabolic adaptations (Villarroya et al., 2017; Huh, 2018). So far, only little is known on how aging affects the ability of these organs to produce and secrete their bato- and myokines. The identification of bato- and myokines which can improve metabolic health, would be of great interest for drug development.

1.8. Metabolomics

1.8.1. Omics Technologies

Omics technologies are large scale, high-throughput analyses that can map genetic or molecular changes in biological samples to provide great amount of information on distinct profiles. Common omics like genomics, transcriptomics, proteomics or metabolomics are widely used to characterize the genome, transcriptome, proteome or metabolome (Figure 7). Omics aim to analyse biological networks and organization at different levels by combining multidisciplinary bioanalytics with biostatistics and informatics (Junot et al., 2014).

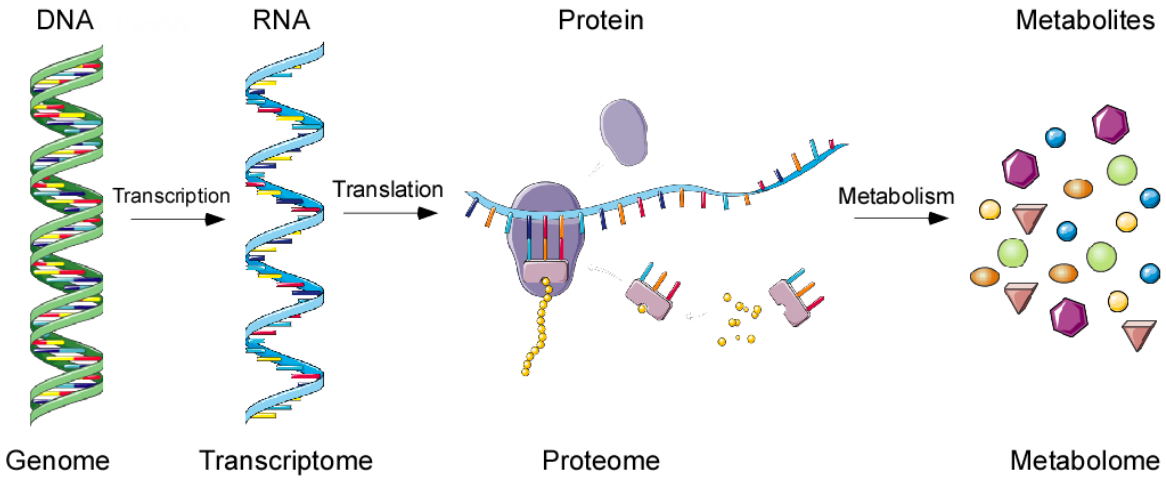

Figure 7: Omics analysis: From genomics to metabolomics. Adapted from (Zhao and Lin, 2014).

1.8.2. Metabolome and Metabolomics

Metabolites are defined as small molecules with low molecular weight (<1500 Da) like lipids, amino acids, sugars and carbohydrates, nucleotides, vitamins and more. The metabolome is the global set of endogenous molecules which can be found in a given biological sample and condition (Zhang et al., 2012).Metabolites can also originate from foods or other exogenous sources that are consumed or from microorganisms in the body (Barnes et al., 2016)

Metabolomics describes the identification of all metabolites in a biological sample (Idle and Gonzalez, 2007; Patti, 2011). It is a powerful tool to systematically screen for a high number of various metabolites and can be used to identify the regulation and role of metabolites regarding influences of, for example genetics, lifestyle, sex, age or dietary factors. To identify and quantify metabolites, powerful analytical tools with high resolution and high sensitivity are required. This was only made possible by the developments in analytical chemistry from low resolution to high resolution instruments (Idle and Gonzalez, 2007; Junot et al., 2014).

Typically, high resolution approaches like NMR, HPLC/UHPLC coupled to MS or GC-MS are used to detect numerous metabolites within a small amount of time. Every method has its advantages and disadvantages: NMR can be used for bulk metabolites, GC-MS for volatile metabolites and LC-MS for a wide range of polar to unpolar compounds (Zhang et al., 2012).

In general, there are two different types of metabolomics: targeted and untargeted (Patti, 2011; Bingol, 2018).

Using a targeted approach, a limited number of known metabolites are determined and quantified using exogenious standards. With the untargeted approach a large number of unknown metabolites are identified by comparing the relative abundancies of these molecules in different samples. After the samples are run, the spectra will be analysed using online libraries to identify the single molecules. This is a semi-quantitative approach,as the metabolite levels are only comparable within on sample set to see if levels are up- or down regulated (Dettmer et al., 2007; Bingol, 2018).

1.9 UPLC/MS-MS

Ultra-high performance liquid chromatography (UPLC) is a standard sample separation technique that separates molecules due to their chemical properties between a mobile phase (eluent) and the stationary phase of a column (Rathod et al., 2019). Based on the molecules' chemical structure (polarity and size) they will be retarded on the column which leads to different retention times (Rt) of each molecule. Additionally, the composition of the mobile and stationary phase both influence the sample separation. UPLC systems operate at a very high pressure which allows a short time analysis (Kang, 2012).

After the separation, the molecules are analysed in the MS, where they are turned into ions by e.g. Electrospray Ionization (ESI) in an ion source, or by matrix-assisted laser desorption/ionization (MALDI). This leaves the molecules with either a positive or negative charge, which is vital for the MS analysis, as non-ionic particles will not be detected by the MS. The MS sorts the ions according to their mass-to-charge ratios (m/z) and measures the relative abundance of each ionic species. When the ions reach the detector, they are quantitatively converted into a measurable electrical signal. In the MS2

(two consequent MS analysators), ions can be separated and proceeded to ion fragmentation which gives in-depth information of the molecules' structure (Kang, 2012; Rathod et al., 2019).

1.9.1 High Resolution Mass Spectrometry

The field of metabolomics was only made possible by the development of high resolution und highly sensitive machines. Mass spectrometers can measure the m/z of ions, by forcing them into an electric or magnetic field. The power of a mass spectrometer is defined by its resolution, the ability to separate ions with close m/z ratios. For a proper determination, it should provide a mass accuracy level below 5 ppm and a mass resolution over 10.000 ($m/\Delta m$) (Marshall and Hendrickson, 2008). For biochemical applications these commonly used analyzers are time-of-flight (TOF) and Fourier transformation (e.g. orbitrap) instruments which can be coupled to liquid chromatography (Marshall and Hendrickson, 2008).

1.9.2 Orbitrap Exploris 120^{TM} Mass Spectrometer

The Orbitrap Exploris consists of an ESI ion source, Stacked Ring Ion Guide (S- Lens), Advanced Quadrupole Technology (AQT), C- Trap, Ion Routing Multipole and the High Field Orbitrap Mass Analyzer (Fig. 2).

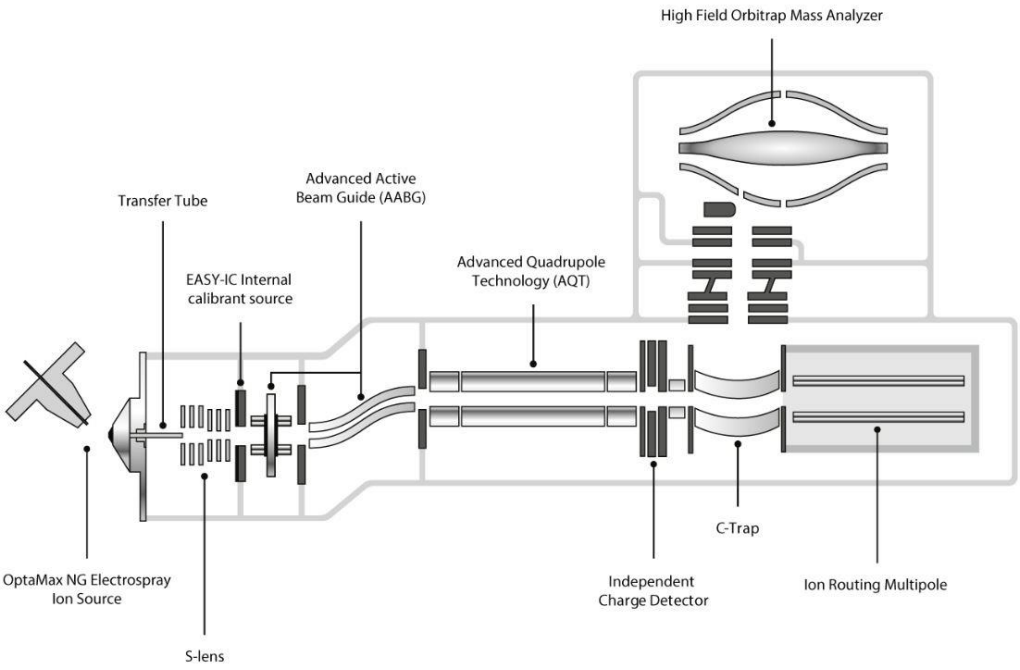

Figure 8: Schematic Orbitrap Exploris 120^{TM} set up. Adapted from Orbitrap Exploris Series Operating Manual (P/N BRE0014471, Revision E)

After the molecules have been separated on the UPLC and ionized in the ion source, they are passing the S- lens. This allows high ion transmission, removal of solvent vapour and focusing and transmission of the ions. The AQT is used for precursor isolation and the Ion Routing Multipole leads to the fragmentation of the ions (Yan et al., 2022).

The Orbitrap™ mass analyser is an ion- trapping device built of a central spindle- shaped electrode and two outer electrodes which detect the image current and establish the ion- trapping field. Once the ions enter the analyser they will start to oscillate around the central electrode, then the image current is received and generates the mass spectrum. The C- Trap regulates the number of ions entering the analyser (Yan et al., 2022).

1.10. Metabolomics in Aging and Exercise

A number of studies have been conducted to analyse the aging metabolome. In 2008 (Lawton et al.) observed significant changes in the plasma levels of metabolites related to protein, energy and lipid metabolism and oxidative stress with increasing age. For example, they found that the levels of essential and non-essential amino acid were higher in the elderly group. Furthermore, they detected higher levels of a number of fatty acids and citric acid cycle intermediates in the older group (Lawton et al., 2008). In a two-population based study serum samples from male and female participants from different ages were analysed. The authors could identify a set of 11 (women) and 12 (men) metabolites associated with incomplete mitochondrial fatty acid oxidation which were associated with age. These five metabolites were changed in both male and female samples: the acylcarnitines C12:1 and C18:1, the amino acids histidine and tryptophan and the phosphatidylcholine acyl-alkyl PC ae C36:1 (Yu et al., 2012).

Uchitomi et al. analysed whole gastrocnemicus muscle homogenate from young and old mice and showed significant changes in glucose, phospholipid and polyamine metabolism (Uchitomi et al., 2019). Another study from Tokarz et al. analysed the impact of age, dietary interventions and exercise in young and old mice. Among others, they identified arginine and lysine metabolites to be downregulated and various ceramides and acylcarnitines to be upregulated in skeletal muscle from aged and high fat diet-fed mice (Tokarz et al., 2021).

Various studies on how exercise influences whole body metabolism have been made. These studies conclude that PA induces quantifiable changes in the metabolome (Kelly et al., 2020). Generally, PA induces changes in fatty acid metabolism, mobilization and lipolysis, TCA cycle, glycolysis, amino acid metabolism, carnitines, purines and cholesterols. Schranner et al. reviewed 27 publications and report that lactate and pyruvate increase whereas formate and the sugar rhamnose are decreased after one

bout of exercise. Furthermore, they report that, among others, TCA cycle intermediates, free fatty acids, acylcarnitines or purines are upregulated after exercise (Schranner et al., 2020).

The majority of metabolomics studies is performed with blood or urine samples rather than with samples from the tissue itself (Kelly et al., 2020; Schranner et al., 2020). This may give insights into bigger metabolic adaptations, but the underlying biological processes remain under-investigated. Meanwhile, also whole tissue homogenates or cell culture lysates are used for metabolomics analyses (Gohlke et al., 2019; Kumar et al., 2020; Tokarz et al., 2021; Whitehead et al., 2021). This allows the interpretation of metabolite dynamics within the cell or tissue itself but gives no information about the secretion of metabolites. Furthermore, the studies often do not contain any stimulus on the tissue or the stimulus/exercise is not directly before the tissue biopsies are taken. A direct stimulation right before the sample preparation is of great importance, if not only the resting but also the activated metabolic profile shall be analysed. The analysis of secreted metabolites under unstimulated and stimulated conditions is of great importance to understand the auto-and paracrine influence and therefore the cross-talk between a donor and a receiving organ.

2. Aim and Objectives

Obesity, Physical Inactivity and Aging are three major and related health threats affecting a large part of the worldwide population. Consequently, combating these threats has to be addressed globally, highlighted by the strategy on diet, PA and health of the WHO. This strategy's main objectives are to reduce risk factors for chronic diseases, increase awareness and understanding about diet and PA, monitor and promote research and develop policies and action plans to improve diets and PA (WHO, 2004).

Overall, most of the literature focus on the potential parameters of individual signalling pathways that cause, impact, and/or worsen obesity, exercise/physical inactivity, or aging. However, not much is known about metabolome profiles from adipose tissue and skeletal muscle in the context of aging and with regard to stimulation with the central signalling molecule of fat and muscle cAMP.

In this PhD Thesis the influence of aging and exercise on the cAMP regulated metabolome was analysed to answer the following research questions:

1. To what extent can secreted metabolites from murine and human skeletal muscle and adipose tissue biopsies be characterised using untargeted metabolomics?
2. Are there differences in the secretome profile of adipose tissue and SKM between young and old mice?
3. Which influence does cAMP stimulation have on the secretome of young and old mice? Which tissue and which age group is most affected?
4. Which metabolites are the most regulated by age, or by cAMP stimulation? Are there metabolites which are exclusively released from young/old or treated/untreated samples?
5. Which influence does exercise and aging have on the human secretome of skeletal muscle?

3. Materials and Methods

3.1. General Chemicals, Materials and Equipment

The majority of all chemicals and materials was purchased from ThermofisherScientific (Massachusets, USA), Agilent Technologies (California, USA), Water Corporation (Massachusets, USA), VWR Chemicals (France), Sarstedt (Nümbrecht). All plastic laboratory ware (e.g. Micro Tubes, 6-, 12-well plates, tissue culture flask, conical tubes 15mL, 50mL) was purchased from Sarstedt (Nümbrecht).

This list provides general chemicals, materials and equipment that were used:

- Autoclave, Varioklav 135 T (Faust)
- Centrifuge 5430 R (Eppendorf)
- Forskolin (Sigma Aldrich, Cat. No. F6886)
- Thermomixer comfort (Eppendorf)
- Dimethylsulfoxid (Roth)
- Milli-Q Water Purification System (Merck EMD Millipore)
- Ministar Silver Centrifuge (VWR)
- Nanodrop200 Spectrophotometer (ThermoScientific)
- Pipet Boy acu 2 (Integra)
- Vortex (VWR)
- Ranin Pipete Lite XLS Size, L2, 20, 200, 1000 (Mettler Toledo)
- Ranin Pipete Filter Tips BioClean Ultra TM Size: 20,200,1000 µL (Mettler Toledo)
- Preparation tools scissors, forceps (Fine science tools)

HEPES Buffer; pH adjusted to 6.8-7,2

Component	**Final concentration (mM)**
NaCl	125 mM
KCl	4,8 mM
CaCl2 x 2 H2O	1.3 mM
HEPES	25 mM
Glucose	5,55 mM

3.2. Animal experiments:

3.2.1. Housing:

Wildtype (WT) male C57Bl/6 mice were housed under specific- pathogen- free conditions at the “Genetisches Ressourcen Centrum” at the Life & Medical Sciences Institute at University of Bonn. All

mice were kept under a 12-hour light/ darkness cycle (06:00- 18:00; 18:00- 06:00) and fed standard chow and water ad libitum.

Alternatively, male C56Bl/6 mice were purchased from Charles River Laboratory at similar age.

Mice were sacrificed for organ isolation at an age of either 6 weeks or 18-19 months.

3.2.2. Isolation and treatment of sample tissues:

Soleus muscle, interscapular BAT and WATi were dissected from each mouse. Soleus muscle tissues were taken from both legs; one tissue was handled for one condition (1x Control, 1x Forskolin stimulation). BAT and WATi were cut into two pieces (1x Control, 1x Forskolin stimulation). Tissue weights were noted for data normalization.

Tissues were then transferred into a 2 mL Eppendorf tube and washed with 200 µL HEPES. Afterwards either 200 µL of pure HEPES-buffer or 200 µL of a 30 µM Forskolin-HEPES-solution was added to the samples and incubated on a thermomixer at 37°C for 30 minutes. The supernatant was used for further metabolomics analysis; the tissue was immediately frozen at -80°C.

3.3. Human soleus biopsy preparation

3.3.1. MALICoT Study

The sampling and analysis of human soleus biopsies was done in collaboration with Prof. Dr. med. Jörn Rittweger, Deutsches Institut für Luft- und Raumfahrt (DLR), Institute of Aerospace Medicine. DLR carried out the study „Master Athletic, Laboratory Study of Intramuscular Connective Tissue" short MALICoT. The study received ethical approval (Ärztekammer Nordrhein, lfd. Nr. 2018269) and was registered at the German clinical trials register (www.drks.de, registration number DRKS00015764) prior to the start of the study. MALICoT study was conducted at the DLR, Institute of Aerospace Medicine, Linder Höhe, Cologne. For the study, healthy male volunteers were recruited which had to be of specific age and training status. The inclusion criteria were either young (20-35 years old) or old (60-75 years old) and BMI ≤25 kg/m². Furthermore, the participants had to be either untrained or trained. Untrained was defined as little or no physical activity: ≤25 metabolic units of physical activity per week. Trained was defined as training ≥4 hours per week and the participation in track and field competitions like jumping, sprinting, or throwing events. The following numbers of participants were included for metabolomic analysis: young untrained: n=12, young trained: n=10, old untrained: n=11, old trained: n=7. Detailed parameters about the study participants is displayed in Table 1. The study was performed between September 2020 and May 2021. Due to the SARS-CoV-2pandemic, the recruitment and study realisation was restricted and delayed.

Table 1: MALICoT Study participant parameters: n (number of participants), age, height, bodyweight, BMI and body fat of all participants. Values are displayed as median (except for n).

Parameter	young_untrained	young_trained	old_untrained	old_trained
n	12	10	11	7
Age [years]	29,5	23	65	63
Height [cm]	183,9	180	180	180
Bodyweight [kg]	77,0	79,3	81,1	74,9
BMI [kg/m2]	22,9	23,2	25,8	23,6
Body Fat [%]	15,0	9,8	24,4	8,7

3.3.2. Muscle Biopsy

Tissue samples were obtained from the soleus muscle by Prof. Dr. med. Jörn Rittweger. The sampling was done under sterile conditions with local anaesthesia (Lidocain 1%). A 12 mm incision was made into the skin and fascia, and the biopsy was obtained with a biopsy rongeur (Ferr. Smith, Fa. Zepf, Dürbheim). After the removal of the tissue, the wounds were closed by intracutaneous suture and covered with a sterile plaster.

3.3.3. Sample Treatment

The obtained soleus biopsy was cut into two pieces (1x Control, 1x Forskolin treatment). Tissue weights were noted for data normalisation. Tissues were then transferred into an 1,5mL Eppendorf tube and washed with 200 µL HEPES. Afterwards, either 200 µL of pure HEPES- Buffer or 200 µL of a 30 µM Forskolin-HEPES-Solution was added to the samples and incubated on a thermomixer at 37°C for 30 minutes. Next, the tissue was immediately frozen at -80°C. The supernatant was inactivated by heat at 67°C for 10 minutes and then frozen at -80°C.The supernatant was used for further metabolomics analysis.

3.4. Untargeted metabolomics

3.4.1. Materials and equipment

- Acetonitrile (UPLC/MS-CC/SFC, Biosolve)
- Accucore™ C30 (2,6 µm, 2,1mm x 150mm, ThermoFisher scientific)
- Accucore™ Defender guards (2,6 µm, 2,1 mm x 10 mm, ThermoFisher scientific)
- Ammonium acetate 99%, Ammonium formiate (VWR Chemicals)
- ddH_2O (Milli-Q Water Purification System)
- Cortecs®UPLC®C18 (1,6 µM, 2,1 mm x 150 mm, Waters)
- Elmasonic S 60 H, Elma

- Filter Vials 0,2 µm PES
- Formic acid 99% (VWR Chemicals)
- InfinityLab Deactivator Additive
- InfinityLab Poroshell 120 HILICz (2,7 µm, 2,1 mm x 150 mm, Agilent Technologies)
- Methanol (VWR Chemicals)
- Orbitrap Exploris 120 (ThermoFisher Scientific)
- SureStart™ CAP AVCS ™ Screw 0,3 mL
- SureStart™ Vial 0,3 mL
- UHPLC Guard InfinityLab Poroshell 120 HILICz (2,7 µm, 2,1 mm x 5 mm, Agilent Technologies)
- Vanquish Flex System, ThermoFisher Scientific

Untargeted metabolomics was performed with an UHPLC system coupled to a high-resolution Orbitrap mass spectrometer (Vanquish Flex, ThermoFisher Scientific, Orbitrap Exploris 120, ThermoFisher Scientific). For data analysis Thermo Scientific Xcalibur v.4.4.16.2 software was used.

The applied methods and settings have been established in our lab relying on our preliminary experiments to cover a broad range of analytes. Several conditions regarding LC and MS/MS settings have been tested. All applied settings were those which have performed best in our hands.

Column settings have been chosen according to manufacturers' information.

3.4.2. Sample preparation:

Fresh supernatant from tissue explants was taken and either immediately mixed with ice-cold ACN (1:5 (v/v), total volume 300 µL) or was heatshock inactivated (67°C, 10 min) and mixed with ice-cold ACN (1:5 (v/v), total volume 300 µL) prior to sample analysis depending on the sued separation method. All samples were stored at -80°C until analysis. Before metabolomics analysis samples were filtered using 0,2 µm nano filter vials and then stored in the 4°C-tempered auto-sampler.

3.4.3. Liquid Chromatography:

Prepared samples were analysed using three different columns: Agilent HILICz, Waters Cortecs C18, ThermoFisher Scientific Accucore C30. The combination of the three different columns allows the analysis of a broad range of polar and unpolar metabolites: Hydrophilic interaction liquid chromatography (HILIC) allows the separation of polar analytes and ionic metabolites (Xu et al., 2007).C18 and C30 are reverse phase columns. Reversed-phase LC methods are widely used for the identification of unipolar and hydrophobic metabolites and biomarkers (Patti, 2011). C30 columns are designed for the separation of hydrophobic, long-chain, structural isomers. C18 has shorter carbon chains than C30 and is therefore an intermediate column. The combination of the complementary RP

and HILIC methods allows a broad metabolite coverage (Patti, 2011). The applied conditions and settings are displayed in Table 2; the gradient profiles in Table 3 -Table 8. Solvents were degassed with ultrasonication before being used.

Quality controls (QC): Two types of QC were used to monitor sufficient stability of the system throughout the whole measurement: A) matrix blank sample to remove background noise, and B) pooled sample put together from all individual samples to control intrarun accuracy. Furthermore, QC were used for spectral integration and processing (see section 3.4.5).

Table 2: UHPLC and column parameters applied for untargeted metabolomics

Column	**Column Chamber Temperature**	**Injected sample volume [µL]**	**Flow[µL /min]**	**Average column pressure**	**Ionization mode**	**Solvent A**	**Solvent B**
HILICz	45°C	25	250	200-300 bar	positive	H2O+ 10 mM Ammoniumformiat + 0,1% FA	ACN+ 10% H2O+ 10mM Ammoniumformiat + 0,1% FA
HILICz	45°C	25	250	200-300 bar	negative	H2O+ Ammoniumacetat (pH=9)+ Deactivator	100% ACN
C18	30°C	3	250	600-800 bar	positive	H2O+ 0,1% FA	ACN+ 0,1% FA
C18	30°C	3	250	600-800 bar	negative	H2O + 10 mM Ammoniumacetat (pH=7)	ACN+ 10% H2O+ 10mM Ammoniumacetat(pH=7)
C30	60°C	3	400	400-500 bar	positive	H2O+ 0,1% FA	ACN+ 0,1% FA
C30	60°C	3	400	400-500 bar	negative	H2O+ 10 mM Ammoniumacetat (pH=9)+ Deactivator	100% ACN

Table 3: Gradient profile for HILICz positive mode

Time [min.]	Gradient
0-3	87% B
3-11	87% B to 59% B
11-12	59% B to 49% B
12-16	49% B to 29% B
16-18	29% B

Table 4: Gradient profile for HILICz negative mode

Time [min.]	Gradient
0-2	80% B
2-5.5	80% B to 73% B
5.5-8.5	73% B
8.5-9	73% B to 71% B
9-12	71% B

Table 5: Gradient profile for C18 positive mode

Time [min.]	Gradient
0-2	5% B
2-10	5% B to 100% B
10-12	100% B
12.00-12.01	100% B to 5% B
12.01-14.00	5% B

Table 6: Gradient profile for C18 negative mode

Time [min.]	Gradient
0-2	5% B
2-9	5% B to 100% B
9-11.5	100% B
11.5-11.6	100% B to 5% B
11.6-14.00	5% B

Table 7: Gradient profile for C30 positive mode

Time [min.]	Gradient
0-2	5% B
2-10	5% B to 100% B
10-14	100% B
14-14.1	100% B to 5% B
14.1-20	5% B

Table 8: Gradient profile for C30 negative mode

Time [min.]	Gradient
0-2	3% B
2-10	3% B to 100% B
10-14	100% B
14-14.1	100% B to 3% B
14.1-20	3% B

3.4.4. Mass Spectrometry

Samples were identified using and Orbitrap Exploris 120 instrument. The following settings were consistent in all sample analyses:

- Ion Source Type: H-ESI
- Internal Mass Calibrant: Easy-IC™
- Orbitrap Resolution: 60.000

- Scan Range (m/z): 100-1500, 50-750 (HILICz)
- RF Lens: 70% (C18), 85% (C30), 90/100% (HILICz)
- Intensity threshold: 1.0e3
- Mass Tolerance: +/- 5ppm
- ddMS^2: Isolation window= 1.5 (m/z), normalized Collison Energy Type, HCD Collision Energies: 30,45,60 %, Orbitrap Resolution 30.000

Table 9 shows the Ion Source Settings which were adjusted for each method.

Table 9: Orbitrap Exploris Ion Source Settings

Ion Source Parameter	HILICz positive	HILICz negative	C18 positive	C18 negative	C30 positive	C30 negative
Positive Ion (V)	3000	3000	3500	3000	3000	3000
Negative Ion (V)	2000	3500	3500	3500	3500	3500
Sheath Gas (Arb)	50	60	60	60	60	60
Sweep Gas (Arb)	0	0	2	0	0	5
Aux Gas (Arb)	15	15	15	15	15	15
Ion Transfer Tube (°C)	200	200	320	320	275	275
Vaporizer Temp (°C)	350	350	350	350	350	350

Metabolites were ionized with electrospray technique in positive and negative mode.

In each sample batch, a matrix blank sample to remove background noise and a pooled sample from all samples as a QC was included. QC was run after every 12 samples. To guarantee intrarun accuracy, analytes with <30% SD in the pooled samples were further processed. An internal mass calibration was included in each run to ensure mass accuracy. MS scan involved alternating MS1 (60.000 mass resolution) and MS2 (30.000 mass resolution) mode using a scan range of 40-1.500 m/z.

Compound Discovery 3.2 software was used for untargeted analysis, peak identification and integration of mass spectrometric data.

MS Data was further analysed using spectral libraries. Metabolites were assigned according to their m/z data, chromatographic data and MS2 fragmentation patterns.

3.4.5. Spectral Integration & Processing

Spectral data was analysed using Compound Discoverer 3.2. Processing involved spectrum processing, peak area refinement and compound identification. The following settings were applied:

Table 10: Compound Discoverer Filter settings for Spectral Integration and Processing

Spectrum Processing Alignment	Adaptive curve
Peak Area Refinement	Mass Tolerance=5ppm Peak Intensity=50.000 Signal/noise ratio=3 Max. peak width at half peak height was set at 0,5min
Group compound node	Mass Tolerance=10ppm Rt Tolerance=1min.
Data normalisation	Tissue weight (highest tissue weight was set as factor 1, all data was recalculated with normalised tissue weight factor for each sample)
QC Correction	Min. Coverage: 50% (compound has to be be refound in QC pooled sample, otherwise it will not be processed further) 80% max. QC Area RSD Max. Sample/Blank: 3
Compound libraries	ChemSpider (KEGG,HMDB,BioByc) mzCloud (endogenous metabolites, Steroid/Vitamins/Hormones) Metabolika Pathways (exclusion of non-eucaryotic pathways) Precursor mass: 5ppm, FT Fragment: 10ppm, IT Fragment: 0.4 Da DIA Scan, max. isolation width: 500, activation energy: 100, match factor: 70

3.4.6. Statistical Analysis & Data Processing

For Data Analysis the online free website tool *https://www.metaboanalyst.ca/* was used. Its analyses are based on the open-source MetaboAnalystR packages.

Compound ID Conversion:

Compound labels were standardized by conversion of the metabolite names into KEGG or HMDB ID. This way they could be compared with metabolite and pathway libraries in a next step.

Metabolite names were pasted into the Metabolite ID Conversion tool. Input Type was set as Common Name. After submitting and converting the samples, the results were exported into an excel sheet. Since this online tool did not find a match to every metabolite, the non-converted names had to be further identified manually. Consequently, every non-converted metabolite name was again checked in KEGG or HMDB database to find the correct ID.

Statistical Analysis:

Statistical analysis [one factor] was used for further analysis. Data files were uploaded as .csv files and the following conditions were applied:

- Data type: Peak Intensities

- Format: Samples in columns (paired)
- Samples labels were adjusted according to the condition (e.g. Cntl, FSK)
- Data Filtering: by Interquantile Range
- Sample normalization: None (this has already been done in the step before)
- Data transformation: Log transformation (base 10)
- Data scaling: Auto scaling

Volcano plot Analysis:

The Volcano Plot analysis is a combination of T-test and Fold Change (FC) Analysis. Paired Analysis, FC threshold of 2 and p- value threshold of 0.05 raw p- value was set, Group variance was equal.

Principal Component Analysis:

2D Scores Plot were chosen for PCA with PC1 on the x-axis, and PC2 on the y- axis with display of 95% confidence regions.

Hierarchical Clustering Heatmaps:

The following settings were used to create heatmaps: Data source: Normalized data; Standardization: Autoscale features, Distance measure: Euclidean, Clustering method: Ward

Quantitative Enrichment Analysis

For Quantitative Enrichment Analysis (QEA) all metabolite names were either used as names after Compound ID Conversion or as HMDB IDs. If metabolites could not be linked to HMDB or KEGG IDs, these metabolites could not be evaluated in QEA. Data was log transformed and auto-scaled. As metabolite library, KEGG pathway set using 84 metabolite sets based on KEGG human metabolic pathways (Oct.2019) was used.

3.5. Cell culture

The following materials and equipment was used for cell culture:

- 10 cm^2 TC dishes (ThinCertTM; Greiner, Cat. No. 664160)
- 10 cm^2 TC dishes, Standard (Sarstedt, Cat. No. 83.3902)
- 12-well TC plates (Greiner, Cat. No. 662160)
- 12-well TC plates, Standard (Sarstedt, Cat. No. 83.3921)
- 12-well TPP plates (TPP Techno Plastic Products AG, Cat. No. 92412)
- 3,3’,5-Triiodo-L-thyronine sodium salt (Sigma Aldrich, Cat. No. T6397)

- 30 µM and 100 µM nylon meshes (Millipore, Cat. No. NY3002500, NY1H00010)
- 3-Isobutyl-1-methylxanthine, IBMX (Sigma Aldrich, Cat. No. I5879)
- 6-well tissue culture (TC) plates (Sarstedt, Cat. No. 83.3920)
- 6-well TPP plates (TPP Techno Plastic Products AG, Cat. No. 92406)
- Cannulas (Braun, Sterican 0,90 x 40 mm, Cat. No. 4657519)
- Collagenase, Type II (Worthington, Cat. No. CLS2)
- Countess Automated Cell Counter (Invitrogen, Cat. No. C10227)
- Cryogenic vials (Sarstedt, Cat. No. 72.379.992)
- D(+)-Biotin (Novabiochem, Cat. No. 58-85-5)
- Dexamethasone (Sigma Aldrich, Cat. No. D4902)
- DMEM, high glucose, GlutaMAX(TM), pyruvate (Gibco, Cat. No. 31966)
- DMEM, high glucose, GlutaMAX(TM) (Gibco, Cat. No. 61965)
- Fetal Bovine Serum, FBS (Biochrom, Cat. No. S0015)
- F-12 Media (gibco, Cat. No. 21765029)
- FGF-b (PetroTech, Cat. No. 100-18B)
- Horse serum (Sigma Aldrich, Cat. No. H1270
- Insulin solution human (Sigma Aldrich, Cat. No, I9278)
- Laminin (Sigma Aldrich, Cat. No. 114965-81-9)
- L-Gutamine (Sigma Aldrich, Cat. No. G7513)
- Non-essential amino acids (Gibco, Cat. No. 11140050)
- Pantothenate (Sigma Aldrich, Cat. No. P5155)
- Penicillin/streptomycin (P/S; Merck, Cat. No. A2213)
- Rosiglitazone (Sigma Aldrich, Cat. No. R2408)
- Sodium ascorbate (Carl Roth, Cat. No. 3149)
- Syringe filter 0.22 µm (VWR, Cat. No. 514-0061)
- Syringes 5 ml (BD Discardit II, Cat. No. 309050)
- T175 tissue culture flasks (Sarstedt, Cat. No. 83.3912.002)
- Trypan Blue Stain (Gibco, Cat. No. 15250)
- Trypsin-EDTA (0.05 %), phenol red (Gibco, Cat. No. 25300054)

3.5.1. Cell culture of C2C12 cells

C2C12 cells were purchased from CLS, Cat. No. 400476.

The following culture media were used for the cultivation of C2C12.

Table 11: Cell culture media used for the cultivation of C2C12

Growth Medium		**Differentiation Medium**	
DMEM GlutaMAX (+pyruvate) + Substances		DMEM GlutaMAX + Substances	
Substance	Concentration	Substance	Concentration
FBS	10%	Horse Serum	2%
P/S	1%	NEAA	1%
		P/S	1%

3.5.1.1. Expansion and cryo preservation of C2C12

C2C12 were cultured in Growth Medium (GM, Table 11) in T175 flasks until they reached ~90% confluency. Cells were washed with PBS and trypsinized for 3 minutes at 37°C to detach the cells from the cell culture flasks, followed by an inactivation by adding GM. The cell suspension was centrifuged for 5 minutes, 1000rpm. The cell pellet was resuspended in GM and cells were counted using Tryphan Blue Stain. Afterwards, cells were frozen in GM +10% DMSO and stored at -150°C.

3.5.1.2. Differentiation of C2C12

1 Mio. cells were seeded in 6- or 12-well culture plates in GM (Table 11) and grown until the cells were confluent. Afterwards the medium was switched to differentiation medium (Table 11) for 7 days. The medium was refreshed every second day.

3.5.2. Cell culture of human skeletal muscle cells

Human skeletal myoblasts were purchased from ThermoFisher, Cat. No. A12555.

The following media were used for the cultivation of human skeletal muscle cells (hSKM).

Table 12: Cell culture media used for the cultivation of hSKM

Seeding Medium		**Growth Medium**		**Differentiation Medium**	
F12 Medium + Substances		DMEM GlutaMAX + Substances		DMEM GlutaMAX + Substances	
Substance	Concentration	Substance	Concentration	Substance	Concentration
FBS	20%	FBS	20%	HS	2%
HS	10%	HS	10%	P/S	1%
FGF-b (2.5 µg/mL)	2.5 ng/mL	P/S	1%	L-Glutamine	1%

P/S	1%	L-Glutamine	1%		
L-Glutamine	1%				

For the expansion and cultivation of hSKM, laminin-coated cell culture plates were used. Therefore, a sterile laminin solution (10 µg/mL in PBS) was added to the flasks/ to every well and incubated for at least 30 minutes at 37°C, 5% CO2. Afterwards, the laminin was removed and cells were seeded.

3.5.2.1. Expansion and cryo preservation of hSKM

Purchased cells were seeded in Seeding Medium (Table 12) into a laminin-coated T75 flask and cultured until they reached 70-80% confluency. Medium was refreshed every second day. For cell passaging the medium was removed and cells were washed with PBS. 1.5 mL trypsin was added to cover the surface of the cells and incubated for 10 seconds before it was removed. Then the cells were kept at 37°C, 5% CO2 for 5 minutes to detach the cells before 5mL GM (Table 12) was added to stop the reaction. The cells were suspended in the GM and split into new flasks in a ratio 1:4 or frozen in GM +10% DMSO and stored at -150°C.

3.5.2.2. Differentiation of hSKM

1 Mio. cells were seeded in laminin-coated 6- or 12-well culture plates in GM (Table 12) and grown until the cells reached 70-80% confluency. Afterwards the medium was switched to differentiation medium (Table 12) for 7 days. The medium was refreshed every second day.

3.5.3. Cell culture of BA

The following buffers and culture media were used for the isolation and cultivation of BA

Table 13: Buffers and Media used for the isolation of BA from interscauplar BAT

Isolation Buffer		**Culture Medium**	
H2O + Substances, pH=7.4, sterile filtered		DMEM GlutaMAX + Substances	
Substance	Concentration	Substance	Concentration
NaCl	123 mM	FBS	10%
KCl	5 mM	HEPES	10 mM
CaCl2	1.3 mM	Insulin	4 nM
Glucose	5 mM	P/S	1%
HEPES	100 mM	Sodium-Ascorbate	25 µg/mL
BSA	1.5%	T3	4 nM
Collagenase II	2 mg/ml		

Table 14: Cell culture media used for the cultivation of BA

Growth Medium		**Differentiation Medium**		**Induction Medium**	
DMEM GlutaMAX + Substances		DMEM GlutaMAX + Substances		Differentiation medium + Substances	
Substance	Concentration	Substance	Concentration	Substance	Concentration
FBS	10%	FBS	10%	Dexamethason	1 µM
P/S	1%	Insulin	1 nM	IBMX	0.5 mM
		P/S	1%		
		T3	20 nM		

3.5.3.1. Isolation and immortalization of BA

Newborn mice were sacrificed and interscapular BAT was dissected. The tissue was then chopped with a scissor in 3 mL of Isolation Buffer (Table 13) and kept in a water bath for 30 minutes at 37°C. To ensure proper digestion of the whole tissue, the flasks were shaken every 5 minutes. Undigested tissue parts were then filtered out with a 100 µm nylon mesh. Samples were then kept on ice for 30 minutes. The middle phase of the cell suspension was used for the further procedure. Cells were again filtered with 30 µm nylon mesh and centrifuged for 10 minutes, 700g. The pelleted cells were resuspended in 2 mL BA Culture Media (Table 13) and cultivated in 6- well plates for 24h, 37°C, 5% CO2. On the next day, BAs were immortalized with lentivirus containing SV40 large T antigen (200 ng/well).

3.5.3.2. Expansion and cryo preservation of BA

Immortalized BAs were cultured in GM (Table 14) until they reached ~90% confluency. Cells were washed with PBS and trypsinized for 3 minutes at 37°C to detach the cells from the cell culture plates, followed by an inactivation by adding BA GM. The cell suspension was centrifuged for 5 minutes, 1000rpm. The cell pellet was resuspended in BA GM and cells were counted using Trypan Blue Stain. Afterwards, cells were either frozen in GM +10% DMSO or reseeded and cultured to passage 4 to be used for experiments.

3.5.3.3. Differentiation of BA

1 Mio. BA cells were seeded in BA GM in 6- or 12- well TC plates (Day -4) and cultured for 2 days. At day -2, medium was switched to BA Differentiation medium (DM, Table 14) for 2 days, followed by a switch to BA Induction medium (Table 14) for another two days (Day 0). Afterwards, BAs were cultured in DM until day 7. The medium was replaced every second day. Cells were kept at 37°C and 5% CO2.

3.5.4. *In vitro* treatment of C2C12, hSKM and mBA with selected metabolites

The following list provides all compounds used for the treatment of the different cell types (Table 15).

Table 15: Compounds used in vitro testing in C2C12, hSKM and mBA

Compound	**Supplier**	**Catalog Number**
21-Desoxycortisol	Iso Sciences	13407
Choline chloride	Sigma Aldrich	C7017
Corticosterone	Cayman Chemical Company	16063
DL-Carnitine hydrochloride	Merck KGaA	8.41774.0025
Forskolin	Sigma Aldrich	F6886
Histamin	Sigma Aldrich	H7125
L-(-)-Norepinephrinebitartrate salt monohydrate	Sigma Aldrich	A9512
Oleamide	Sigma Aldrich	2136
Prostaglandin E2	Tocris Bioscience	2296
Prostaglandin E3	Cayman Chemical Company	14990

C2C12, hSKM and mBA were differentiated as described. The acute treatment started at day 6 of differentiation. The old media was removed and replaced by fresh DM with or without the selected compounds. The cells were incubated overnight for 16 hours. On the next morning, cells were washed twice with PBS and the plates were stored at -80°C for further RNA isolation.

C2C12 were also treated chronically for 7 days. When media was switched from GM to DM, the compounds were applied. Fresh media with or without the selected compounds was refreshed every second day. At day 7, cells were washed twice with PBS and the plates were stored at -80°C for further RNA isolation.

3.6. RNA Methods

The following materials were used for RNA isolation:

- InnuSOLV RNA Reagent (Analytik Jena AG, Cat. No. 845-SB-2090100)
- Nanodrop200 Spectrophotometer (ThermoScientific)
- Luna qPCR Master Mix (NEB, Cat. No. M3003)
- Real-time PCR machine, HT7900 (Applied Biosystems)
- SYBR-Green PCR master mix (Applied Biosystems, Cat. No. 4309155)
- Thermocycler Biometra TOne (Analytik Jena)
- Thermomixer comfort (Eppendorf, Cat. No. 2050-120-04)
- Protoscript® II First Strand cDNA Synthesis Kit (New England BioLabs, Cat. No. E6560S)

3.6.1. RNA Isolation and cDNA Synthesis

Cell samples were lyzed using 1mL InnuSolV RNA Reagent. 200 µL chloroform was added to all sample lysates, shaken manually for 15 seconds, kept at RT for 5 minutes and then centrifuged at 13.000 rpm, 4°C for 10 minutes. Then the upper phase was transferred to a new 1.5 mL Eppendorf tube and 500 µL isopropanol were added. To pellet the RNA all samples where centrifuged (13.000 rpm, 4°C, 10 min.). After discarding the supernatant, pellets were washed with 1 mL Ethanol 75% (in DEPC-H_2O) and centrifuged (13.000 rpm, 4°C, 10 min.). All samples were washed two more times. The resulting RNA pellet was then dried using a vacuum centrifuge and dissolved in nuclease free water. RNA concentrations were measured with the Nanodrop Spectrophotometer.

In the last step 1 µg of RNA was used for cDNA synthesis. cDNA synthesis kit was used according to manufacturer's protocol.

3.6.2. mRNA analysis using Quantitative Real Time Polymerase Chain Reaction (qRT-PCR)

mRNA expression levels were examined by qRT-PCR using the fluorescent dye Luna qPCR Master Mix. A HT7900 instrument (Applied Biosystems) was used with the program shown in Table 16. mRNA levels were quantified with the Second Derivative Maximum Method. For murine samples, Glyceraldehyde-3-phosphate dehydrogenase (GAPDH), and for human samples TATA-box-binding protein (TBP) was used as an internal control. The primer sequences of the target genes are shown in Table 17.

Table 16: qPCR Program

Step	Temperature (°C)	Time (s)	Repetition
1	95	600	
2	95	15	40 cycles
3	60	60	
4	95	1	
5	65	15	
6	95		

Table 17:Primers used for qRT-PCR

	Target	Forward (5'-3')	Reverse (5'-3')
murine	GAPDH	GGC TGC CCA GAA CAT CAT	CGG ACA CAT TGG GGG TAG
	UCP1	GGCCTCTAGGACTCAGTC	TAAGCCGGCTGAGATCTTGT
	PPARg	ACAAGACTACCCTTTACTGAAATTACCAT	TGCGAGTGGTCTTCCATCAC
	AP2	GCGTGGAATTCGATGAAATCA	CCCGCCATCTAGGGTTATGA
	MyoD	GGCTACGACACCGCCTACTA	GTGGAGATGCGCTCCACTAT
	Myf5	CAGGAATGCCATCCGCTACA	ATTCAGGCATGCCGTCAGAG
	Myogenin	AGTGAATGCAACTCCCACAG	ACGATGGACGTAAGGGAGTG
	Myomaker	ATCGCTACCAAGAGGCGTT	CACAGCACAGACAAACCAGG
	Mef2c	CCCTCAGTCAGTTGGGAGCTTGC	GTGGCGCGTGGTGTGTTGTG
	Pax3	TCAACCAGCTCGGAGGAGTA	ATGGAGCCTGTCTCCTGGTA

human	MyoD	TGCTGGACAGGCAGTCTA	CTCCGACGGCATGATGG
	Mef2c	CTGTCTGGCTTCAACACTG	TGGTGGTACGGTCTCTAGGA
	TBP	CACGAACCACGGCACTGATT	TTTTCTTGCTGCCAGTCTGGAC

4. Results

The global population is becoming older and, in parallel, obesity prevalence is rising constantly in the last decades. Hence, understanding the impact of aging on metabolism is getting ever more important. BAT, WAT and SKM are all highly metabolic tissues, which influence whole body metabolism. To analyse the effects of aging on the metabolic capacity of these tissues, state of the art untargeted metabolomics was performed to identify so far unknown secreted small molecules/metabolites that could function as auto-or paracrine regulators of metabolic capacity.

Untargeted metabolomics was performed from murine BAT, WAT and SKM from young and aged mice. Moreover, untargeted metabolomics was performed from human SKM taken from young or old male healthy participants, that were either highly active in sports (trained) or not active in sports (untrained).

Initially, the following protocol was established to ensure proper sample handling and treatment in order to receive the best possible results: biopsies were taken from mouse/human and immediately divided into two parts. One part was treated with HEPES buffer only, the other part with a 30 µM FSK-HEPES solution to increase cAMP levels. After 30 minutes incubation time at 37°C the tissue supernatant was taken for untargeted metabolomics analysis. The remaining tissue was frozen at -80°C (Figure 9).

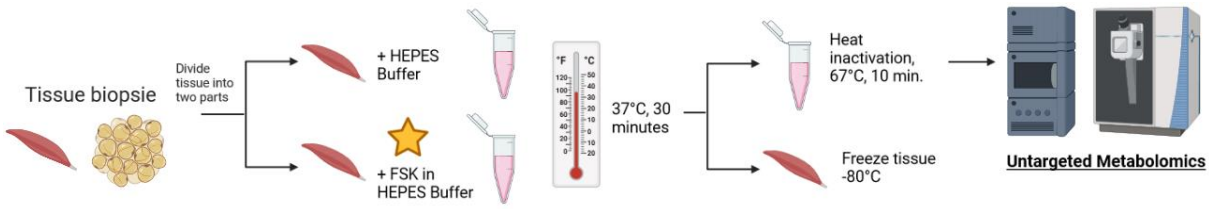

Figure 9: Scheme of sample treatment for untargeted metabolomics analysis

4.1. Untargeted Metabolomics of murine BAT, WATi and SKM from young and aged mice

In general, untargeted metabolomics of murine tissue samples yielded a high number of detected metabolites which were assigned to seven metabolite classes (Figure 10). For BAT, WAT and soleus a total of 391, 195 and 295 metabolites were detected, respectively. In BAT 41,5% of all metabolites were assigned to the class of “Lipids”. 25,2% were “Amino acids” or metabolites related to “Amino acid metabolism”, while 4,9% were “Nucleotides or Purines”. Similarly, the most abundant metabolites were “Lipids” (36,4%), “Amino acid/Amino acid metabolism” (29,7%) and “Nucleotides/Purines” (10,3%) in WATi, whereas in soleus samples also “Lipids” represented the largest class of metabolites (42,7%), followed by “Amino acid/Amino acid metabolism” (24,6%) and “Nucleotide/Purines” (8,9%).

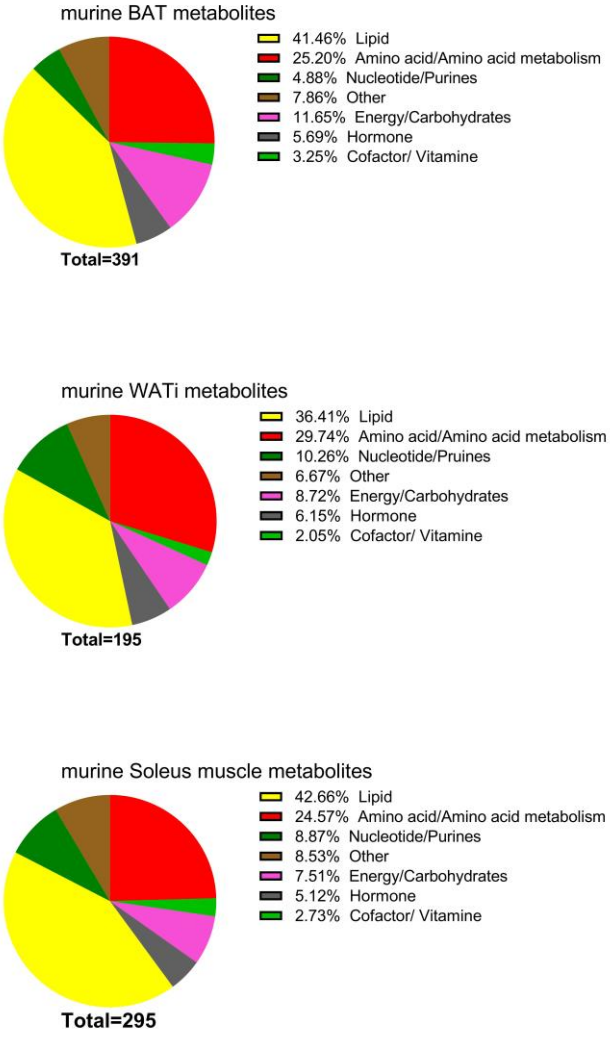

Figure 10: Classification of detected metabolites in BAT, WATi and Soleus Metabolomics

4.1.1. Untargeted Metabolomics of murine brown adipose tissue from young and old mice

4.1.1.1. Effects of aging on the BAT metabolome

First the influence of aging on the metabolome of murine BAT was analysed (Figure 11). For this, samples from young and old BAT were compared.

In order to better identify the distribution and relation of the samples from young and old BAT, Principal Component Analysis (PCA) was performed. PCA allows the visualisation of clusters, patterns and trends in data sets. It is a dimensionality reduction technique that transforms a high-dimensional data set into a lower-dimensional space but retains most of the variation (Ringnér, 2008). It identifies the most informative features, known as principal components, which capture the maximum amount of variance in the data. These principal components are linear combinations of the variables that explain the maximum variance of all the variables (Greenacre et al., 2022). By this, one sample can be

represented by a few numbers instead of by thousands of variables (Ringnér, 2008). The data can then be plotted and each data point represents one individual sample. Proximity of data points means high similarities, whereas a great distance means a great variance between the data sets.

Each data point represents one sample/one individual. The blue points depict old BAT; the green young BAT. The circles around the data points show the correlation between the samples. PCA showed that samples cluster to each other according to age, resulting in the formation of two opposing clusters (Figure 11 A). This means that young/old BAT samples showed a high similarity within their sample groups. On the other hand, PCA showed a great variance between young and old samples. PCA also showed that the variance within the sample group is greater in the old group, than in the young group.

Volcano Plot Analysis (VP) was used visualize significant changes in the individual metabolites' abundancies. In this type of analysis, the x-axis represents the magnitude of change and the y-axis represents the statistical significance of the change: metabolites displayed in the outer right or left region show a high fold changes. Metabolites in the upper region of the graph show a high significance. VP showed 69 significantly upregulated metabolites in old BAT compared to young BAT, which were mainly classified as "amino acids/amino acid metabolism" (36/69) (Figure 11 B,C). Of these 69 metabolites, the dipeptide aspartylphenylalanine was by far the most significantly upregulated. 3-phosphoglyceric acid, anserine and carnosine were three other highly regulated metabolites standing out (Figure 11 B).

Aspartylphenylalanine and carnosine (alanyl-L-histidine) are both β-dipeptides which were already identified in human plasma and urine (Burton et al., 1989). The source of these small peptides might be directly by ingestion or the breakdown of ingested proteins, or a de novo synthesis from e.g. asparagine and phenylalanine. Like carnosine, anserine is a histidine-containing dipeptide and a methylated derivative of carnosine (Boldyrev et al., 2013). Carnosine and anserine are highly abundant in skeletal muscle and nervous system of, especially long-lived, mammals (Hipkiss et al., 2002). Many studies on carnosine and anserine have been conducted in SKM which describe several potential physiological roles: antioxidant function, regulator of excitation-contraction coupling by the regulation of calcium release from the SR, and a provider of extracellular histidine and histamine (Boldyrev et al., 2013). Some studies also report anti-aging effects of carnosine: Yuneva et al., report that the carnosine-supplementation of senescence-accelerated mice can increase life span by 20% (Yuneva et al., 1999). These beneficial effects could be explained by its function as an antioxidant and modulator of the degradation of aged protein (Hipkiss et al., 2002). So far only little is known about the role of carnosine and anserine in BAT. An effect on sympathetic nerve activity is under discussion (Tanida et al., 2007).

Furthermore, VP showed 55 significantly downregulated metabolites in old mice compared to young mice, which were mainly lipids (30/55) (Figure 11 B,C). Of these metabolites, oleoylethanolamide (OEA), Linoleoylethanolamide (LEA) and sphingosine-1-phosphate (S1P) were the most strongly downregulated metabolites with high significance.

OEA and LEA are both n-acylethanolamides (NAE) and endocannabinoid like lipids (Brown et al., 2017; Tovar et al., 2023). OEA is a well described PPAR-α activator which reduces food intake by promoting satiety, but may also regulate feeding and metabolism via the dopamine or endocannabinoid signalling system (Brown et al., 2017). LEA is the most common NAE in nutrients and was found to be increased in serum levels of overweight humans. An administration of LEA to rats receiving cafeteria or standard diet, showed a weight loss and reduction in circulating cholesterol and triglycerides. Furthermore, LEA could reduce inflammatory markers like IL-6 and TNFα (Tovar et al., 2023). OEA and LEA might therefore be potential contributors to improved lipid metabolism.

S1P is a lysophospholipid and breakdown product of ceramide metabolism, which is mainly found in the blood and lymph (Hla et al., 2008). S1P can be secreted by different transporters and highly influences the vascular and immune system by i.e. angiogenesis and vascular permeability, the regulation of T-, B- and dendritic cell trafficking, and cell proliferation and cytokine expression (Hla and Dannenberg, 2012; Proia and Hla, 2015). Kowalski et al., showed upregulated S1P levels in the serum of obese mice, as well as in the serum of obese humans. They also demonstrated a positive correlation between S1P levels and metabolic abnormalities like BMI, body fat percentage or cholesterol levels (Kowalski et al., 2013). In murine BAT, S1P, together with its transporting apolipoprotein apoM, is as well discussed as a negative regulator of BAT activity, BAT mass and lipid turnover (Christoffersen et al., 2018; Gohlke et al., 2019). However just recently, Borup et al. could show a positive correlation between BAT activity and cold-induced changes in apoM but not S1P plasma levels of humans (Borup et al., 2022). Moreover, sphingolipids, of which S1P is a metabolite, were found to be induced in aged BAT (Gohlke et al., 2019).

Of the total number of 351 metabolites detected, abundance of 227 was not significantly changed between both groups.

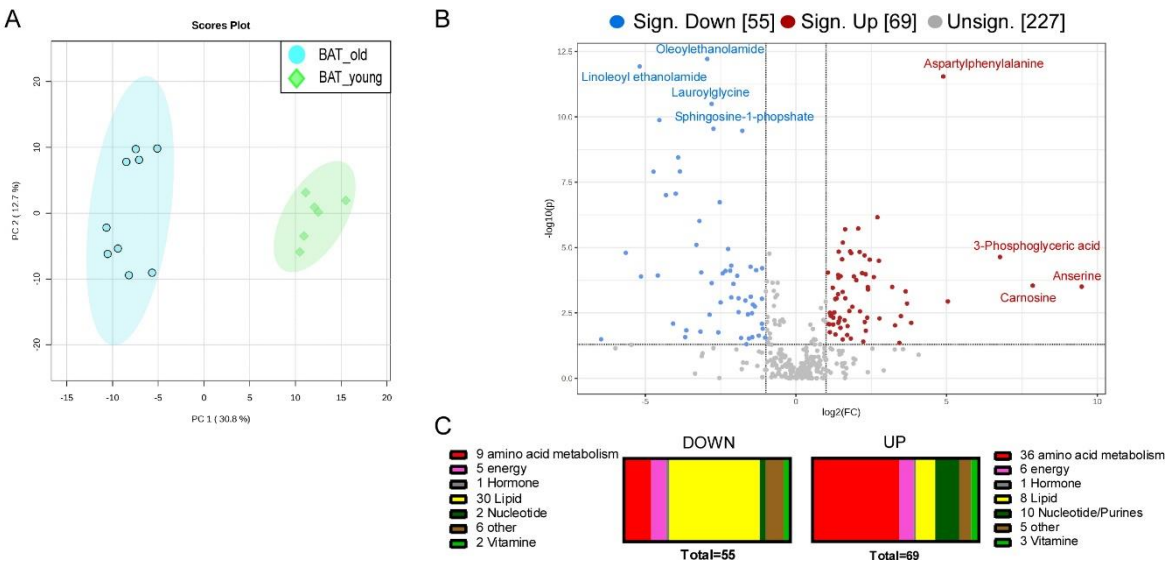

Figure 11: Analysis of young vs. old BAT metabolomics: A: PCA Analysis of young and old BAT B: Volcano Plot of old vs. young BAT metabolomics C: Classification of significantly up- and downregulated metabolites in old vs. young BAT

Quantitative Enrichment Analysis (QEA) was used to assess the over- or underrepresentation of specific pathways within the metabolomics data set. The metabolite abundancies are linked to biological pathways, to highlight potential functional changes. QEA of old and young BAT metabolomics showed the most changes in “Sphingolipid metabolism”, “Glutathione metabolism” and “Valine, leucine and isoleucine biosynthesis” (Figure 12 A). In Sphingolipid metabolism, the top three metabolites were S1P, sphinganine and 3-ketosphingosine, which were all downregulated in old BAT in comparison to young BAT.

In contrast, the top three regulated metabolites connected to “Glutathione metabolism”, glycine, ornithine and glutamic acid were all significantly upregulated. For “Valine, Leucine and Isoleucine Biosynthesis” the three top regulated metabolites were the amino acids leucine, isoleucine and valine. Leucine and isoleucine were both significantly upregulated in old BAT, whereas valine was significantly downregulated in old BAT compared to young BAT (Figure 12 B-D). Glycine, ornithine, glutamic acid, leucine, isoleucine and valine are all amino acids. Glycine, ornithine and glutamic acid are nonessential amino acids, which can be biosynthesized. Leucine, isoleucine and valine on the other hand, are essential amino acids and together form the group of branched-chain amino acids (BCAA). All mentioned amino acids, except ornithine, are proteinogenic amino acids (Lopez and Mohiuddin, 2023). Apart from these five mentioned amino acids, many more belonged to the group of significantly upregulated metabolites in old BAT compared to young BAT. As already described, amino acids or metabolites from amino acid metabolism represented the biggest class of upregulated metabolites in old BAT group (Figure 11 C). BCAA function as nutrient signal and modulate food intake through central signalling in the hypothalamus but also via leptin production in adipocytes (Roh et al., 2003; Lynch et al., 2006). Moreover, BCAA blood levels were shown to be elevated in obese humans and rats, and are

considered to be a predictor of the incidence of type 2 diabetes (Felig et al., 1969; Rafecas et al., 1991; Wang et al., 2011). Kuroiwa et al. analysed plasma samples from young to aged donors and found an age, BMI and body fat percent related upregulation of Glutamate (amongst other amino acids) (Kuroiwa et al., 2021). In BAT, BCAA are utilized in the mitochondria to drive thermogenesis. A defect in BCAA catabolism on the other hand, impairs BAT fuel oxidation and thermogenesis (Yoneshiro et al., 2019) The higher levels of leucine and isoleucine in old BAT might be due to impaired uptake and catabolism of these amino acids.

Together these data showed that young and old BAT clearly differ in their metabolic profiles of secreted metabolites. Especially amino acids and amino acid metabolites, but also small peptides were among the top upregulated metabolites in old samples. On the other hand, a profound downregulation of lipids like fatty acid-ethanolamides or sphingolipids were observed in the old samples.

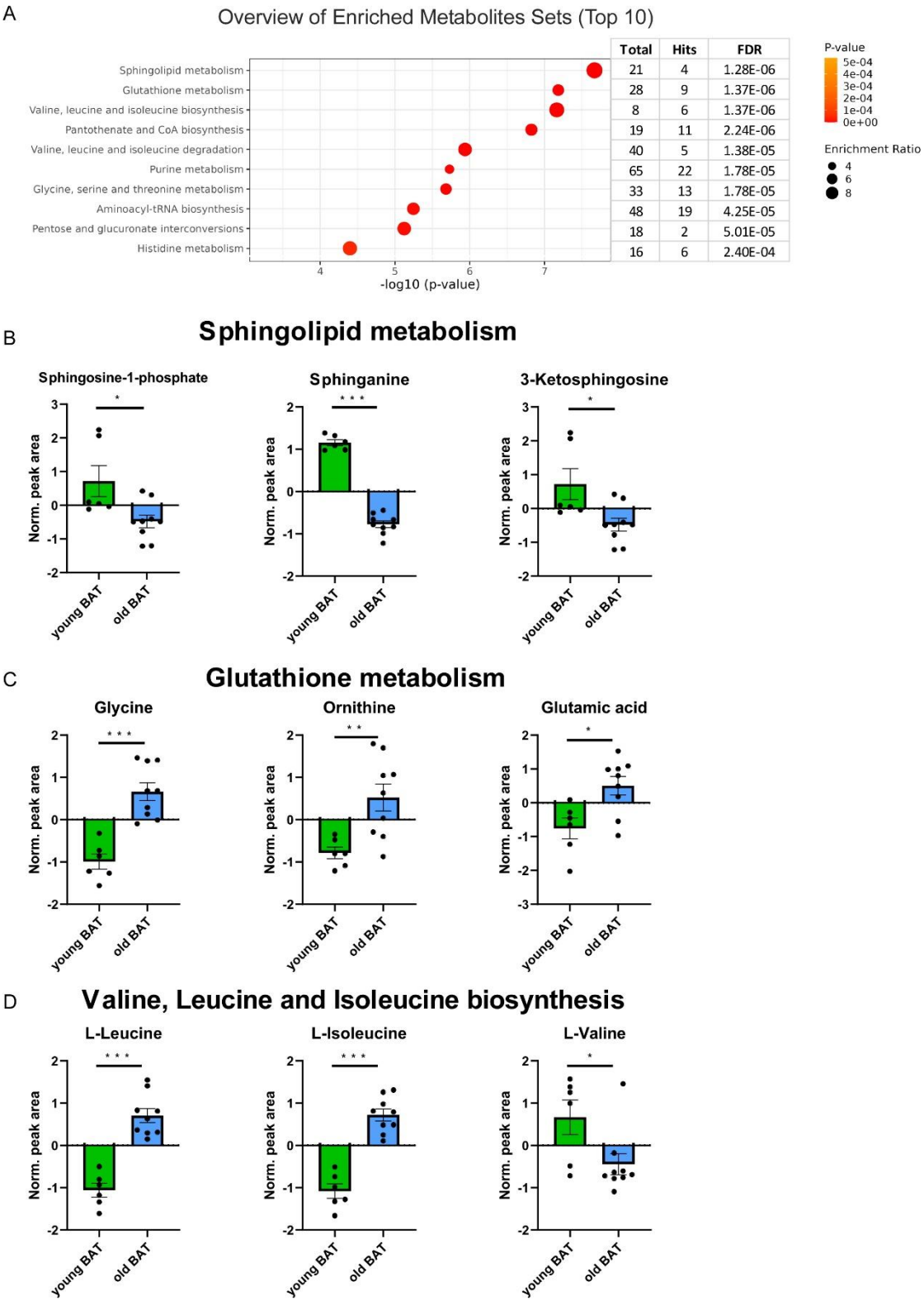

*Figure 12: Quantitative Enrichment Analysis of age-related changes in the metabolome of young and old BAT. A QEA showing enriched pathways sets in the metabolome of young versus old BAT. B-D: Top three enriched metabolites from the top three altered pathway sets; young BAT: n=6; old BAT: n=9; Normalised peak areas are represented as mean ± SEM, unpaired t-test, *p≤0.05, **p≤0.01, ***p≤0.001*

4.1.1.2. Effects of cAMP stimulation on BAT metabolome

Next, the effect of cAMP stimulation on the BAT secretome was analysed. While PCA revealed a distinct subcluster formation in the young group (Figure 13 A), samples from old mice treated with or without FSK showed almost complete overlap (Figure 13 C). This indicates that cAMP stimulation of young BAT, but not old BAT, causes a high variance in the data set implying a great effect of the acute stimulation on the secretome. VP showed 22 significantly up and 6 significantly downregulated metabolites in the young stimulated samples. 323 metabolites remained unchanged (Figure 13 B). In BAT from old mice, 12 metabolites were significantly upregulated and 3 significantly down; 340 metabolites were not significantly changed (Figure 13 D). Overall, cAMP stimulation caused a rather modest downregulation (with regard to fold change) of metabolites in both BAT from young and old mice, while several metabolites were strongly increased in both groups upon cAMP treatment. Those metabolites were mainly glucocorticoids/steroid hormones like estradiolacetate, estroneglucuronide, 19-hydroxytestosterone or androstenedione but also lipids like prostaglandin E3 or butenylcarnitine.

Estradiolacetate and estroneglucuronide are metabolites of the C18-steroids estradiol and estrone. 19-hydroxytestosterone and androstenedione are metabolites of the C19-steroid testosterone. Sex steroid hormones are usually produced by the gonads or adrenal gland but other organs, like the adipose tissue has been shown to express enzymes involved in steroid hormone biosynthesis as well (Wierman, 2007). BAT mass and function and the responsiveness to cold differ according to sex: for example, female rodents show a higher amount and higher prevalence of active BAT and female rats display higher amounts of UCP1 and larger mitochondria. Therefore, it seems likely, that these effects are mediated by steroid hormones (Law et al., 2014; Kaikaew et al., 2021). Furthermore, estradiol and progesterone were shown to reduce BAT thermogenic activity in rats and inhibit NE-mediated UCP1 increase in murine BA (Quevedo et al., 1998). Additionally, steroid hormones can act in a crosstalk together with glucocorticoids (Kaikaew et al., 2021). Glucocorticoids (GC) are usually secreted from the adrenal cortex under the influence of the hypothalamic-pituitary-adrenal axis and regulate numerous processes like cellular growth and development but also the response to stress or energy metabolism (Macfarlane et al., 2008). In rodents, GCs are known to suppress BAT activation and chronic high levels of GCs in humans can cause obesity, type 2 diabetes or dyslipidemia (Larson, 2019). But the effects might be highly species-specific: Ramage et al. demonstrated that in humans the GC prednisolone could acutely increase BAT activity and energy expenditure during cold exposure in vivo and lead to an increase in isoprenaline-stimulated respiration and UCP-1 in vitro. But in a murine in vitro model prednisolone decreased isoprenaline-stimulated respiration (Ramage et al., 2016).

Prostaglandins (PG) like prostaglandin E3 are eicosanoids, which are synthesized from the membrane lipid arachidonic acid via the cyclooxygenase COX-1 or COX-2. Prostaglandins can be synthesized in all cells, except red blood cells, and affect practically all major body systems (Miller, 2006). PGI2, PGE2, and $PGF_{2\alpha}$ are already known PGs produced by the adipose tissue (Maurer et al., 2019). Vegiopoulos et al. showed, that adrenergic stimulation can increase COX-2 mRNA levels and the secretion of PGE2 and PGI2, accompanied by the induction of a BAT-like phenotype in murine WAT (Vegiopoulos et al., 2010). PGE2 itself increases calcium concentrations and oxygen consumption in rat BAT and the activation of its receptor EP4 can improve glucose tolerance and insulin resistance and have anti-inflammatory effects in obese mice (Nagai et al., 1996; Yasui et al., 2015).

Together these data show that cAMP stimulation of young BAT led to larger changes in the metabolome compared to old BAT. Despite that, the significant upregulation of hormones and eicosanoids in both young and old BAT might indicate that the production or secretion of those metabolites might be conserved throughout aging. These secreted metabolites could in turn affect neighbouring cells or could be released into the blood stream to influence peripheral organs.

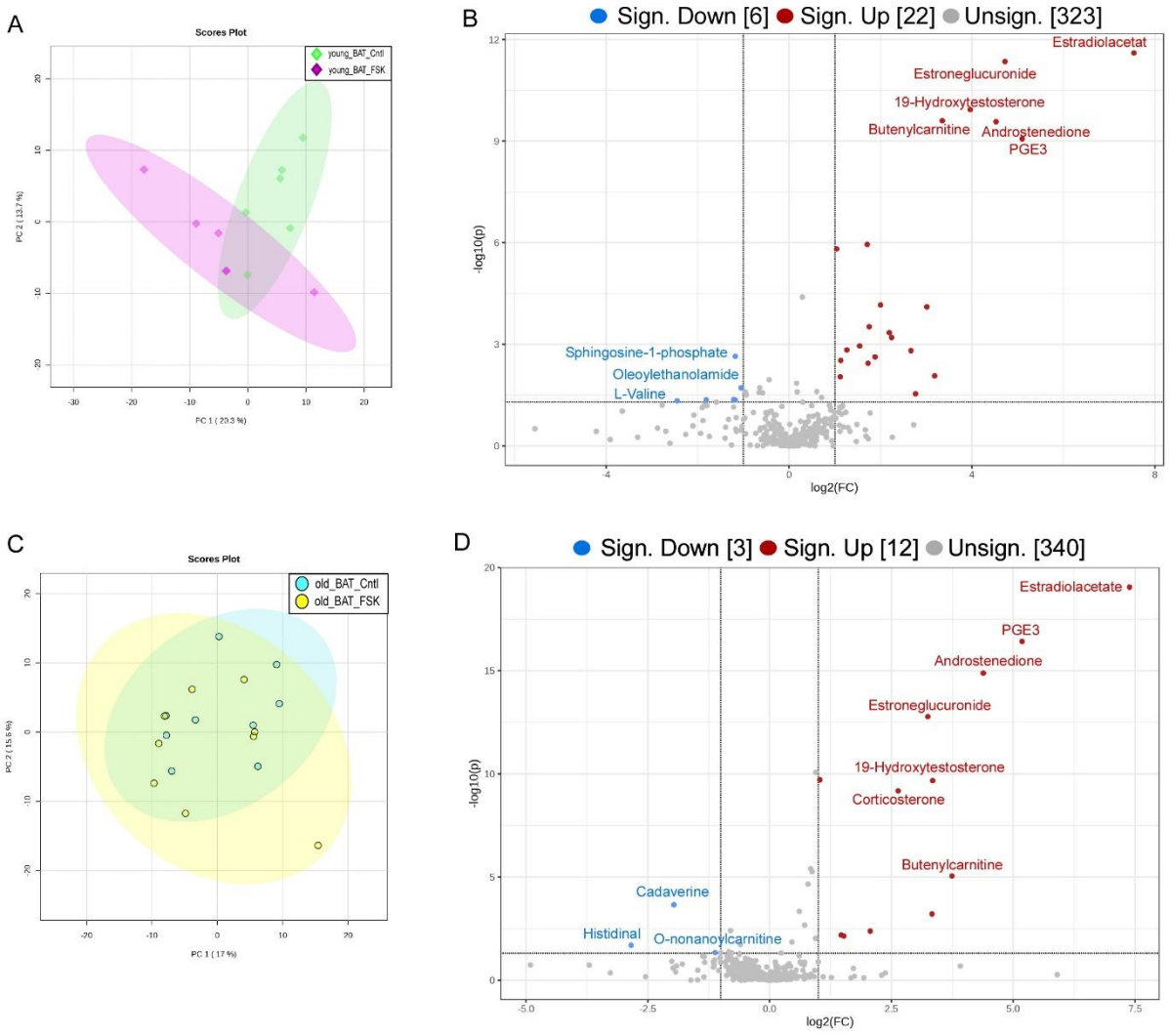

Figure 13: Effects of cAMP stimulation on the BAT secretome of young and old mice A: PCA and B: VP of young BAT after FSK treatment. C, D: PCA and VP of old BAT after FSK treatment.

QEA of untreated vs. treated young and old BAT was performed to study the effect of cAMP stimulation on biological processes. The metabolomics data from untreated samples were compared to data from samples with FSK stimulation and linked to pathway sets.

QEA of young BAT showed that cAMP stimulation induced the strongest changes in “Steroid hormone biosynthesis”; followed by “GPI-anchor biosynthesis” and “Riboflavin metabolism” (Figure 14 A). In “Steroid Hormone biosynthesis” 12 metabolites were up- or downregulated. The changes in “GPI-anchor biosynthesis” and “Riboflavin metabolism” revealed FDR values >0.1 which indicates a higher likelihood of mistakenly identified enriched pathways when they are not truly significant.

To analyse whether the metabolites were down- or upregulated, the most significant hits were analysed in detail. In addition to VP analysis, these data showed that the stimulation of young BAT with FSK led to significant increases in metabolites from “Steroid hormone biosynthesis”. For example, corticosterone, estroneglucuronide and 19-hydroxytestosterone were significantly increased after

cAMP stimulation (Figure 14 B). Even though “GPI-anchor biosynthesis” and “Riboflavin metabolism” did not meet the statistical criteria for QEA, the associated metabolites 6-α-glucosaminyl-1D-myo-inositol and riboflavin were significantly upregulated after stimulation (Figure 14 C,D). UDP-acetylglucosamin was not significantly changed by FSK treatment. Interestingly, like in QEA of young compared to old BAT, QEA from young unstimulated and stimulated BAT also showed BCAA metabolism among the enriched pathways. Analysis of BCAA showed increased abundance of leucine and isoleucine in young BAT after cAMP stimulation, whereas valine levels were reduced. However, these effects did not reach statistical significance (Figure 14 E).

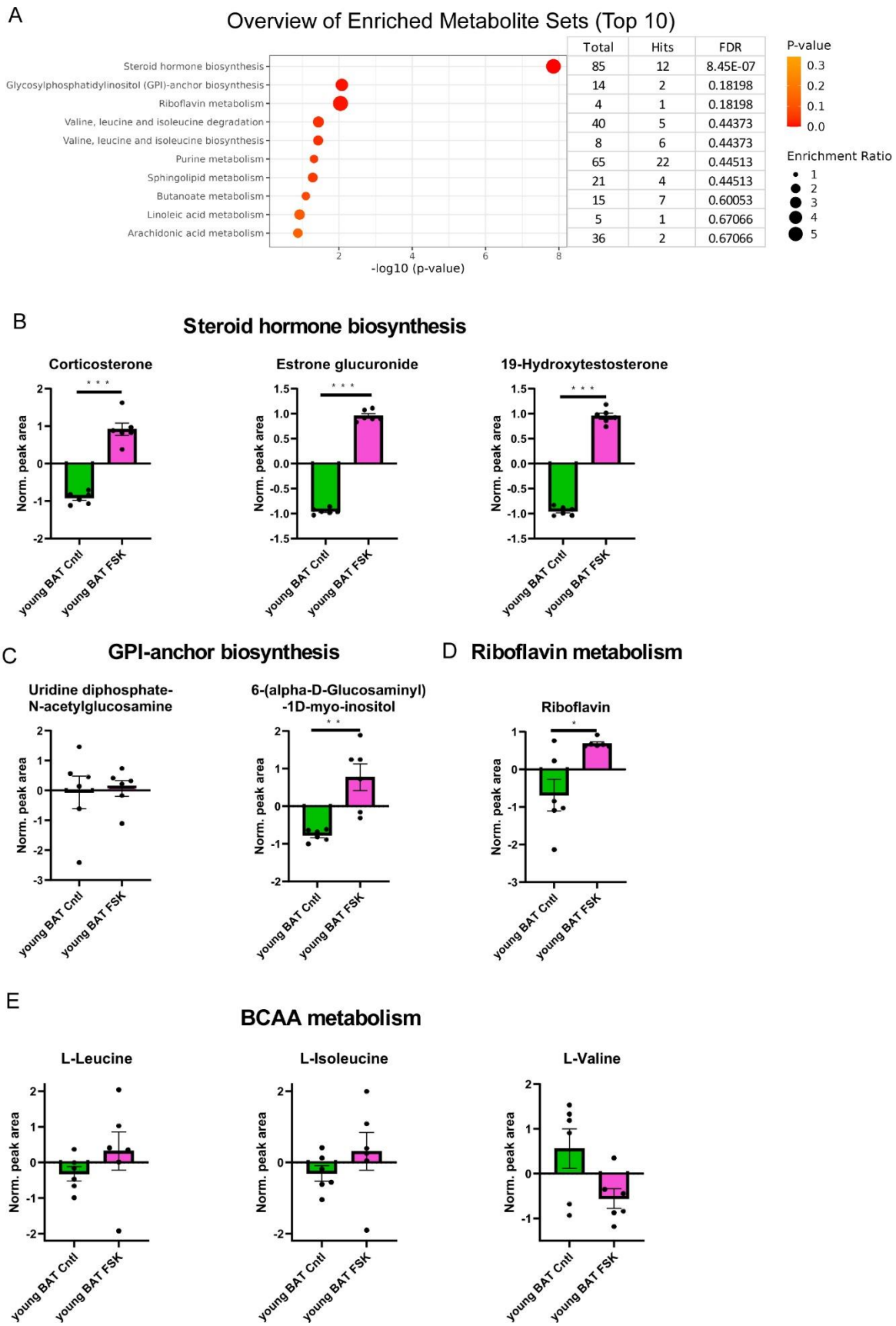

*Figure 14: Analysis of the effect of cAMP stimulation on the enrichment of biological processes in young BAT. A: QEA of unstimulated and stimulated young BAT B-E: Top enriched metabolite hits for the top enriched pathway sets. Normalised peak areas are represented as mean ± SEM, unpaired t-test, *p≤0.05, **p≤0.01,***p≤0.001. n=6.*

To analyse which metabolites/biological signalling pathways were enriched in old BAT stimulated with FSK, QEA was performed as well. The two pathways which met a FDR<0.1 were “Steroid hormone biosynthesis” and “Sphingolipid metabolism”. In “Steroid hormone biosynthesis” 12 metabolites were altered; while 4 were detected in “Sphingolipid metabolism” (Figure 15 A).

In line with VP analysis from old unstimulated and stimulated BAT, QEA showed an upregulation of metabolites from “Steroid hormone biosynthesis”. FSK stimulation led to a marked increase in the abundancies of before mentioned steroids like corticosterone, androstenedione and 19-hydroxytestosterone (Figure 15 B). Noteworthy, S1P was found to be significantly increased after FSK stimulation, which is opposite to the effect observed when comparing young to old BAT (cf. Figure 12 A). 3-dehydrosphingosine and sphinganine were decreased due to cAMP stimulation, albeit not significantly (Figure 15 C). Interestingly, adipocyte sphinganine levels have been shown to be increased in obese individuals (Blachnio-Zabielska et al., 2012).

QEA also revealed “Glutathione metabolism” to be altered due to cAMP stimulation in old BAT: Glutathione (GSH) was decreased significantly; glutamate and glutamylcysteine were decreased as well, even though not significantly (Figure 15 D). GSH is a tripeptide composed of glutamic acid, glycine and cysteine and can be synthesized by the two enzymes γ-glutamylcysteine synthase (γ-GCS) and GSH synthase. Together with its antioxidant enzyme glutathione peroxidase (GPX), they represent a major redox system in all cell types. Under oxidative stress, like observed during obesity, this system is induced to detoxify ROS (Kobayashi et al., 2009). In adipose tissue of obese mice, low GPX activity levels but high expression levels of γ-GCS were detected, which resulted in high GSH content. In murine WAT, cold exposure reduces GSH content and in vitro treatment of 3T3L1-adipocytes with GSH led to impaired insulin signalling (Kobayashi et al., 2009). Reduced levels of GSH and its metabolites due to cAMP stimulation could indicate an induction of the antioxidant system towards pro-oxidant conditions. To fuel the higher demand of GSH synthesis, the metabolites glutamate and γ-glutamylcysteine might be used which decreases the abundancies.

Together these data showed that in young as well as in old BAT, cAMP signalling led to significant elevations particularly of metabolites connected to “Steroid hormone biosynthesis”. Moreover, Sphingolipid metabolism was significantly altered in BAT from old mice. In both young and old BAT, FSK stimulation changed the levels of BCAA.

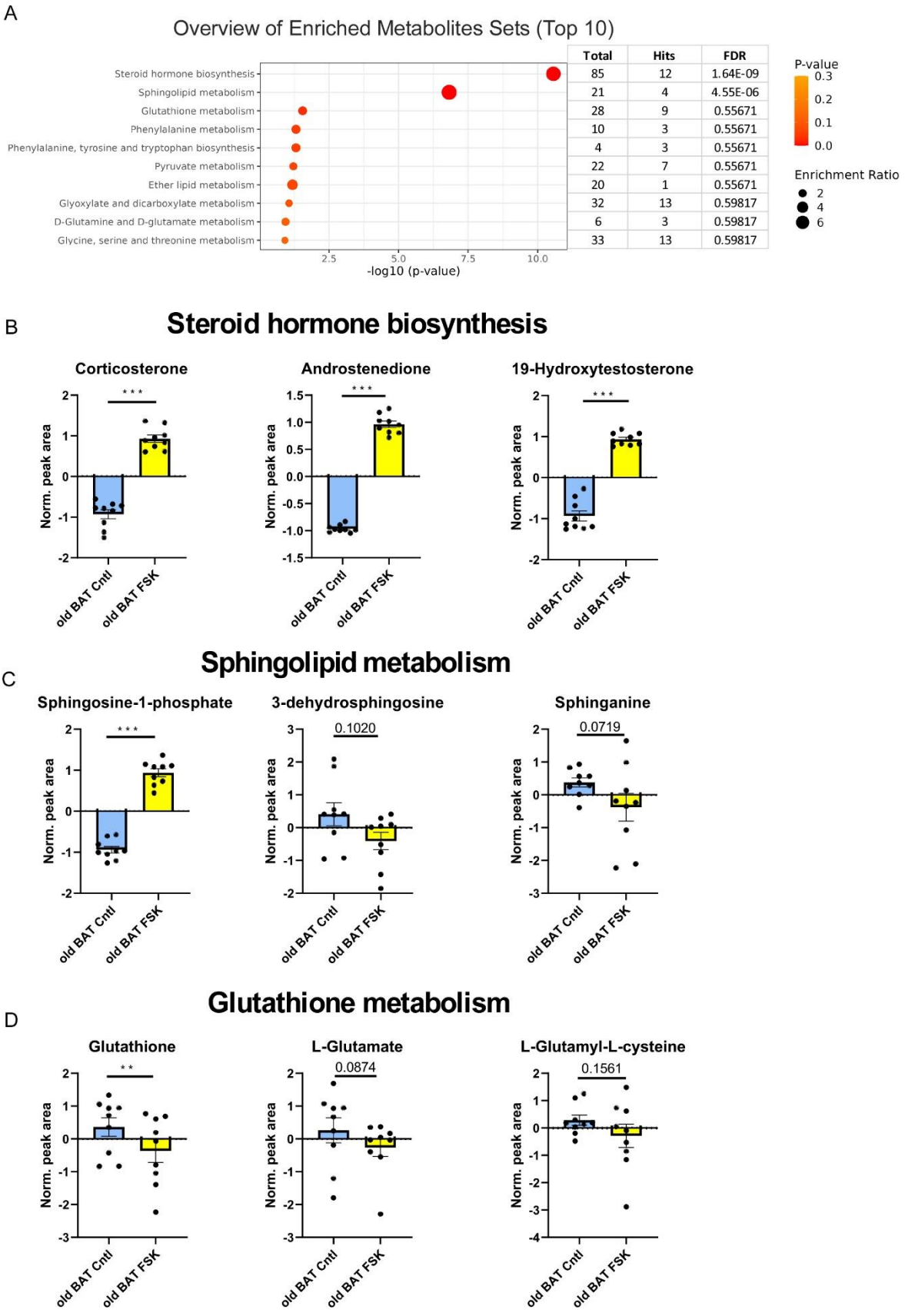

*Figure 15: Analysis of the effect of cAMP stimulation on the enrichment of biological processes in old BAT. A: QEA of unstimulated and stimulated old BAT B-D: Top enriched metabolite hits for the top enriched pathway sets. Normalised peak areas are represented as mean ± SEM, unpaired t-test, *p≤0.05, **p≤0.01, ***p≤0.001. n=9.*

4.1.1.3. Analysis of common and unique metabolites in the secretome of young and old BAT

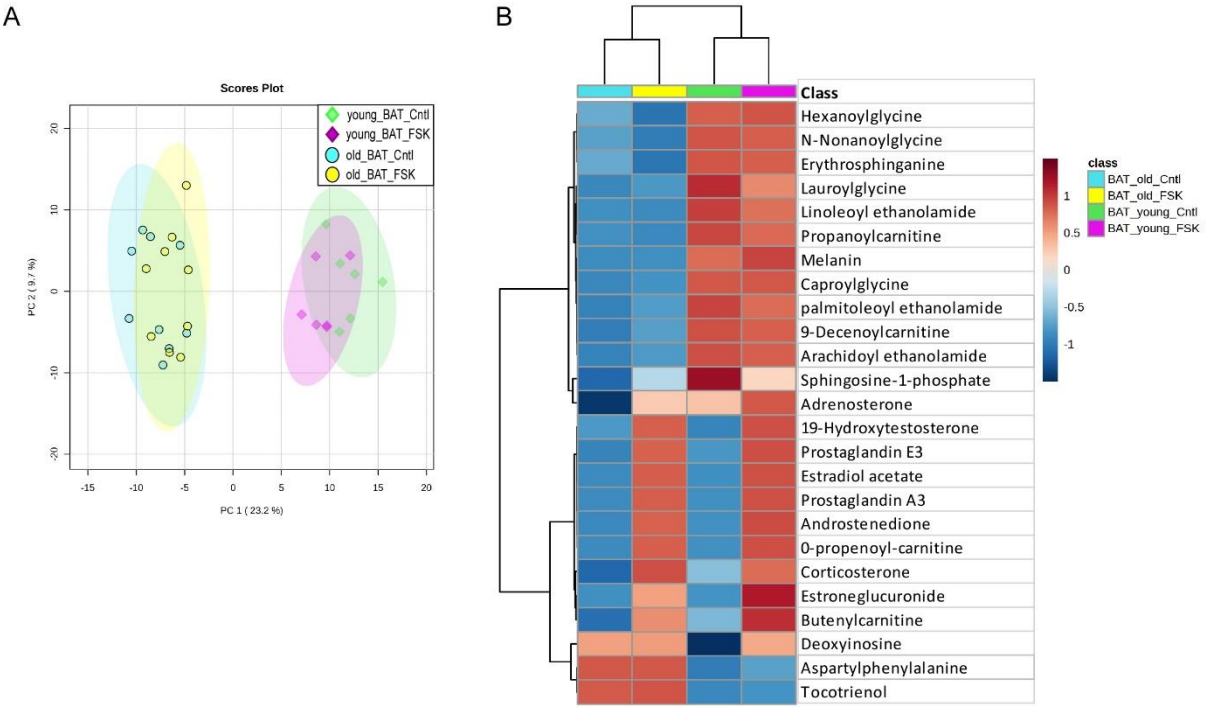

Figure 16: Comparison of all BAT groups: young and old samples with and without FSK. A: PCA of all four groups. B: Heat Map of Top 25 regulated metabolites in all groups

Next, the effect of aging on the BAT secretome was directly compared to cAMP stimulation by a comparison of all groups in one complete data set. Still, PCA showed a clear separation according to age with only minor effects of cAMP stimulation (Figure 16 A), indicating a higher impact of aging on the metabolic profile, rather than the acute stimulation.

Similarly, heat map analysis depicting the top 25 changed metabolites between all groups showed clustering according to age (Figure 16 B). Moreover, a grouping of metabolites which differ according to age could be observed. Notably, four short and medium chain n-acylglycines, hexanoylglycine, caproylglycine, nonaloylglycine and laroylglycine were higher in young than old samples. The acylethanolamide LEA was already among the top downregulated metabolites in old BAT compared to young BAT (cf. Figure 11 B): Here, two additional NEAs palmitoleoylethanolamide and arachidoylethanolamide were shown to be of higher abundancy in the young groups compared to the old groups. N-acylglycines belong to the group of N-acylamino acids which can occur in countless variations of acyl chains attached to an amino acid (Anderson and Merkler, 2017). N-acylamino acids, just like N-acylethanolamides, belong to the class of N-acylamides and show structural similarities with endocannabinoids (Bradshaw et al., 2009). Two well studied acylglycines are n-arachidonoylglycine

and n-palmitoylglycine. N-arachidonoylglycine can have antinociceptive and anti-inflammatory effects; and n-palmitoylglycine is involved in sensory and neuronal signalling (Bradshaw et al., 2009). In relation to BAT, Guijas et al. detected elevated levels of myristoylglycine in the supernatant of cells committed to BA differentiation and further identified it as potential inducer of brown adipocyte differentiation (Guijas et al., 2022). To date, nothing is known about the effects of the above mentioned acylglycines and NEAs, but the pronounced difference in their abundancies between young and old BAT, could imply an important role in BA differentiation and aging.

Vice versa, metabolites like aspartylphenylalanine were found more prominent in old samples. This tripeptide was already identified as one of the top upregulated metabolites in old compared to young BAT (cf. Figure 11 B), but did not alter due to cAMP stimulation. Furthermore, heat map analysis showed ten commonly upregulated metabolites in young and old samples after FSK treatment. Those metabolites were steroid hormones like 19-hydroxytestosterone, estradiolaceate and corticosterone and prostaglandins like PGE3 and PGA3. This was already indicated by VP analysis of young and old BAT after cAMP stimulation (cf. Figure 13 B,D).

To analyse whether there are common or uniquely cAMP-regulated metabolites in young or old BAT, the significantly altered metabolites were compared. Ten metabolites were found to be upregulated in young and old samples after FSK stimulation (Figure 17 A). As expected, these common metabolites were hormones like 19-hydroxytestosterone and corticosterone, but also lipids like PGE3 (Figure 17 C). Further analysis of the normalised peak areas of the commonly upregulated metabolites showed that these metabolites were upregulated with similar intensities (Figure 16 D). There were no shared downregulated metabolites between the experimental groups.

In order to better understand the detailed mechanisms underlying tissue-specific aging, uniquely regulated metabolites are of special interest. 12 metabolites were found to be uniquely upregulated in young BAT, whereas 3 metabolites were unique in old BAT (Figure 17 A). On the other hand 6 metabolites were solely downregulated in young BAT and 3 in old BAT (Figure 17 B).

A

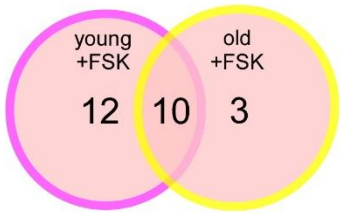

B

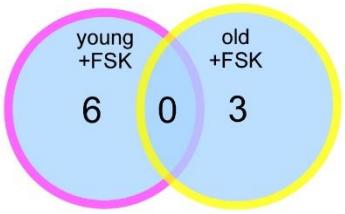

C

	Name
1	19-Hydroxytestosterone
2	Androstenedione
3	Butenylcarnitine
4	Corticosterone
5	Estradiol acetate
6	Estratetraenol
7	Estroneglucuronide
8	O-propenoyl-carnitine
9	Prostaglandin E3
10	Estradiol

D

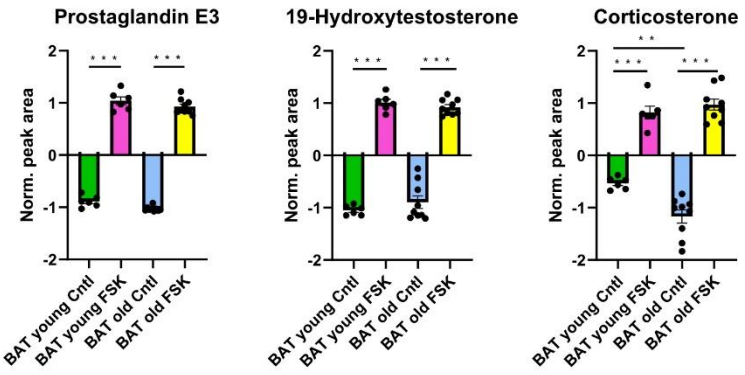

*Figure 17: Comparison of significantly regulated metabolites from young and old BAT. A: Venn Diagramm of shared upregulated; B: Venn Diagramm of shared downregulated metabolites between young and old BAT after FSK treatment. C: Table of 10 shared upregulated metabolites between young and old BAT. D: Normalised peak area of three exemplary shared metabolites between young and old BA. Normalised peak areas are represented as mean ± SEM, one-way ANOVA, young BAT n=6, old BAT n=9, *p≤0.05, **p≤0.01, ***p≤0.001.*

The 18 unique metabolites (12 upregulated, 6 downregulated; Figure 18 A) from young BAT were further analysed. First, the metabolites were linked to biological pathways by performing Overrepresentation Analysis (ORA), which compares a list of compounds with human and mammalian metabolite libraries and identifies enrichment of biological processes.

In young BAT only one pathway was found to be enriched: “Valine, leucine and isoleucine biosynthesis”. The two metabolites ketoleucine and the BCAA L-valine, were linked to this pathway (Figure 18B). Interestingly, ketoleucine is an initial metabolite of BCAA leucine which regulates BAT thermogenesis (Yoneshiro et al., 2019). Moreover, it has been shown to increase the expression of Sirt1, which is a well described regulator of lipid and glucose metabolism (Bruckbauer and Zemel, 2011). As already described in section 4.1.1.1. and 4.1.1.2., leucine and isoleucine were upregulated in old BAT compared to young BAT, and elevated after cAMP stimulation in young BAT. ORA of the unique metabolites from young BAT further indicates BCAA levels to be affected by aging and stimulation of BAT.

ORA only revealed one statistical significant biological process to be associated with the unique metabolites from young BAT. Therefore, the metabolites were analysed individually: the normalised peak areas from young and old BAT with and without FSK stimulation were analysed together to directly compare their abundance. Notably, 7/12 of the significantly upregulated metabolites in young

BAT were of low abundancy under basal conditions when compared to old BAT. However, cAMP stimulation elevated the metabolites to similar levels. The metabolites' abundancies were not changed in old BAT due to the FSK treatment (Figure 18 C). On the other hand, metabolites which were downregulated in young BAT after cAMP stimulation, were of higher abundancy before the treatment in comparison to after the stimulation, but also in comparison to the levels observed in BAT (Figure 18 D).

A

	Name
1	2-Deoxyglucose
2	6-(alpha-D-Glucosaminyl)-1D-myo-inositol
3	L-beta-aspartyl-L-aspartic acid
4	Xanthine
5	Deoxyinosine
6	Glycerol 1-hexadecanoate
7	Carboxyspermidine
8	Ketoleucine
9	N6-Acetyl-L-lysine
10	Isoleucylprolylisoleucine
11	19-Hydroxy-PGE2
12	Riboflavin
1	Oleoylethanolamide
2	Sphingosine-1-phosphate
3	5-Methylcytosine
4	PC(14:0/16:1(9Z))
5	3-Methylglutarylcarnitine
6	L-Valine

B

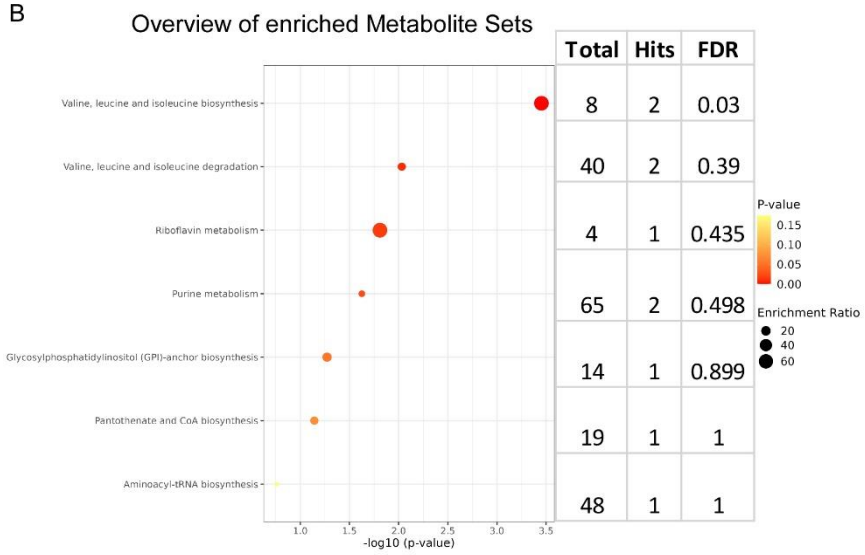

	Total	Hits	FDR
Valine, leucine and isoleucine biosynthesis	8	2	0.03
Valine, leucine and isoleucine degradation	40	2	0.39
Riboflavin metabolism	4	1	0.435
Purine metabolism	65	2	0.498
Glycosylphosphatidylinositol (GPI)-anchor biosynthesis	14	1	0.899
Pantothenate and CoA biosynthesis	19	1	1
Aminoacyl-tRNA biosynthesis	48	1	1

C

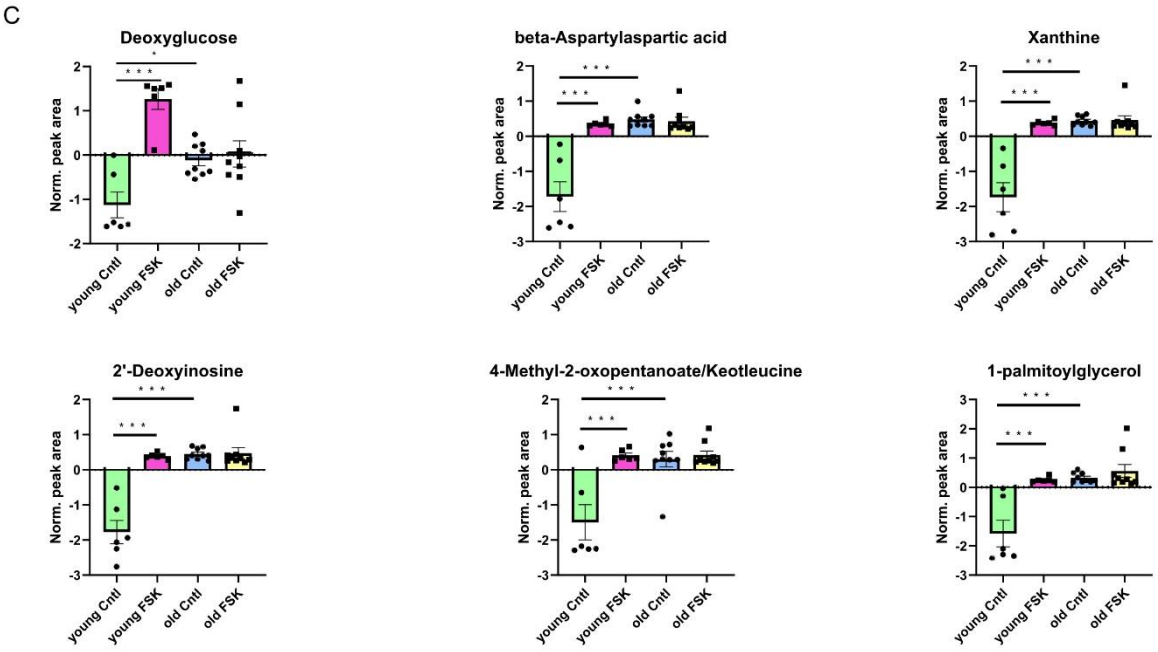

D

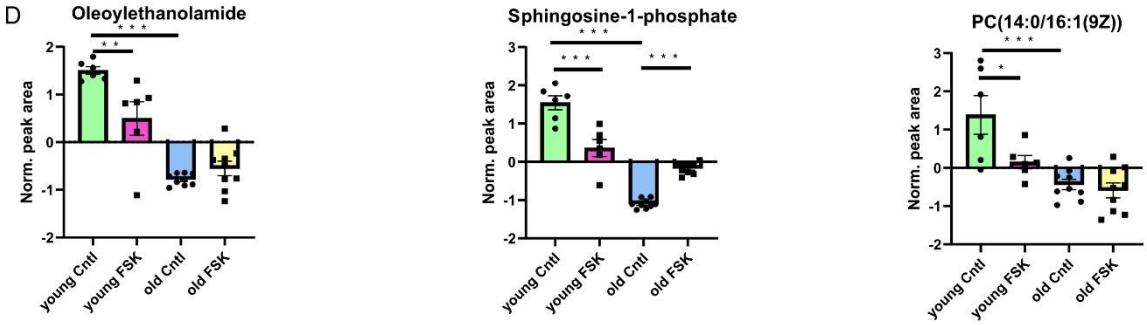

*Figure 18: Analysis of unique metabolites from young BAT after FSK stimulation A: Table with all metabolites which were significantly up or downregulated after FSK stimulation of young BAT B: QEA of unique metabolites from young BAT. C: normalised peak area of 6 of 12 significantly up regulated metabolites. D: normalised peak area of 3 uniquely downregulated metabolites in young BAT. Normalised peak areas are represented as mean ± SEM, one-way ANOVA, young BAT n=6, old BAT n=9, *p≤0.05, **p≤0.01, ***p≤0.001*

4.1.2. Untargeted Metabolomics of murine white adipose tissue from young and old mice

4.1.2.1. Influence of aging on WAT metabolome

White adipose tissue is well known to secrete a multiplicity of factors, including lipids and proteins and is a known regulator of systemic energy homeostasis. Therefore, alongside to BAT, inguinal WAT from young and old mice were analysed.

Initial PCA, showed a separation according to age, even though not as clear as in BAT (Figure 19 A). Nonetheless, the separation indicates distinct metabolome profiles. VP analysis revealed 20 metabolites to be significantly up and 38 metabolites to be significantly downregulated in old vs young WATi samples (Figure 19B), whereas zhe abundancies of 127 metabolites showed no significant changes. 8/20 upregulated metabolites were amino acids or linked to amino acid metabolism; the majority of downregulated metabolites (18/38) were lipids (Figure 19 C).

Among the most prominent upregulated metabolites were acetylphenylalanine, 3-hydroxydodecanoylcarnitine, aspartylphenylalanine and anserine. Interestingly, aspartylphenylalanine and anserine were upregulated in old BAT as well. Acetylphenylalanine is an amphiphatic metabolite of phenylalanine and classified as a uremic toxin. Uremic toxins are endogenous metabolites that can cause damages in the kidney, in neurons and in the cardiovascular system, if they accumulate in the body (Okajima et al., 1985). The elevated abundance of aspartylphenylalanine and acetylphenylalanine could result from increased protein degradation and insufficient clearance in old WAT compared to young WAT. So far nothing is known about direct effects of the two amino acid metabolites on white adipose tissue function. Strikingly, anserine was found to be elevated in both old WATi and BAT. Anserine is a highly abundant dipeptide which was already detected in adipose tissue and can have antioxidant effects, as already described in section 4.1.1.1. (Heidenreich et al., 2021). Increased levels of anserine in aged tissues might indicate a higher demand for antioxidant reagents to counteract increased ROS levels.

Two noticeable downregulated metabolites were oleamide and D-myo-inositol-cyclicphosphate. Oleamide is a fatty acid amide of oleic acid and shows structural similarities with endocannabinoids. It is known for its role in sleep regulation and has analgesic and cannabinoid-like effects (Hiley and Hoi, 2007). Oleamide was shown to interact with multiple targets like the cannabinoid receptor CB1, the serotonin receptors 5-HT_{1A}, 5-HT_{2A}, and 5-HT_{2C}, several ion channels or the modulation of GABA. Furthermore, it can induce hypothermic effects which could also influence adipose tissue metabolism (Hiley and Hoi, 2007). Strikingly, downregulated levels of fatty acid amides were as well detected in old BAT (cf. Figure 11). Possibly, aging could affect fatty amide metabolism in both BAT and WATi and contribute to increased fat mass and impaired metabolic parameters.

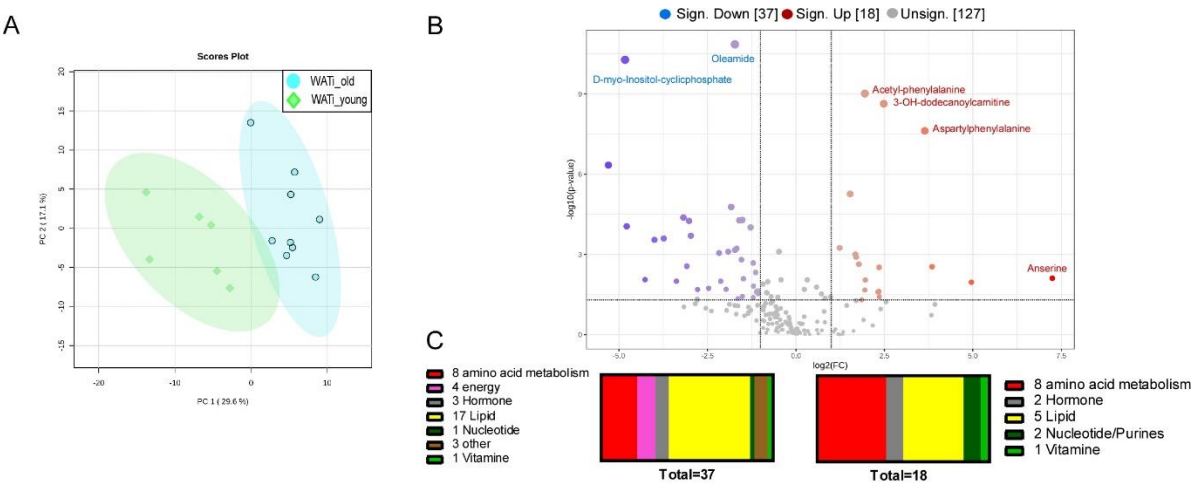

Figure 19: Analysis of young vs. old WATi metabolomics. A: PCA Analysis of young and old WATi. B: Volcano Plot of old vs. young WATi metabolomics C: Classification of significantly up- and downregulated metabolites in old vs. young WATi.

Similar as described for BAT, QEA was performed to link the changes of metabolites to biological processes. Interestingly, different pathways than in BAT were enriched in old compared to young WATi. The top enriched pathways were “Biosynthesis of unsaturated fatty acids”, “Taurine and hypotaurine metabolism” and “Nicotinate and nicotinamide metabolism” (Figure 20 A). The monounsaturated omega-9 fatty acid oleic acid and the saturated fatty acid (SFA) stearic acid were found to be significantly upregulated in old WAT. On the contrary, the polyunsaturated FAs α-linolenic acid and docosahexaenoic acid were significantly decreased in old WATi compared to young WATi (Figure 20 B). It is well known that aging *per se* is a risk factor for the accumulation of fat and the development of insulin resistance (Picard and Guarente, 2005). Palmitic acid and stearic acid are abundant FAs in human tissues and are known for their proinflammatory potential (Jamar and Pisani, 2023). Higher levels of stearic acid have been detected in patients suffering from obesity or type 2 diabetes. Both stearic and palmitic acid can lead to the induction of leptin gene expression and its secretion. On the other hand the polyunsaturated FA docosahexaenoic acid reduces the secretion of proinflammatory cytokines like Il-6 and TNF-α of macrophages (Jamar and Pisani, 2023). Increasing age is known to be associated with an imbalance between de novo fatty acid synthesis and the uptake of FFA into the adipocytes. This might explain the higher abundancy of long-chain fatty acids in old WATi (Picard and Guarente, 2005).

The second most enriched pathway was “Taurine and hypotaurine” metabolism. Here, two metabolites were found to be changed of which only hypotaurine was significantly decreased in old WATi (Figure 20 C). Hypotaurine is a precursor of the semi-essential micronutrient taurine, which is one of the most abundant amino acids in humans and other eukaryotes (Singh et al., 2023). Recently,

taurine blood levels were found to be inversely correlating with increasing age and the supplementation of this micronutrient identified as potential supplement to counteract aging (Singh et al., 2023). For “Nicotinate and nicotinamide metabolism” the one significantly changed metabolite was niacinamid, which was reduced in old WATi (Figure 20 D). Noteworthy, niacinamide has been shown to protect against diet-induced weight gain and induces browning of WA (Méndez-Lara et al., 2021).

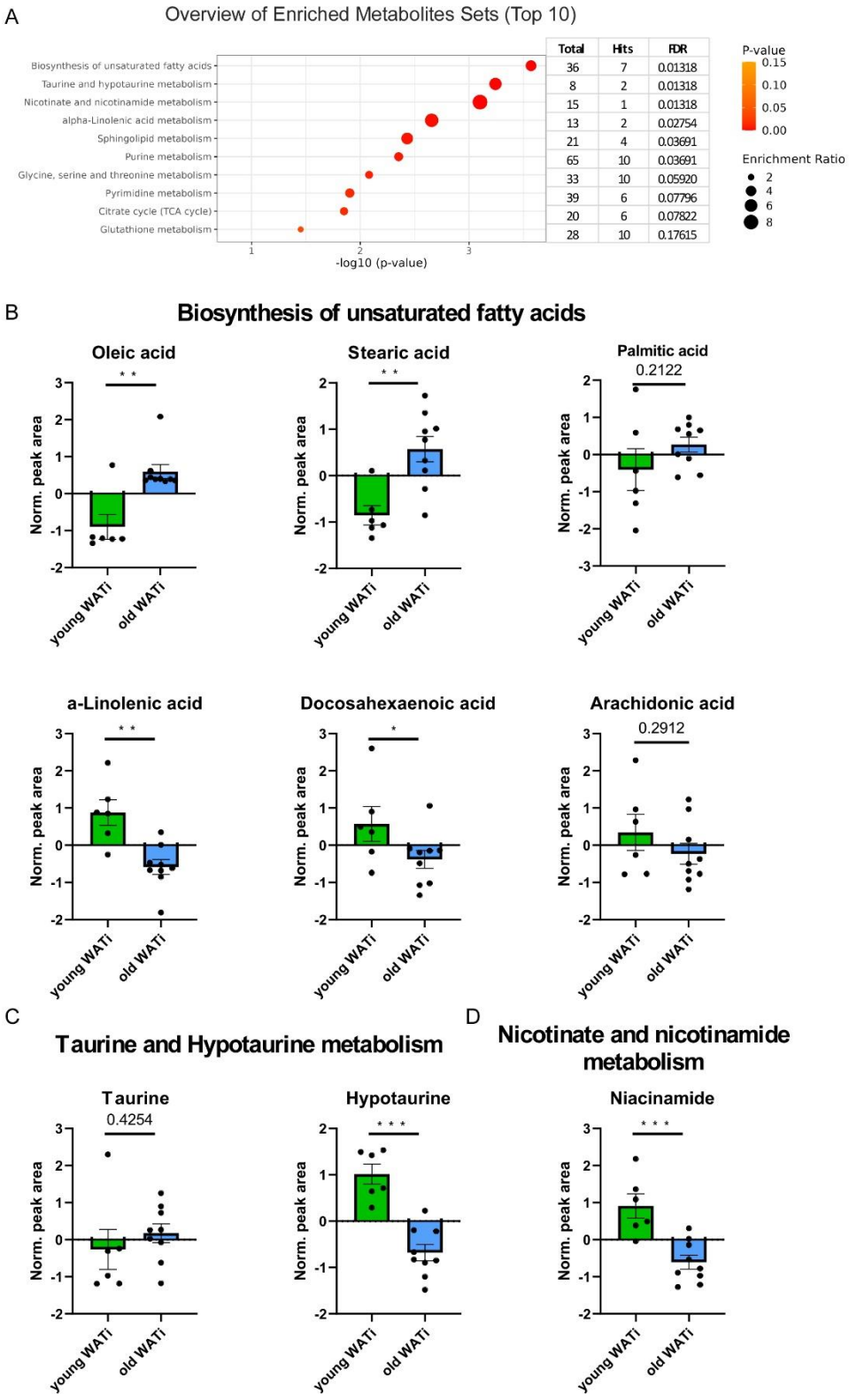

*Figure 20: Quantitative Enrichment Analysis of age-related changes in the metabolome of young and old WATi. A QEA showing enriched pathways sets in the metabolome of young versus old WATi. B-D: Top three enriched metabolites from the top three altered pathway sets; young WATi: n=6; old WATi: n=9; Normalised peak areas are represented as mean ± SEM, unpaired t-test, *p≤0.05, **p≤0.01, ***p≤0.001.*

In summary, metabolomics of young and old WATi revealed pronounced changes in the metabolic profile according age. In total 55 metabolites were significantly changed in old compared to young WATi. These metabolites highly indicate an effect of aging on lipid metabolism. Furthermore, hypotaurine, which is a precursor of the known aging-associated metabolite taurine, was as well found to be reduced in aged WATi.

4.1.2.2. Effects of cAMP stimulation on WATi metabolome

Next, the effect of cAMP stimulation on the secretome of young and old WATi was analysed. Similar to BAT samples, the secretome of young WATi clearly showed the formation of two distinct clusters due to FSK treatment. In old WATi, both groups showed virtually complete overlap and no separation of the two sample groups (Figure 21 A,C). This indicates a higher response of young WATi to cAMP stimulation in comparison to old WATi. Additionally, VP showed a higher number of significantly changed metabolites in young than in old WATi samples: 18 metabolites were upregulated in young samples whereas only 9 metabolites were upregulated in old samples. Moreover, 15 metabolites were downregulated in young, and only 1 metabolite in old WATi samples (Figure 21 B,D).

Strikingly, and in line with metabolomics from BAT, both young and old WATi shared the same metabolites with pronounced upregulation after cAMP stimulation. 19-hydroxytestosterone, androstenedione, corticosterone, estradiolacetate, PGE3 and PGA3 were significantly upregulated in young and old WATi after cAMP induction. Steroids can influence adipose tissue through a combination of genomic and non-genomic mechanisms. Estrogen and androgen receptors are expressed in white adipose tissue and can regulate adipocyte proliferation and differentiation, as well as the activation of lipolysis or the secretion of adipokines like leptin (Mayes and Watson, 2004). A knockout of estrogen receptor, on the other hand, showed significant increases in WAT with age in male and female mice (Heine et al., 2000). PGE2 is the most abundant PG in white adipose tissue and is recognized as an inducer of browning in WAT (Vegiopoulos et al., 2010). PGE3 is so far most described in the context of cancer (Yang et al., 2014) but nothing is known about its role in WAT.

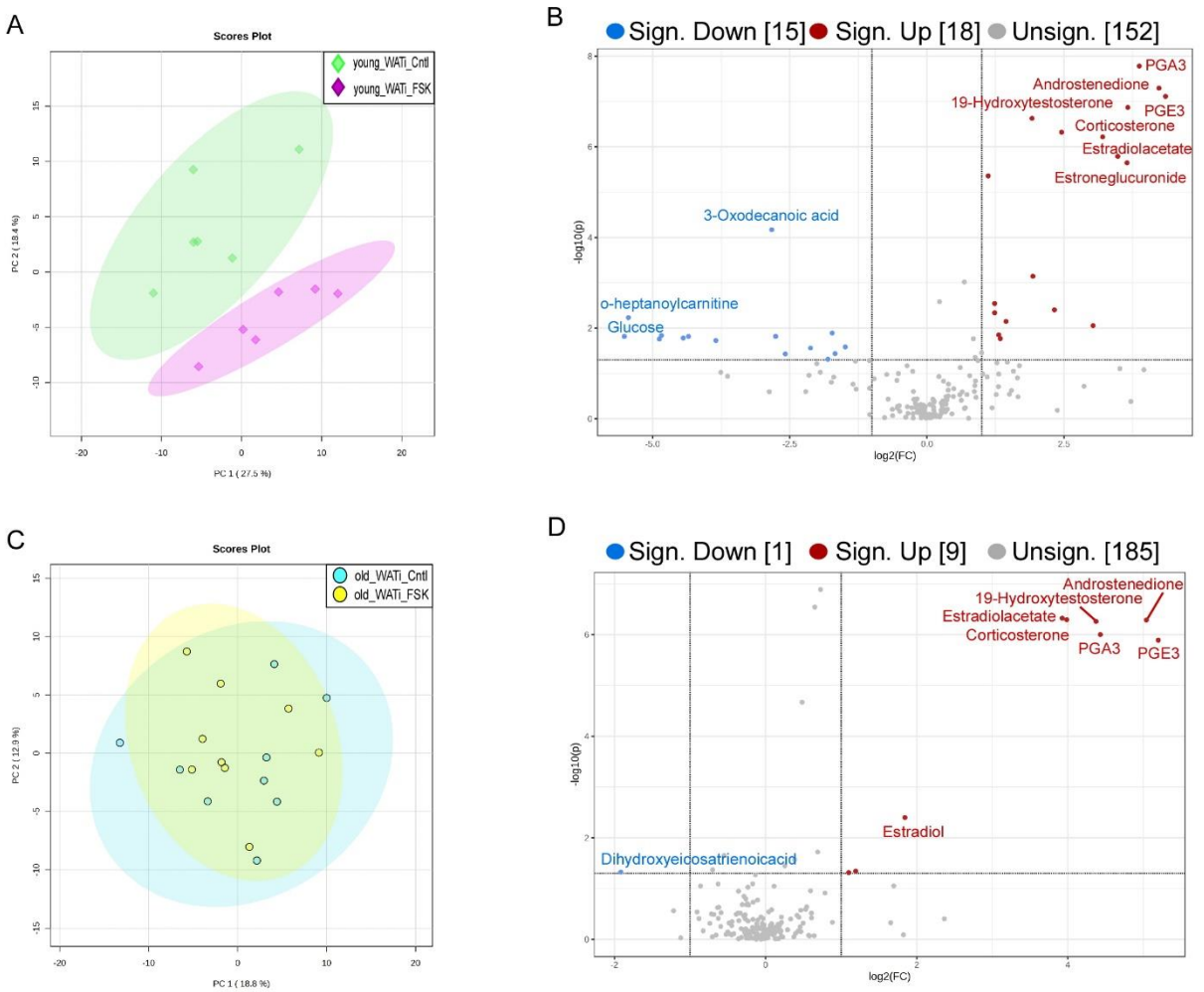

Figure 21: Effects of cAMP stimulation on the WATi secretome of young and old mice. A: PCA and B: VP of young WATi after FSK treatment. C, D: PCA and VP of old WATi after FSK treatment.

In the next step, the impact of cAMP treatment on biological processes was analysed in the metabolome of young WATi. As expected, QEA showed the enrichment of "Steroid hormone biosynthesis" for which 7 metabolites were found to be changed (Figure 22 A). These metabolites were for example corticosterone, estrone glucuronide or 19-hydroxytestosterone which were significantly upregulated after FSK treatment (Figure 22 B). All other listed enriched metabolite sets did not show a FDR< 0.1 and are therefore not significantly enriched (Figure 22 A). Nevertheless, N-acetyl-glucosamine-1-phosphate and D-xylose-5-phosphate were significantly downregulated after cAMP stimulation (Figure 22 C). D-xylose-5-phosphate is an intermediate of the pentose phosphate pathway, which can supply glycolysis to generate energy (Stincone et al., 2015). As glucose was among the top downregulated metabolites in VP from cAMP stimulated young WAT, the decreased levels of the two metabolites could result from increased glycolysis. Albeit not significantly, upregulated UDP-D-glucuronate might still be of relevance, since lower levels of this metabolite were detected in the blood metabolome of type-2-diabetes patients compared to healthy controls (Teruya et al., 2023).

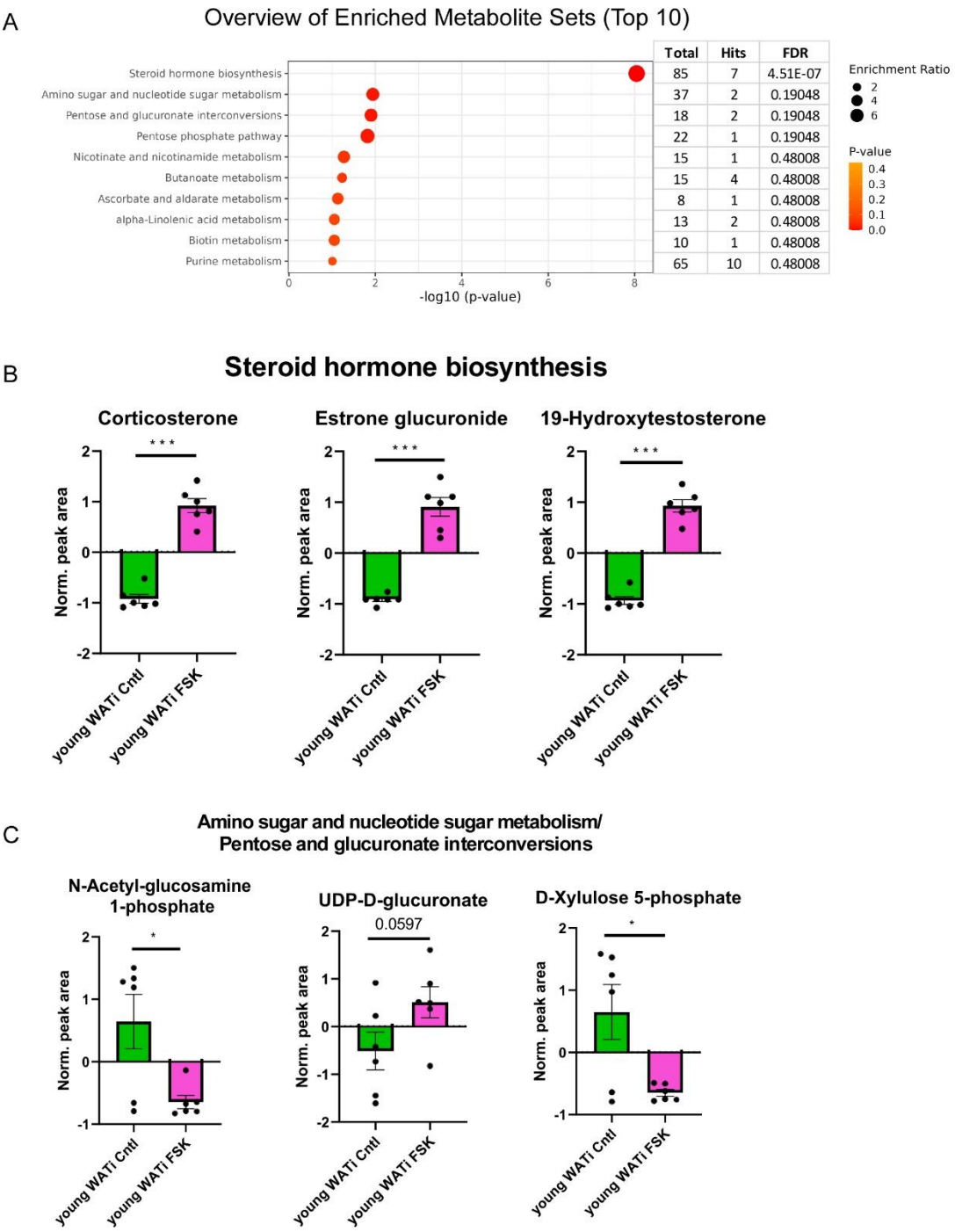

*Figure 22: Analysis of effect of cAMP stimulation on the enrichment of biological processes. A: QEA of unstimulated and stimulated young WATi B, C: Top enriched metabolite hits for the top enriched pathway sets. Normalised peak areas are represented as mean ± SEM, unpaired t-test, *p≤0.05, **p≤0.01, ***p≤0.001. n=6.*

QEA of old WATi metabolomics revealed "Sphingolipid metabolism" as the top enriched pathway. 4 metabolites were altered due to FSK treatment. Especially, sphinganine and 3-dehydrosphinganine showed a marked increase upon cAMP stimulation (Figure 23 A,B). Strikingly, cAMP stimulation altered sphingolipid metabolism in old BAT as well, even though in the opposite direction. Sphinganine and 3-dehydrosphinganine are precursors in the synthesis of S1P, sphingolipids and ceramides. The metabolites were found to be elevated in the abdominal subcutaneous adipose tissue of obese adults

(Blachnio-Zabielska et al., 2012). A deficiency of the generating enzyme of 3-keto-sphinganine on the other hand, can impair adipocyte function and adipocyte death (Fang et al., 2019).

As in young WATi, “Steroid hormone biosynthesis” was enriched in old WATi due to cAMP stimulation. In this metabolites set 7 metabolites were detected, which were all significantly upregulated (Figure 23 A,C). Those metabolites were hormones like corticosterone, estradiol and 19-hydroxytestosterone which were already described in this section.

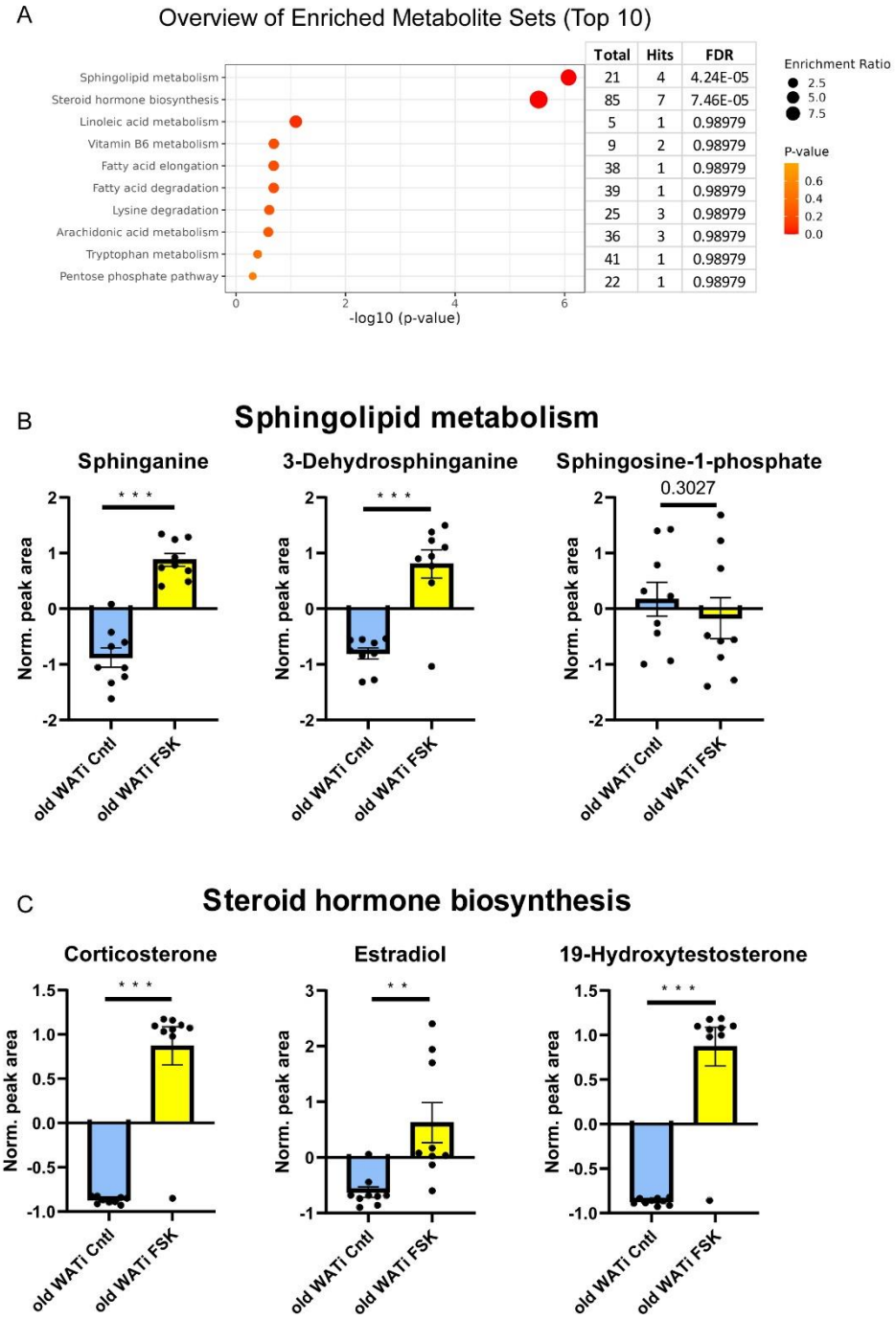

*Figure 23: Analysis of the effect of cAMP stimulation on the enrichment of biological processes of old WATi. A: QEA of unstimulated and stimulated young WATi B, C: Top enriched metabolite hits for the top enriched pathway sets. Normalised peak areas are represented as mean ± SEM, unpaired t-test, *p≤0.05, **p≤0.01, ***p≤0.001. n=9.*

Taken together, cAMP stimulation of WAT had a stronger influence on young WAT, as indicated by PCA and VP analyses. Strikingly, in young as well as in old WAT, and similar to BAT, cAMP stimulation increased levels of several steroid hormones and prostaglandins. Despite that, FSK stimulation might increase glycolysis in young WAT which results in decreased levels of glucose and D-xylose-5-posphate. In old WAT, sphingolipid metabolism was highly impacted by cAMP stimulation even though in a different manner than observed in BAT.

4.1.2.3. Analysis of common and unique metabolites in the secretome of young and old BAT

Next, all sample groups were analysed in one data set to visualize the effects of aging and cAMP stimulation together. PCA showed that the effects of aging led to a clearer subclustering than cAMP stimulation (Figure 24 A), indicating that aging itself has a greater influence on the metabolome than an acute cAMP stimulation. As already indicated by individual PCA of young and old WATi (cf. Figure 21), cAMP stimulation had a greater effect on young than old WATi, resulting in the formation of two clusters for the young sample groups. Furthermore, heat map analysis of the top 25 metabolites showed that sample groups cluster according to age and not cAMP stimulation.(Figure 24 B). Additionally, heat map showed metabolite grouping according to age or stimulation: 11 metabolites were upregulated in both young sample groups; 3 metabolites were significantly upregulated in both old groups. Among the upregulated metabolites in young WATi were hexadecanamide (which is also known as palmitic acid amide) and pamitoleoylethanolamide, which are metabolites of the C16 fatty acids palmitic acid and palmitoleic acid. Interestingly, palmitoleic acid is produced and secreted by WAT and induces lipolysis, glucose uptake and glucose utilization in WA (Cao et al., 2008; Bolsoni-Lopes et al., 2013). Furthermore, it was identified as a lipokine which can communicate and influence skeletal muscle and liver (Cao et al., 2008).

Metabolites increased in old WATi were aspartylphenylalanine, which was already described in section 4.1.2.1., and O-heptanoylcarnitine and creatinine. Moreover, heat map highlighted the steroid hormones and prostaglandins, which were upregulated in young and old groups after cAMP stimulation.

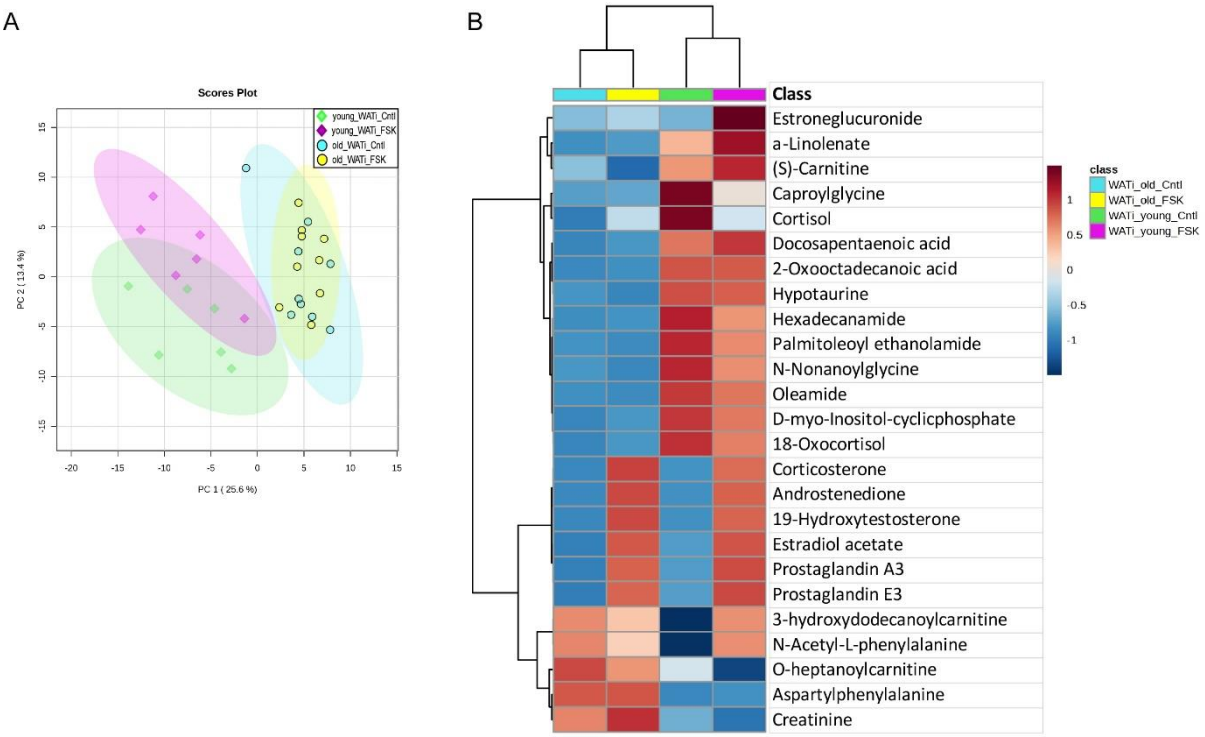

Figure 24: Comparison of all WATi groups: young and old samples with and without FSK. A: PCA of all four groups. B: Heat Map of Top 25 regulated metabolites in all groups

Since young and old WATi showed similar upregulated metabolites and pathways in VP and QEA, the significantly regulated metabolites after cAMP stimulation were analysed for common up- or downregulated metabolites. Six metabolites were commonly upregulated in young and old WATi samples after cAMP stimulation (Figure 25 A). No metabolites were commonly downregulated (Figure 25 B). As expected, the six commonly upregulated metabolites were 19-hydroxytestosterone, androstenedione, corticosterone, estradiolacetate, PGA3 and PGE3 (Figure 25 C). Those metabolites also showed a similar magnitude of increase (Figure 25 D). Alike metabolites were also commonly upregulated after cAMP stimulation in young and old BAT, as described in section 4.1.1.2. This might indicate that the secretion of these metabolites might be due to a common mechanism that is activated in both brown and white adipocytes, or from a different cell type, which is present in both tissues. Nevertheless, the metabolites' secretion seems to be unaffected by aging in both BAT and WAT.

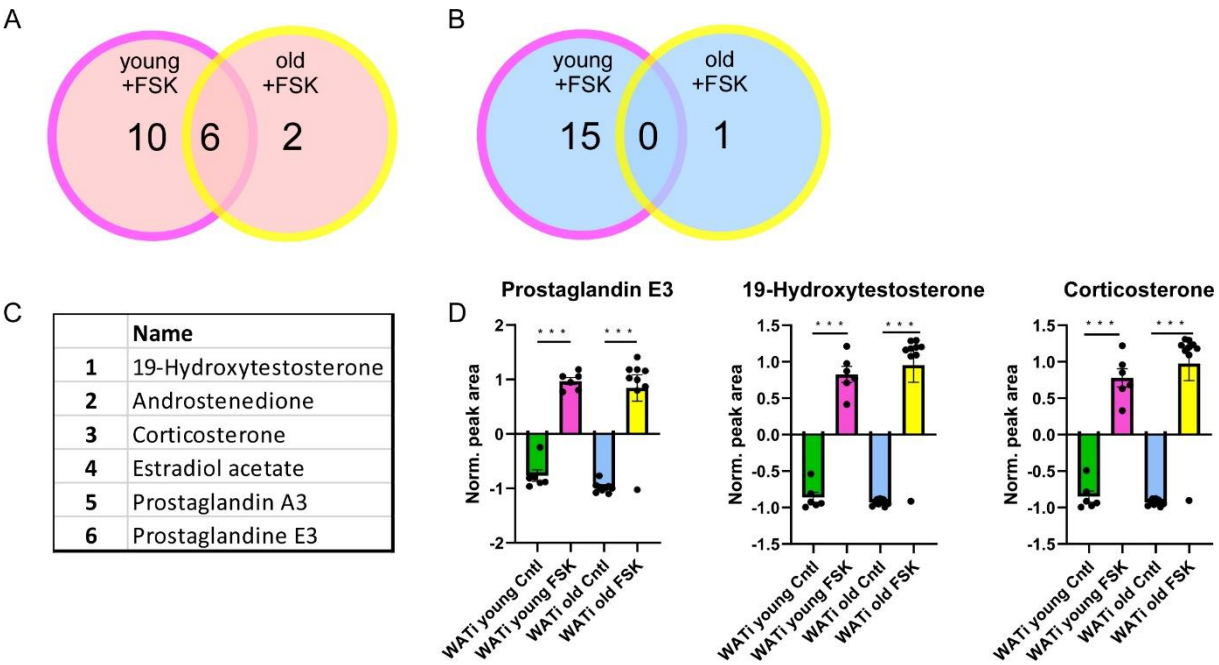

	Name
1	19-Hydroxytestosterone
2	Androstenedione
3	Corticosterone
4	Estradiol acetate
5	Prostaglandin A3
6	Prostaglandine E3

*Figure 25: Comparison of significantly regulated metabolites from young and old WATi. A: Venn diagram of shared upregulated; B: Venn diagram of shared downregulated metabolites between young and old WATi after FSK treatment. C: Table of 6 shared upregulated metabolites. D: Normalised peak area of three exemplary shared metabolites. Normalised peak areas are represented as mean ± SEM, one-way ANOVA, young WATi n=6, old WATi n=9, *p≤0.05, **p≤0.01, ***p≤0.001*

Next the uniquely regulated metabolites from young WATi were analysed in detail: 10 metabolites were uniquely upregulated, whereas 15 were uniquely downregulated after cAMP stimulation in young WATi (Figure 25 A). The unique metabolites were analysed in ORA, which did not show any enriched pathway with a FDR <0.1 (Figure 26 B). Individual analysis of the metabolites revealed that the long chain fatty acids 16-hydroxypalmitic acid, 3-oxopalmitic acid and thapsic acid were significantly upregulated in young, but not old WATi samples after cAMP stimulation. The increased levels of fatty acids and fatty acid metabolites could be a result of increased lipolysis which is a known downstream effect of cAMP stimulation (Figure 26 C). On the other hand, the medium-chain keto acid 3- oxododecanoic acid and 10- oxodecanoic acid were downregulated in young WATi samples. Moreover, the β-hydroxyketone 3-dehydrosphinganine and fatty acid metabolite capryloylglycine were downregulated due to cAMP stimulation (Figure 26 D).

A

	Name
1	Octadecenoicacid
2	Inosinic acid
3	N-lauroylglycine
4	16-Hydroxyhexadecanoic acid
5	3-oxopalmitic acid
6	N-Acetyl-L-phenylalanine
7	Hexadecanedioic acid
8	3-hydroxydodecanoylcarnitine
9	Citrate
10	Estroneglucuronide
1	Beta-D-Glucose 1-phosphate
2	O-heptanoylcarnitine
3	Glutathione disulfide
4	sn-Glycerol 1-phosphate
5	N-Acetyl-D-glucosamine 1-phosphate
6	Melanin
7	2-Hydroxyglutaric acid
8	3-Oxododecanoic acid
9	D-Xylulose 5-phosphate
10	Capryloylglycine
11	Cortisol
12	9,10-Epoxy-10,12Z-octadecadienoate
13	3alpha-Hydroxy-5beta-pregnane-20-one
14	3-Dehydrosphinganine
15	10-Oxodecanoate

B

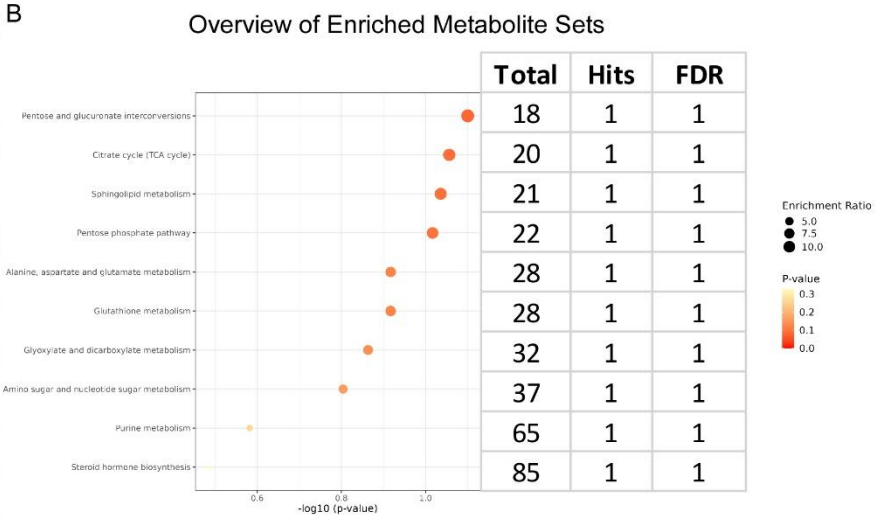

C

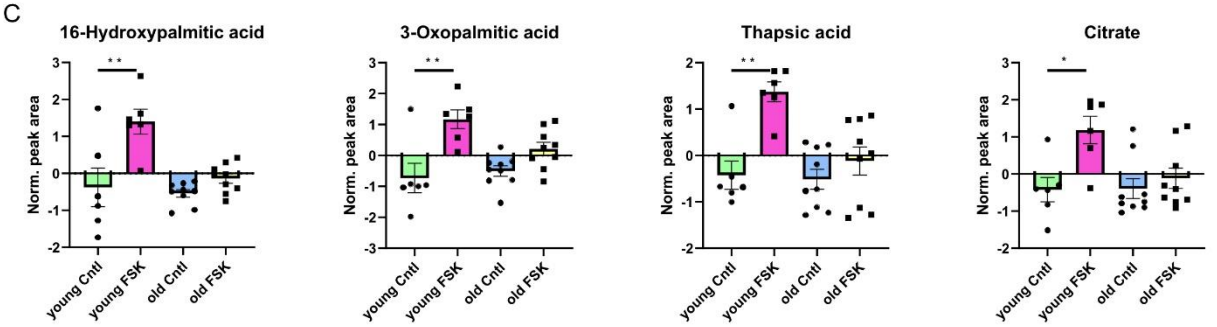

D

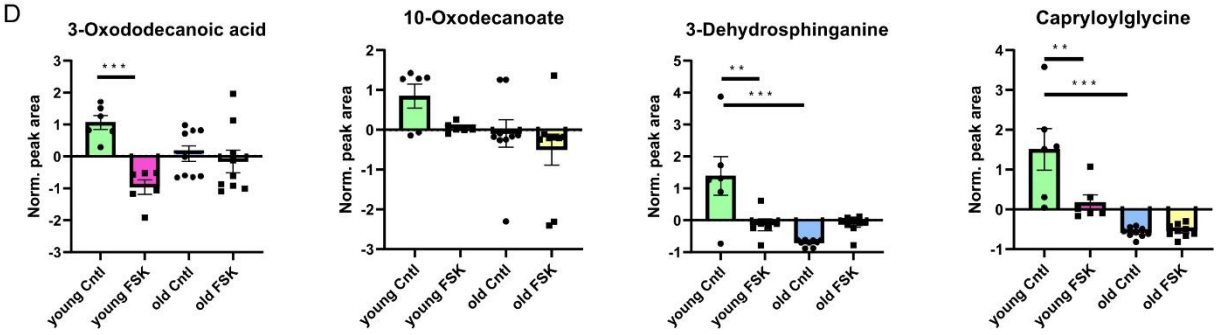

*Figure 26: Analysis of unique metabolites from young WATi after FSK stimulation A: Table with all metabolites which were uniquely up or downregulated after FSK stimulation of young WATi B: QEA of unique metabolites from young WATi. C: normalised peak area of 4 of 11 significantly up regulated metabolites. D: normalised peak area of 4 of 15 unique downregulated metabolites in young WATi. WATi: n=6; old WATi: n=9; Normalised peak areas are represented as mean ± SEM, One Way ANOVA, *p≤0.05, **p≤0.01, ***p≤0.001.*

4.1.3. Untargeted Metabolomics of murine soleus muscle from young and old mice

4.1.3.1. Influence of aging on skeletal muscle metabolome

Skeletal muscle plays a major role in energy metabolism. On the one hand, it stores metabolites like amino acids and carbohydrates, on the other hand SKM is also known to secrete various factors called myokines. SKM is highly affected by aging, which can lead to impaired mobility and metabolism. To analyse the effects of aging on soleus muscle, untargeted metabolomics was performed.

PCA analysis of young and old soleus samples was performed to visualize the distribution and grouping of the samples. Young and old SKM samples showed a pronounced formation of two opposing clusters according to age, indicating a strong influence of aging on the metabolome profile of soleus muscle. Old samples showed a higher distribution within the group compared to young samples (Figure 27 A). Notably, PCA of soleus samples showed a more pronounced effect of aging compared to WATi, but a similar effect compared to BAT. VP analysis showed 56 significantly upregulated and 34 significantly downregulated metabolites in old soleus samples compared to young soleus samples (Figure 27 B). Of 56 significantly upregulated metabolites, 18 were assigned to the class of “Lipids”. 17 of 56 metabolites were classified to “Amino acid metabolism”. Similarly, the downregulated metabolites were also mainly composed of “Lipids” (19/34) and “Amino acid metabolism” molecules (10/34) (Figure 27C). 172 metabolites showed no significant changes.

Among the top upregulated metabolites were 3-hydroxynonanoic acid, tocotrienol and pregnenolonesulfate. Tocotrienol belongs to the Vitamin E family and is known for its antioxidative effect. Furthermore, it can reduce serum levels of cholesterol and other lipids (Theriault et al., 1999). Tocotrineol can assimilate easily into the cell membrane to enter the cell and accumulates in tissues and organs high in fat (Chung et al., 2018). Tocotrienol can have several effects on skeletal muscle: a low dose of palm-oil derived tocotrienol-rich fraction (TRF) can induce myoblast proliferation, whereas a high dose of TRF showed cytotoxic effects (Chung et al., 2018). Furthermore, TRF can reverse myoblast aging in primary human myoblasts, measured in a reduction of β-galactosidase levels (Lim et al., 2013). Additionally, it was shown that TRF can improve cell viability and restore a young morphology in myoblasts (Khor et al., 2016). Furthermore, TRF supplementation was shown to ameliorate muscle atrophy and plasma insulin concentrations in diabetic mice (Lee and Lim, 2018).

Pregnenolone sulfate is a sulphated steroid and a precursor as well as a product in steroid hormone biosynthesis. Pregnenolone and its sulphated form are both present in muscle and tendon, amongst other tissues (Hackney, 2017). In murine C2C12 skeletal muscle cells, pregnenolone sulfate acts as a substrate for the synthesis of pregnenolone (Fujiki et al., 2018). Interestingly, pregnenolone sulfate itself is a modulator of ion channels (Harteneck, 2013). A broad range of ion channels can be regulated by pregnenolone sulfate, like potassium channels, nicotinic acetylcholine receptor of voltage-gated

sodium channels. Furthermore, it is a negative modulator of $GABA_A$ channels and an activator of TRPM1 and TRPM3 channels (Harteneck, 2013). So far, little is known about the effects of pregnenolone sulfate in SKM.

Among the top downregulated metabolites in old SKM were linoleamide and palmitic amide. Linoleamide and palmitic amide are both fatty acid amides. Interestingly, fatty acid amides were found to be altered in plasma from sarcopenia patients, as well as in plasma samples from aged and sarcopenic mice (Kim et al., 2023). Therefore, they might act as biomarkers for sarcopenia. Strikingly, fatty acid amides were among the top downregulated metabolites in old BAT, as well.

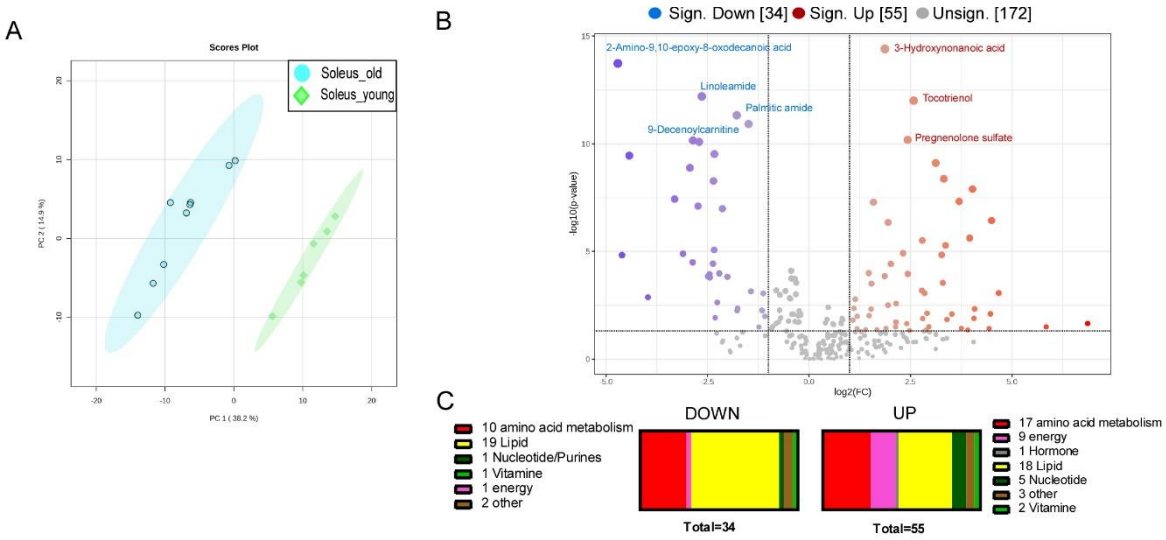

Figure 27: Analysis of metabolomics data of soleus samples from young vs old mice. A: PCA Analysis of young and old soleus B: Volcano Plot of old vs. young soleus metabolomics C: Classification of significantly up- and downregulated metabolites in old vs. young soleus.

With QEA the age-dependent changes in the secretome were linked to biological processes. Highly enriched pathways were “Taurine and hypotaurine metabolism”; “Cysteine and methionine metabolism”, “Vitamin B6 metabolism”, and “Biosynthesis of unsaturated fatty acids” (Figure 28 A). In “Taurine and hypotaurine metabolism”, two metabolites were enriched: Taurine was significantly upregulated and cysteic acid was significantly downregulated in old soleus (Figure 28 A,B). Cysteic acid is a direct precursor of taurine, but also a product of cysteine degradation. Interestingly, taurine metabolism was found to be altered in old WATi as well. As described in section 4.1.2.1. taurine is a semiessential micronutrient and a taurine deficiency has recently been identified as a driver of aging (Singh et al., 2023). Increased levels of taurine in the supernatant of old soleus musclecould indicae that in aging SKM taruine might have another role and that overall decline of serum taurine in mice is independent of taurine secretion from muscle.

In “Cysteine and methionine metabolism”, 9 metabolites were altered. For example, L-cystathionine, pyruvic acid and 3-phospho-glyceric acid were significantly higher in old than in young samples. 3-Phosphohydroxypyruvic acid was significantly lower in old samples (Figure 28 A,C). Appropriately, L-cystathionine and 3-phosphoglyceric acid are precursors in the biosynthesis of L-cysteine and cysteic acid, which in turn can fuel taurine metabolism.

The third highly changed pathway was “Vitamin B6 metabolism” in which the two metabolites pyridoxal and 2-oxo-3-hydroxy-4-phosphobutanoate were of significantly higher abundancy in old than in young soleus samples (Figure 28 A,D). Pyridoxal is part of the vitamin B6 family, which is composed of pyridoxal, pyridoxine, pyridoxamine and their respective phosphate esters (Mukherjee et al., 2011). The different vitamin B6 forms are readily interconvertible. Its active form pyridoxal 5’-phosphate is an essential cofactor in all living species and acts as a coenzyme in over 180 enzymatic reactions ranging from lipid-, glycogen and amino acid metabolism. Pyridoxal and vitamin B6 pathways were shown to be upregulated during differentiation of human skeletal muscle cells (Kumar et al., 2020). The dietary intake of vitamin B6 can increase physical performance in older adults, as measured in better chair rise test time in healthy older adults and greater grip strength in older adults with low physical activity (Grootswagers et al., 2021). Furthermore, serum levels of pyridoxal 5’-phosphate are negatively influenced by increased body fat mass but not aging (Jungert and Neuhäuser-Berthold, 2020).

The forth enriched pathway was “Biosynthesis of unsaturated fatty acids”, in which 7 metabolites were changed. The long chain saturated fatty acids (SFA) stearic acid and arachidic acid, and the monounsaturated fatty acid oleic acid were significantly upregulated in the secretome of old soleus. The polyunsaturated fatty acid (PUFA) α-linolenic acid was significantly downregulated in old soleus (Figure 28 A,E). Interestingly, aging as well as sarcopenia are characterized by the accumulation of intramyocellular lipids (Gueugneau et al., 2015). Additionally, muscle fat infiltration can reduce muscle strength (Visser et al., 2002). However, saturated and unsaturated fatty acids show different effects on skeletal muscle mass and function: SFAs can decrease myotube diameter and suppress insulin signalling. PUFAs, like docosahexaenoic acid, on the other hand, can counteract this SFA induced myotube atrophy. Moreover, feeding dystrophic hamsters with a diet rich in the PUFA α-linolenic acid showed improvements in muscle morphology and function (Lipina and Hundal, 2017). The increased levels of SFA and decreased levels of PUFAs found in old soleus samples might therefore result from an aging-related lipid infiltration of the muscle and an imbalance of SFA and PUFA which can in turn negatively influence muscle mass and function.

In summary, secretomics of young and old soleus, showed a pronounced effect of aging as indicated by clear separation of the two sample groups in PCA and a great number of significantly altered

metabolites. Functional analysis of the top regulated metabolites and pathway analysis, showed an influence in taurine and hypotaurine metabolism, even though the elevated levels of taurine in old soleus are contradicting recent data. Additionally, lipid metabolism seems to be highly impacted in soleus SKM due to aging.

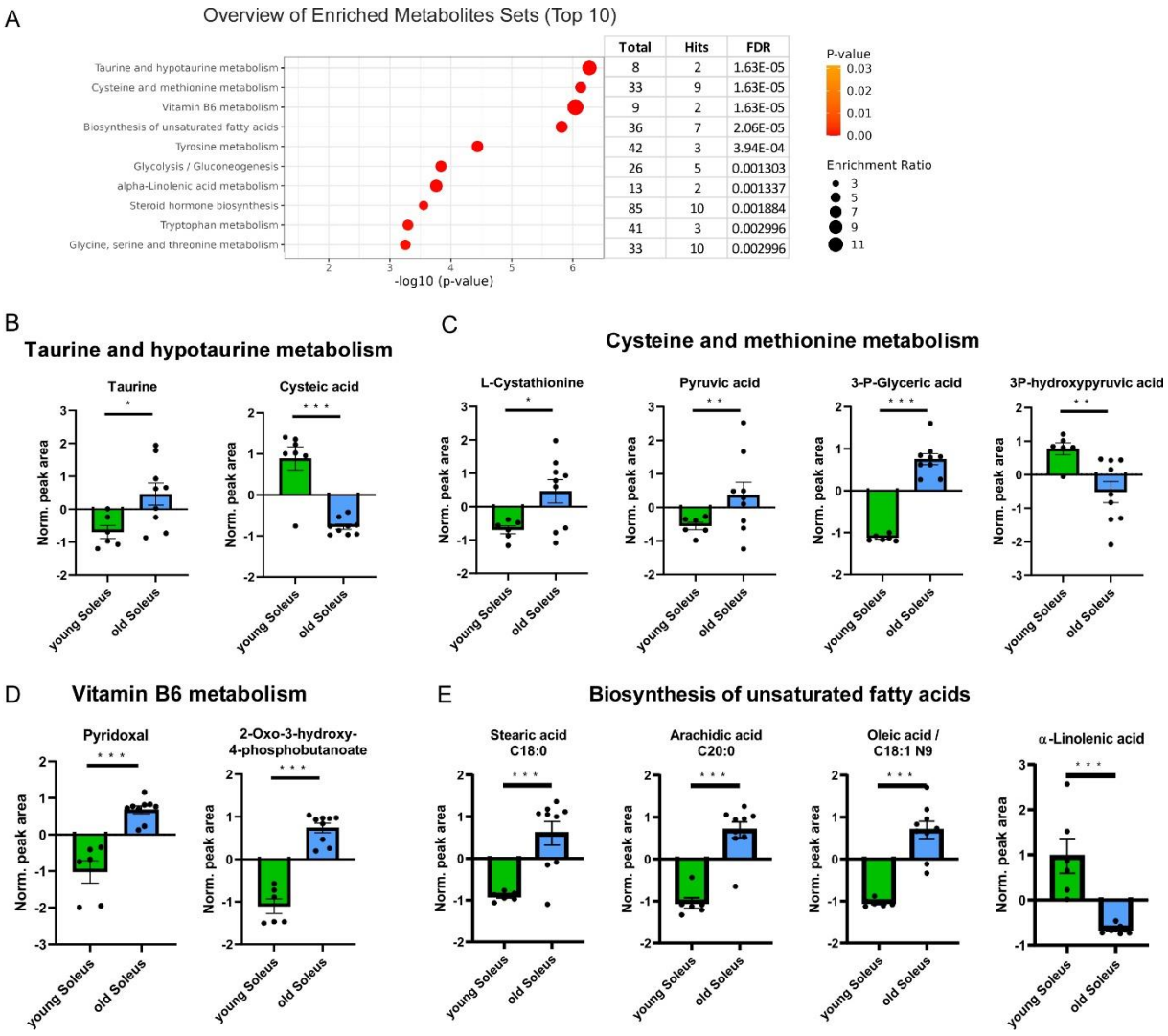

*Figure 28: Pathway analysis of age-related changes in the metabolome of young and old Soleus muscle. A: QEA of young vs. old soleus metabolomics. B-E: Normalised Peak areas of altered metabolites from enriched pathways. Young soleus: n=6; old soleus: n=9; Normalised peak areas are represented as mean ± SEM, unpaired t-test, *p≤0.05, **p≤0.01, ***p≤0.001.*

4.1.3.2. Effects of cAMP stimulation on SKM metabolome

cAMP signalling is vital for full SKM functionality, and the increase of cAMP levels by FSK treatment is widely used as a model for ex vivo exercise. To analyse the metabolome of SKM upon an acute ex vivo exercise mimic, untargeted metabolomics of young and old soleus samples with and without cAMP stimulation were analysed. PCA showed the formation of two distinct clusters in young samples (Figure 29 A). This indicates a high influence of the FSK treatment on young soleus, leading to a strong variance

in the data between the two sample groups. This clustering effect was also observed for the old soleus, however, not as clearly as for the young (Figure 29 D). Like in BAT and WAT, the different clustering of Cntl and FSK treated samples, indicates a higher sensitivity of young tissue to the acute stimulation.

In young soleus, cAMP stimulation led to significant changes in the abundancies of 89 metabolites, of which 73 were significantly up and 16 significantly downregulated due to cAMP treatment (Figure 29 B). The majority of significantly up- and downregulated metabolites in young samples were classified as “Lipids” (27 up and 10 down). Moreover, 19 amino acids or metabolites from amino acid metabolism were upregulated in young soleus samples (Figure 29 C). Interestingly, cAMP stimulation of old soleus samples changed the levels of clearly less metabolites: in total 34, of which 17 were significantly up and 17 significantly downregulated. (Figure 29 E). Of the 17 upregulated metabolites in old soleus, the majority were hormones (7) and lipids (6). Of the 17 downregulated metabolites, 10 were lipids (Figure 29 F).

Strikingly, cAMP stimulation of soleus led to a pronounced increase of several steroid hormones and prostaglandins, just like observed in BAT and WAT. For example, 19-hydroxytestosterone, andostenedione, estradiol and PGE3 were significantly upregulated in young and old SKM after FSK treatment. Usually, sex steroid hormones are synthesized and secreted by the ovary and testis, but SKM is as well capable of producing steroid hormones. Sato et al. showed that testosterone, estradiol and DHT can be synthesized by the enzymes HSD, P450arom and 5α-reductase in skeletal muscle of rats (Sato et al., 2008; Sato and Iemitsu, 2015). The production and the levels of steroid hormones decrease with age which contributes to sarcopenia and muscle weakness (Sipilä et al., 2013). On the other hand, exercise can induce levels of testosterone, dihydrotestsoterone and estradiol in males rats (Aizawa et al., 2008; Aizawa et al., 2010). This effect is highly dependent on the sex and on the type of exercise that is performed. As the stimulation of cAMP production by FSK treatment is a known model for in vitro/ ex vivo exercise, the increased levels of steroids confirm the finding, that exercise increases steroid hormone levels ins SKM independent of age.

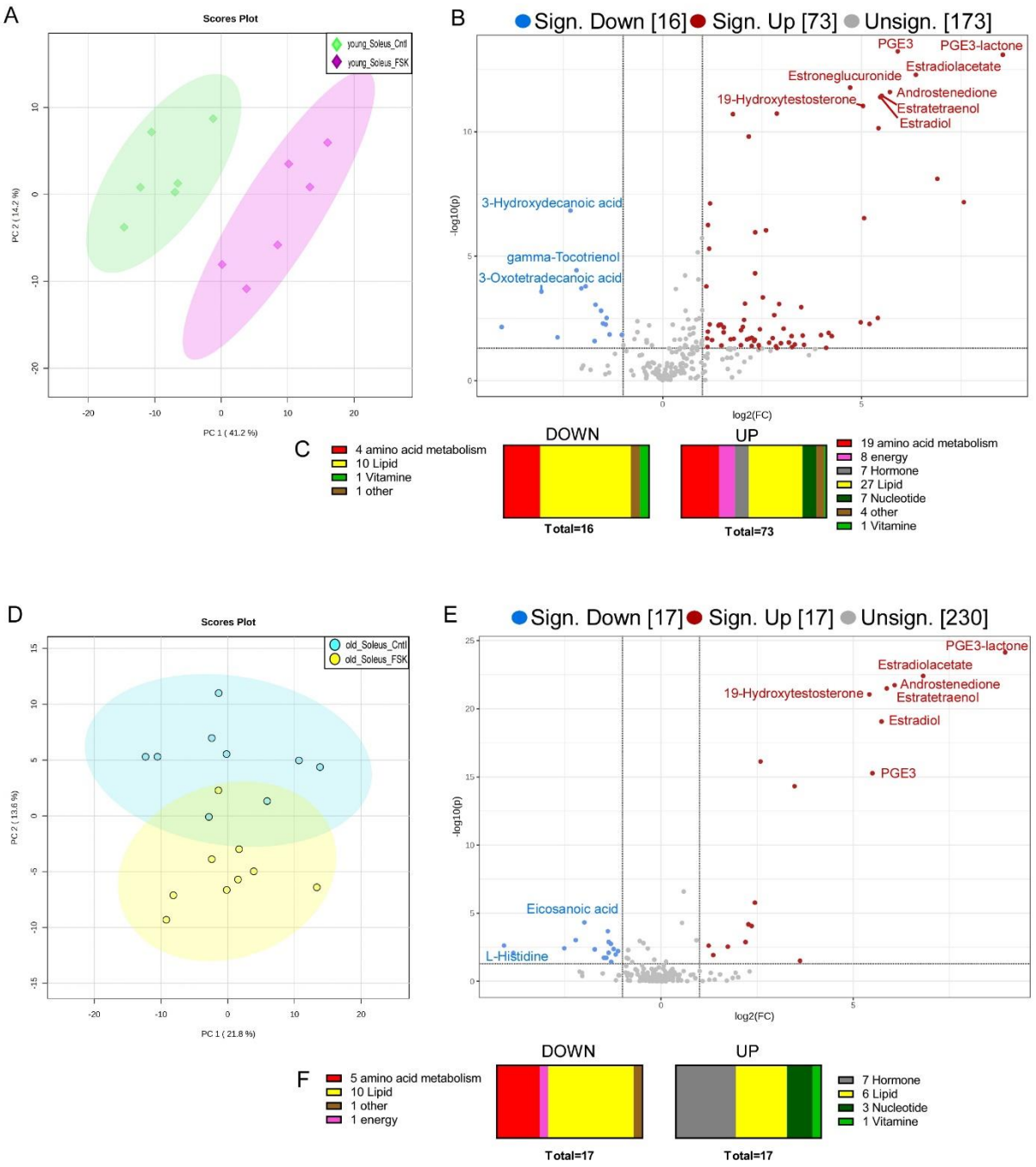

Figure 29:Effects of cAMP stimulation on the soleus secretome of young and old mice. A: PCA and B: VP of young soleus after FSK treatment. D, E: PCA and VP of old soleus after FSK treatment. C, F: Classification of significantly up- and downregulated metabolites.

In a next step the effect of cAMP stimulation was linked to biological processes by QEA. In young soleus samples high changes could be observed in “Steroid hormone biosynthesis”, “Biosynthesis of unsaturated fatty acids”/“Fatty acid biosynthesis” and “Vitamin B6 metabolism” (Figure 30 A).

In “Steroid hormone biosynthesis” 10 metabolites were enriched which were mainly composed of C18- and C19- steroids. The steroid precursor metabolites 20α,22β-dihydroxycholesterol was significantly decreased, whereas the C-19 steroid 19-hydroxytestosterone and the C-18 steroid estrone were

significantly upregulated after FSK stimulation in the secretome of young soleus (Figure 30 B). The reduction in a steroid precursor and an increase in steroid hormones, further indicates that cAMP stimulation activates steroid hormone biosynthesis.

A total of 10 metabolites associated with the biosynthesis of saturated and unsaturated fatty acids were also altered due to FSK stimulation. The C18 and C20 long-chain fatty acids stearic acid, arachidic acid and oleic acid were significantly elevated. Shorter fatty acids like myristic acid (C14) and lauric acid (C12) were significantly reduced (Figure 30 D). The increased energy demand during exercise is mainly fuelled by carbohydrates and fat, the latter being mostly stored as TGs in the adipose tissue. However, SKM also contains TGs, even though in smaller quantities (van Loon, 2004). During exercise these intramuscular TGs are mobilized and oxidized to fuel the energy demand of contracting SKM (Watt et al., 2002). This lipolysis process is mediated by the adipose triglyceride lipase and is activated via PKA (Mason et al., 2012). As cAMP is an activator of PKA, a stimulation of SKM with FSK increases lipolysis via the cAMP/-PKA axis.

Another highly enriched pathway was “Vitamin B6 metabolism”, in which the two metabolites pyridoxal and 2-oxo-3-hydroxy-4-phosphobutanoic acid were significantly upregulated (Figure 30 C). Interestingly, those metabolites were upregulated in old compared to young soleus, as well.

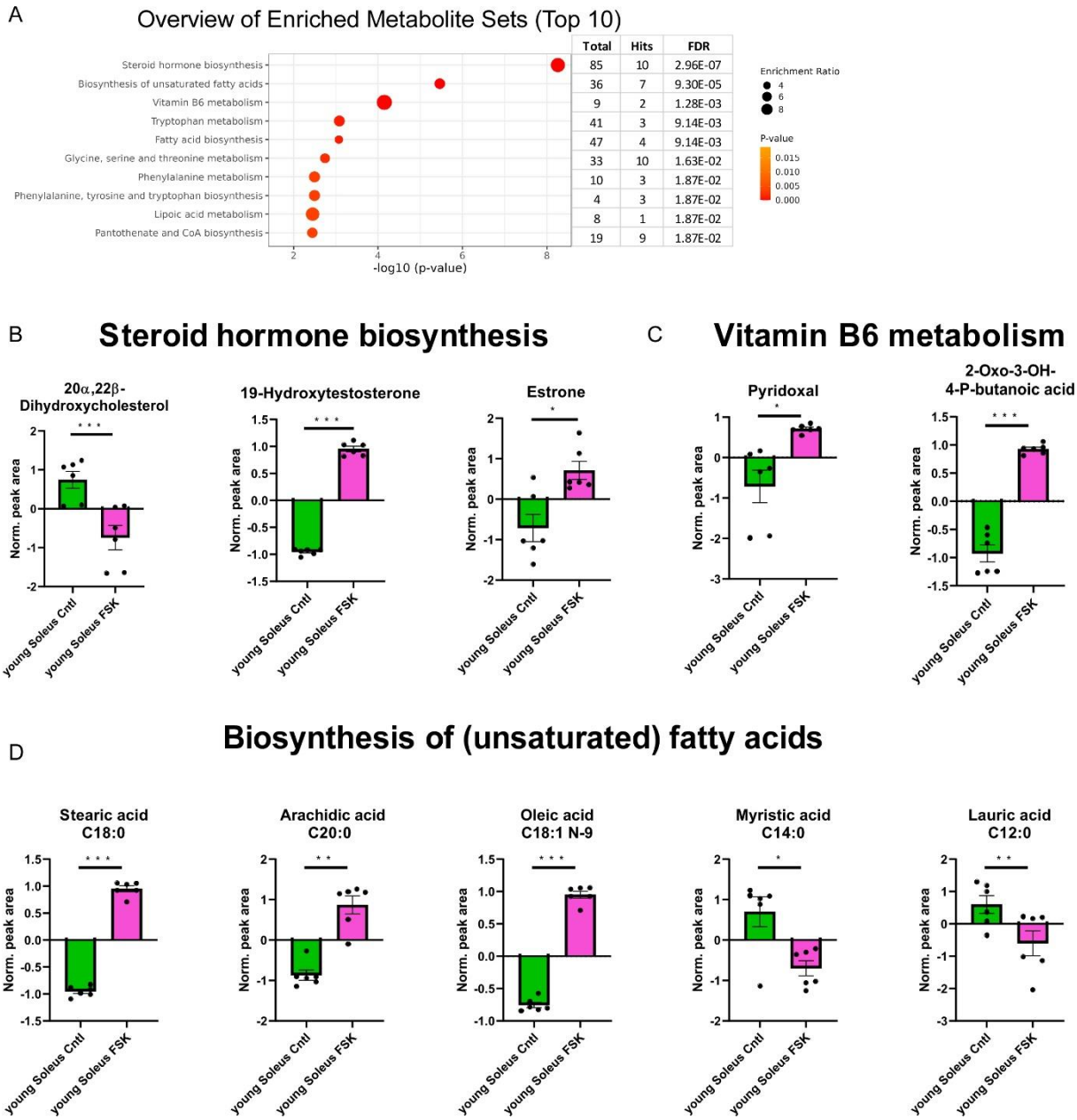

*Figure 30: :Analysis of the effect of cAMP stimulation on the enrichment of biological processes in young soleus. A: QEA of unstimulated and stimulated young soleus B-D: Top enriched metabolite hits for the top enriched pathway sets. Normalised peak areas are represented as mean ± SEM, unpaired t-test, *p≤0.05, **p≤0.01, ***p≤0.001. n=6.*

The secretome of old soleus after cAMP stimulation was analysed in the same way. As in the young samples, QEA showed the enrichment of "Steroid hormone biosynthesis" and "Biosynthesis of unsaturated fatty acids". 10 and 7 metabolites were changed in the pathways respectively (Figure 31 A). Just like in the young samples, several C18 and C19 steroids like androstenedione, 19-hydroxytestosterone and estrone were significantly upregulated in old soleus (Figure 31 B). Strikingly, metabolites from "Biosynthesis of fatty acids" were changed in the opposite direction as in young soleus samples: the long-chain fatty acids stearic acid, arachidic acid and oleic acid were significantly lowered due to cAMP induction (Figure 31 C).

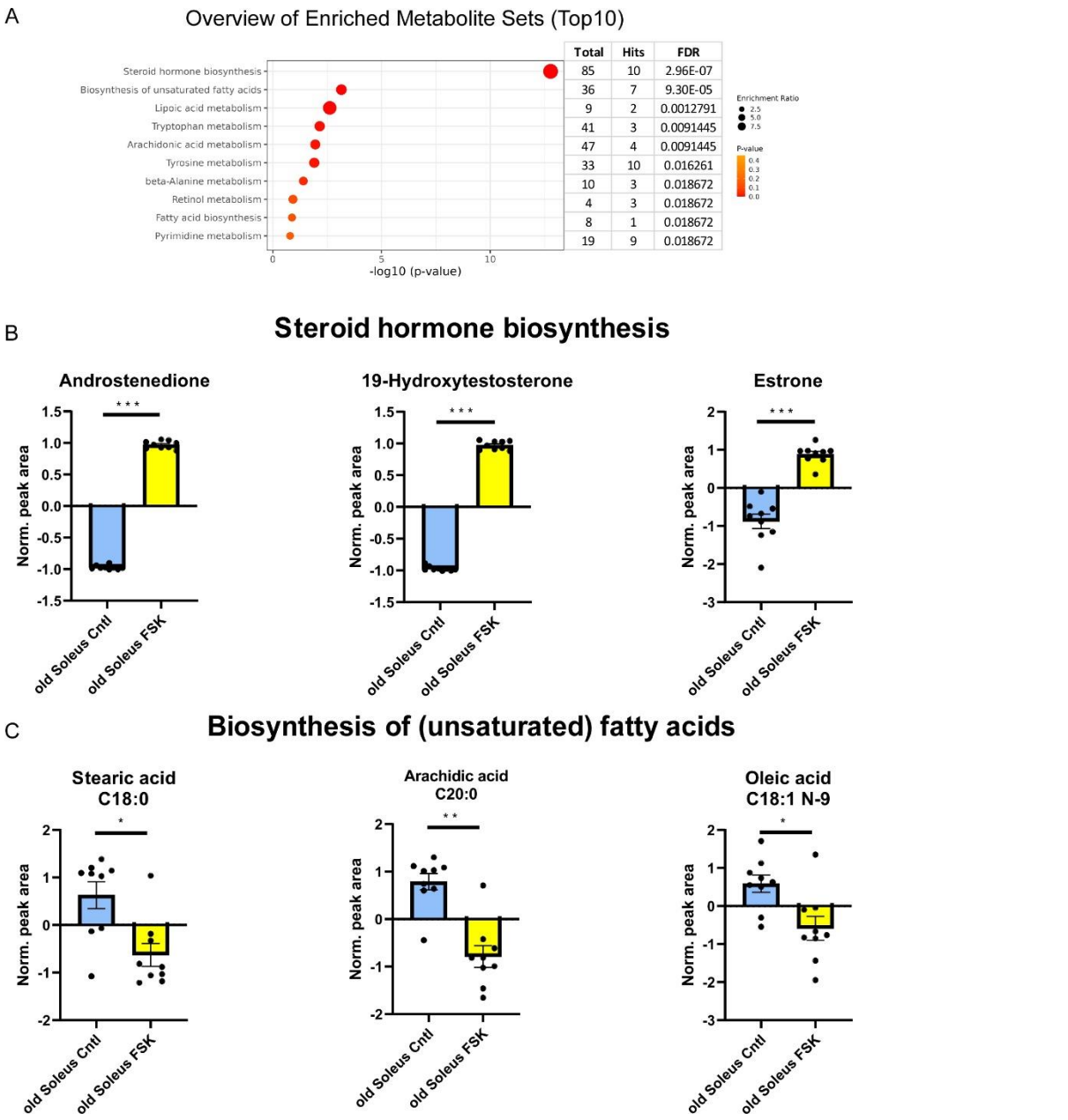

*Figure 31:Analysis of FSK effect on the enrichment of biological processes in old Soleus. A: QEA of unstimulated and stimulated old Soleus B-D: Top enriched metabolite hits for the top enriched pathway sets. Normalised peak areas are represented as mean ± SEM, unpaired t-test, *p≤0.05, **p≤0.01, ***p≤0.001. n=9.*

To compare the different effects of aging and cAMP stimulation directly to each other, again all four groups were analysed in one data set. PCA showed that old and young samples cluster according to age, rather than treatment status. cAMP stimulation in young samples led to the formation of two separated clusters, which could not be observed in the old samples (Figure 32 A). This indicates that aging has a greater effect on the metabolome of soleus SKM than an acute ex vivo exercise treatment. Interestingly, aging showed a greater influence on the metabolic profile of BAT and WATi, as well. Furthermore, Heat map analysis of the top 25 metabolites also showed the highest similarities within the young/old groups (Figure 32 B). Additionally, heat map showed a clustering of several metabolites according to age. For example, acylcarnitines like 2-dodecenoylcarnitine, 9-decenoylcarnitine or

tiglylcarnitine were highly abundant in both young sample groups compared to old groups. Acylcarnitines are fatty acid metabolites and contain an acyl group i.e. a fatty acid or organic acid which is linked to L-carnitine. Their major role is to transport organic acids and fatty acids from the cytoplasm into the mitochondria where they can be broken down to produce energy (Dambrova et al., 2022). Plasma levels of especially short-chain acylcarnitines are increased in type-2 diabetes patients and are therefore discussed to be a relevant biomarker (Hosseinkhani et al., 2022). Elevated concentrations of acylcarnitines in skeletal muscle can occur in insulin-resistance or type 2 diabetes mellitus (McCoin et al., 2015). In mice it was already shown, that exercise can reverse the accumulation of long-chain acylcarnitines in gastrocnemicus muscle during high fat diet. Elevated levels of acylcarnitines in young soleus SKM therefore seem unexpected and demand more thorough analysis on the direct effects of these metabolites on SKM.

On the other hand, metabolites like tocotrienol or pregnenolone sulfate were highly abundant in old but not in young samples. Those metabolites were among the top upregulated metabolites in old compared to young soleus and were already described in section 4.1.3.1..

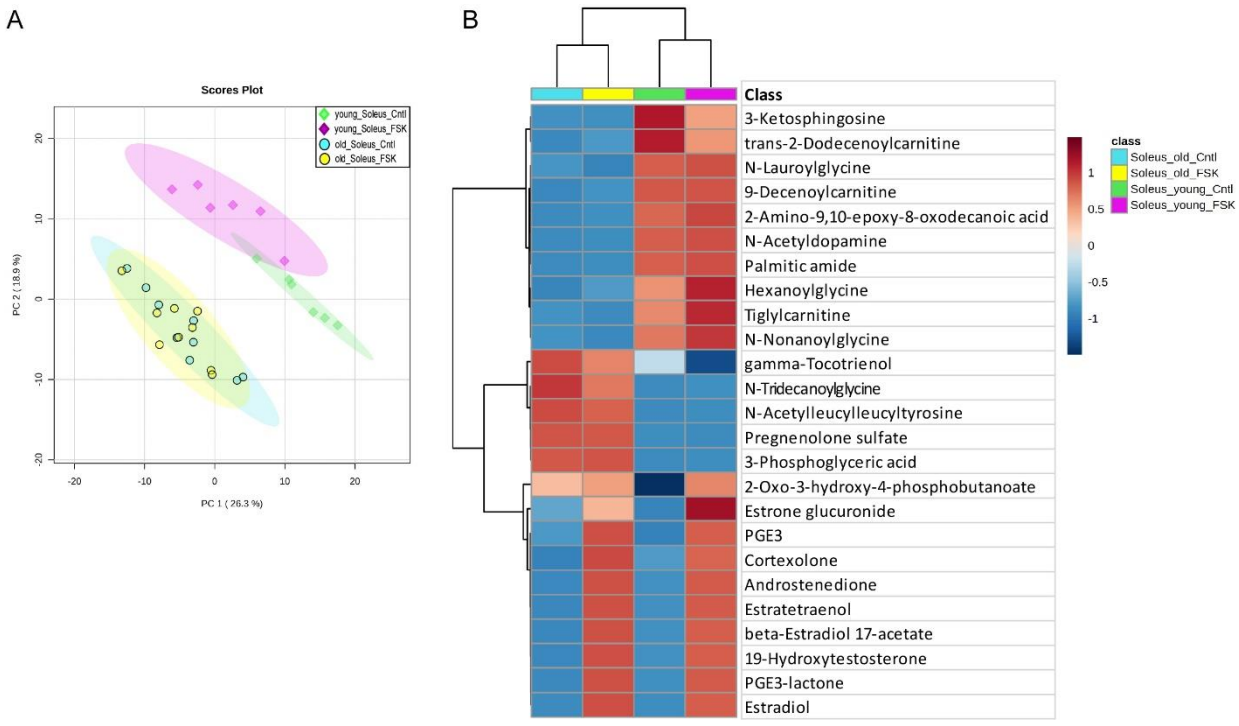

Figure 32: : Comparison of all soleus groups: young and old samples with and without FSK. A: PCA of all four groups. B: Heat Map of Top 25 regulated metabolites in all groups

VP and QEA analysis of young and old samples already highlighted common regulation patterns due to cAMP regulation. For a more detailed analysis, the metabolites which were significantly changed after

cAMP induction in young and old soleus samples were analysed for common features. 12 metabolites were significantly upregulated in both young and old soleus after cAMP stimulation (Figure 33 A). Two metabolites were downregulated in both groups (Figure 33 B). Unsurprisingly, among the shared upregulated metabolites were mainly steroidhormones and prostaglandins. For example the steroids andostenedione and 11-deoxycortisol and PGE3 were significantly upregulated due to FSK stimulation in young and old samples (Figure 33 D). The two metabolites which were commonly downregulated were 3-hydroxydodecanedioic acid and o-adipoylcarnitine. 3-Hydroxydodecanedioic acid was of significant lower abundancy in old than in young samples under unstimulated conditions. In both sample groups the levels were lowered due to cAMP stimulation. 3-Hydroxydodecanedioic acid is a medium-chain hydroxyl acid and involved in the acylcarnitine pathway. O-Adipoylcarnitine on the other hand, is an acylcarnitine.

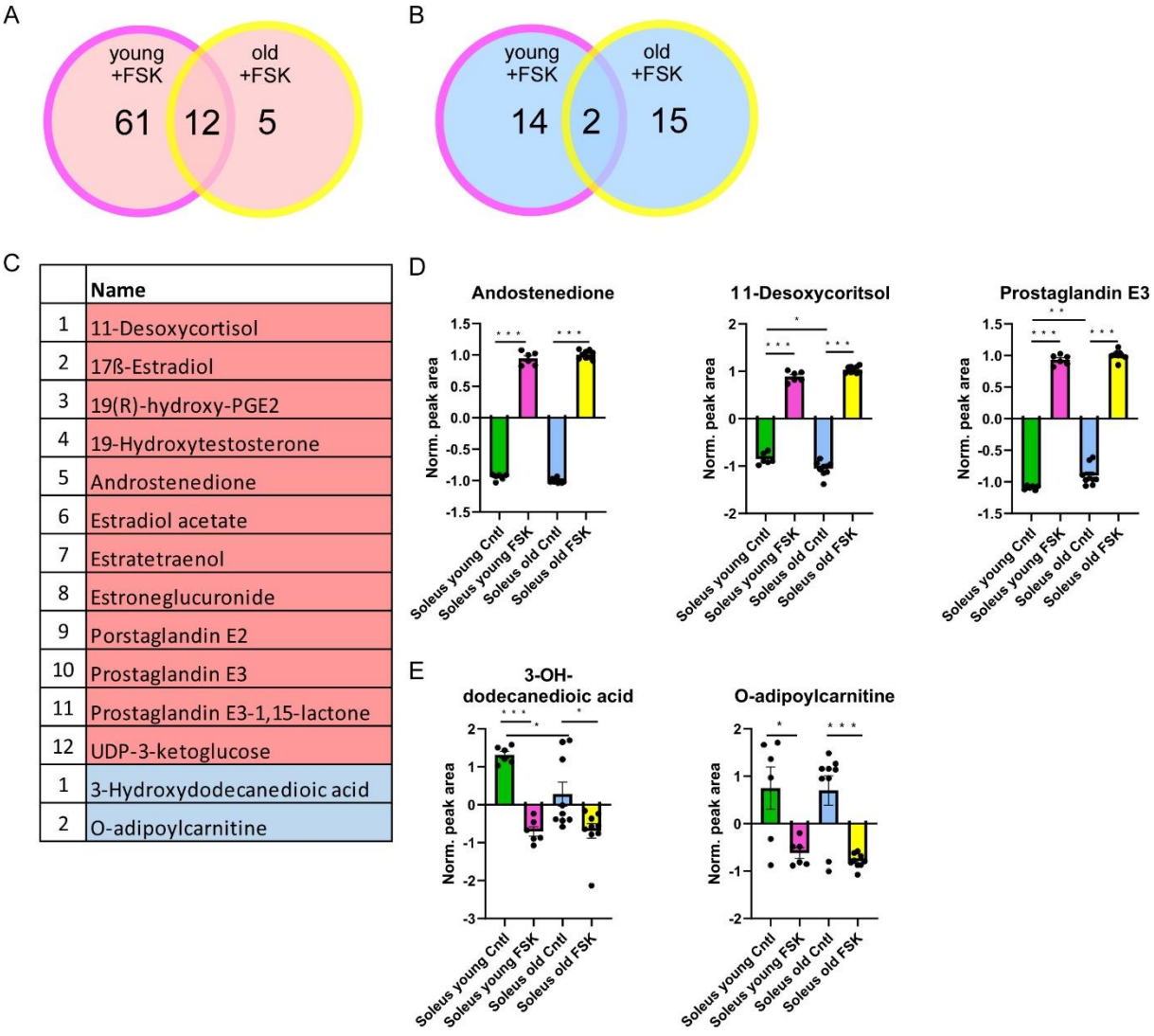

	Name
1	11-Desoxycortisol
2	17ß-Estradiol
3	19(R)-hydroxy-PGE2
4	19-Hydroxytestosterone
5	Androstenedione
6	Estradiol acetate
7	Estratetraenol
8	Estroneglucuronide
9	Porstaglandin E2
10	Prostaglandin E3
11	Prostaglandin E3-1,15-lactone
12	UDP-3-ketoglucose
1	3-Hydroxydodecanedioic acid
2	O-adipoylcarnitine

Figure 33: : Comparison of significantly regulated metabolites from young and old soleus. A: Venn Diagramm of shared upregulated; B: Venn Diagramm of shared downregulated metabolites between young and old soleus after FSK treatment. C: Table of shared up- and downregulated metabolites. D: Normalised peak area of three exemplary shared upregulated metabolites. E: Normalised peak area of the two shared downregulated metabolites between stimulated young and old soleus.

*Normalised peak areas are represented as mean ± SEM, one-way ANOVA, young soleus n=6, old soleus n=9, *p≤0.05, **p≤0.01, ***p≤0.001*

61 metabolites were found to be uniquely upregulated in young soleus after FSK stimulation (Figure 33 A). Those metabolites were analysed for the enrichment of specific pathways by ORA. 8 metabolites were associated with "Aminoacyl-tRNA biosynthesis", 6 with "Alanine, aspartate and glutamate metabolism" and 6 with "Arginine and proline metabolism" (Figure 34 A). Those metabolites, like glycine and proline, were significantly upregulated in young soleus after FSK stimulation, but not in old (Figure 34 C). Taking a closer look at those metabolites, ten amino acids were shared hits in multiple pathways (Figure 34 B). For example, L-glutamic acid was found in seven of the top ten enriched metabolite sets, and L-aspartic acid in five. This indicates a specific alteration of amino acid metabolism in young soleus samples. In SKM, amino acids are mainly present in the form of proteins. A smaller amount (less than 2% of total body amino acid) exist in their free form in plasma or in intra- and extracellular spaces (Gibala, 2001). Nevertheless, this pool of free amino acids participates in a great number of metabolic pathways throughout the body. The size of the free amino acid pool is dynamic and can change upon events such as dietary status or exercise. Especially, glutamate, aspartate, asparagine and BCAA were shown to be released of or taken up from SKM due to exercise. Furthermore, glutamine and alanine are released from SKM after exercise (Gibala, 2001). Amino acid oxidation can fuel energy demand, when lipid and carbohydrate storages are depleted. The increase in free amino acids in young soleus samples after cAMP stimulation could therefore indicate the utilisation of amino acids for energy supply.

In summary, cAMP stimulation of young and old soleus SKM showed a great effect on the metabolome of young soleus and a moderate effect on the metabolome of old soleus. cAMP stimulation of young soleus showed an increase in free long-chain fatty acids and an increase in vitamin B6 metabolites. In old soleus samples, on the other hand, cAMP stimulation decreased the levels of free fatty acids. Interestingly, both young and old samples showed a pronounced increase in steroid hormones and prostaglandins upon cAMP stimulation. The analysis of unique metabolites from young soleus, highlighted amino acid metabolism and strongly indicates an aging effect on the utilisation of amino acids during ex vivo exercise.

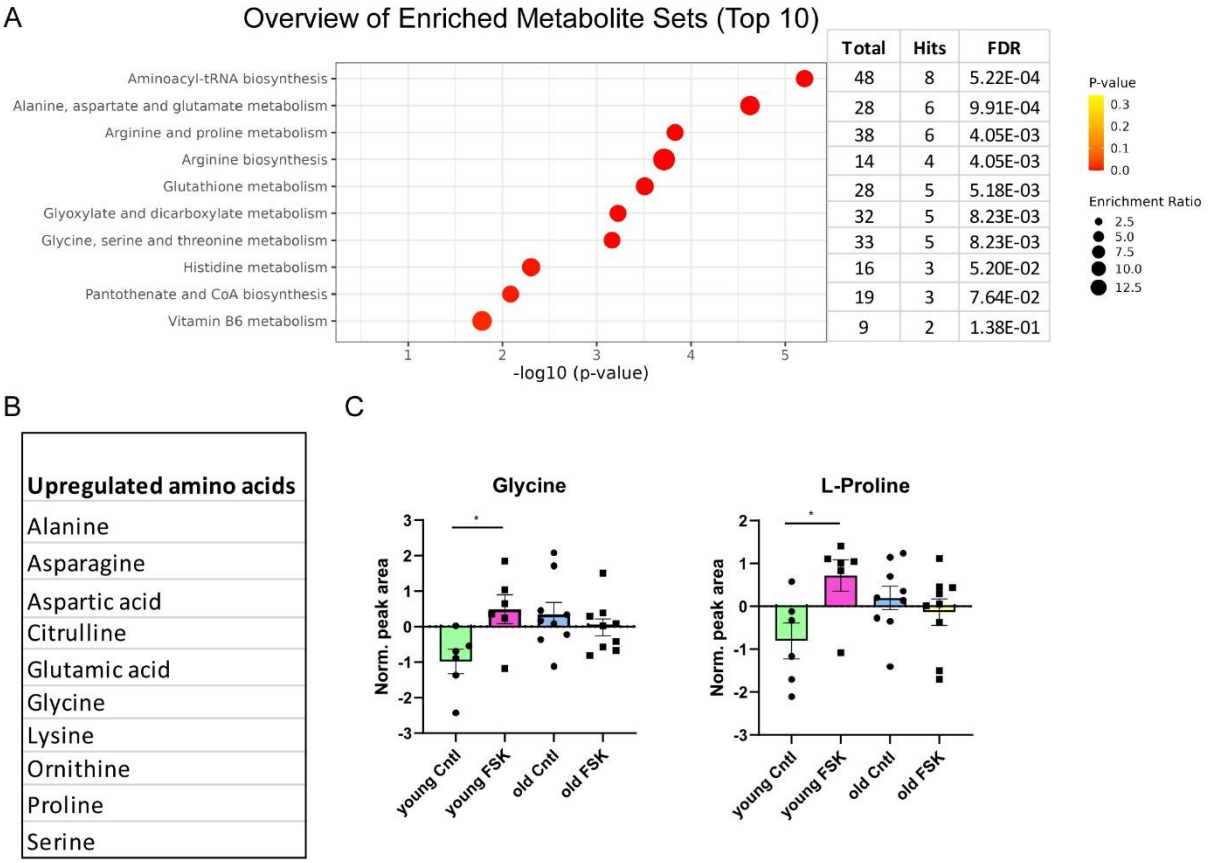

*Figure 34: : Analysis of unique metabolites from young Soleus after FSK stimulation A QEA of unique metabolites from young soleus. B: Table with of ten upregulated amino acids which were found in the top regulated pathways. C: normalised peak area of two significantly up regulated amino acids. Normalised peak areas are represented as mean ± SEM, one-way ANOVA, young soleus n=6, old soleus n=9, *p≤0.05, **p≤0.01, ***p≤0.001*

4.2. Untargeted Metabolomics of human soleus muscle from young and old, untrained and trained healthy men

Untargeted metabolomics from young and old mice revealed a significant influence of aging and ex vivo exercise on the metabolic profile from soleus muscle. However, murine data cannot entirely be transferred to the human organism and cAMP stimulation only serves as a model for acute ex vivo exercise, without displaying the whole impact of training or long-term adaptations. Therefore, human soleus biopsies were analysed in a next step. Soleus biopsies were obtained from healthy male volunteers which were either 20-35 years (young) or 60-75 years (old), and either virtually unactive in sports (untrained) or performed sports on a regular and competitive basis (trained) (see section 3.3.1.).

4.2.1. Effects of training status on the metabolome of soleus muscle from young and old men

The influence of training on the secretome was evaluated by comparison of young or old untrained samples to young or old trained samples. PCA showed major overlapping of untrained and trained samples in the young group, as well as in the old (Figure 35 A, C). Notably, the distribution of the samples was rather high in both groups, which could be a sign of high data variation due to

interindividual differences. This might as well account for similar clustering in PCA and indicate a higher effect of interindividual differences rather than training status in human samples.

Volcano Plot Analysis of young samples showed a significant upregulation of 3 metabolites and a significant downregulation of 16 metabolites in trained compared to untrained samples (Figure 35 B). 322 metabolites showed no significant changes. The top three upregulated metabolites were L-carnitine, heptanoylcarnitine and 1-methylnicotinamide. Among the top downregulated metabolites were inosine, aminohippuric acid and cysteinyl-alanine (Cys-Ala).

L-carnitine is mainly found in SKM (95% of total body carnitine), either in its free form or as acyl carnitine (Brass, 1995). The most studied function of L-carnitine is the transportation of long-chain fatty acids into the mitochondria for β-oxidation. Besides that, it is a prominent supplement in exercise performance, that should increase fat oxidation during prolonged exercise, even though this effect is under great scientific discussion (Stephens et al., 2007). Notably, trained humans and equines seem to have higher total muscle carnitine content than untrained controls (Lennon et al., 1983; Foster and Harris, 1992). Therefore, the increased levels of L-carnitine in trained compared to untrained young samples, likely results from the training status.

1-methylnicotinamide is the methylated metabolite of nicotinamide produced by the enzyme N-methyltransferase which is expressed in SKM amongst other tissues (Aksoy et al., 1994). Interestingly, a single bout of endurance exercise can increase the enzymatic activity of N-methyltransferase in murine liver and a supplementation of diabetic mice with 1-mehtylnicotinamide could increase insulin sensitivity and prolong exercise endurance (Chłopicki et al., 2012; Przyborowski et al., 2015).

The purine inosine was significantly lower in the supernatant of young trained soleus samples. Inosine can be synthesized from adenosine or inosine monophosphate and further metabolised to hypoxanthine. Conflictingly, adenosine concentrations increase upon exercise in the interstitium of human muscle and the activation of the corresponding purinergic receptor A2B was shown to positively influence muscle mass and function and counteract age-related SKM decline (Hellsten et al., 1998; Gnad et al., 2020). On the other hand, Xiang et al. showed, that exercise led to a downregulated of purine metabolites after exercise in SKM of diabetic mice (Xiang et al., 2018).

VP of old soleus samples pictured 13 significantly up and 12 significantly downregulated metabolites in old trained compared to old untrained samples. The top upregulated metabolites in old trained samples were the saturated fatty acids palmitic acid, stearic acid and margaric acid. The increase in long-chain fatty acids in trained samples seems rather unlikely, since an infiltration of lipids in the muscle is mostly observed in sarcopenic or obese individuals (Gueugneau et al., 2015).On the other hand, the long chain fatty acid 11-eicosenoic acid was among the top downregulated metabolites in

old trained compared to untrained samples (Figure 35 D). This indicates that training in old individuals leads to a distinct regulation of lipid metabolism.

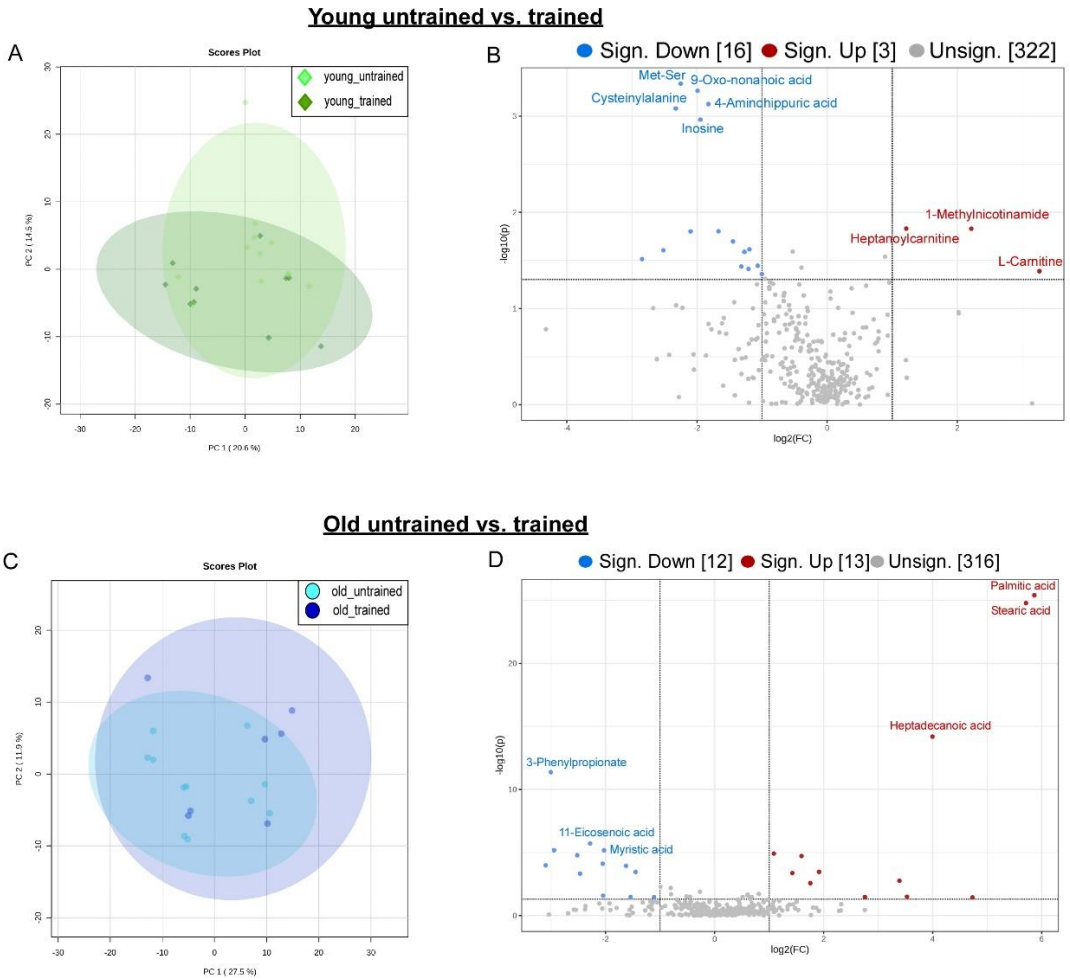

Figure 35: Influence of training status on the secretome of soleus muscle from young and old participants. A: PCA Analysis of young untrained and young trained human soleus samples. B: Volcano Plot Analysis showing significantly increased and decreased metabolites in young trained compared to young untrained samples. C: PCA Analysis of old untrained and old trained human soleus samples. D: Volcano Plot Analysis showing significantly increased and decreased metabolites in old trained compared to old untrained samples.

Overall, untargeted metabolomics of young and old human soleus samples revealed a rather modest effect of training on the basal metabolic profile which likely results from interindividual differences in human participants. In young samples, training showed an influence on (acyl)-carnitines and nicotinamide metabolism. In old samples, metabolomics revealed an influence of training on fatty acid metabolism.

4.2.2. Influence of cAMP stimulation on the metabolome from young trained and untrained soleus muscle

Likewise to murine soleus samples, human soleus samples were treated with the cAMP inducer FSK, to stimulate the muscle and analyse the influence of exercise ex vivo.

PCA of young untrained participants showed that samples cluster according to their treatment group (Control or FSK), but no clear separation of the clusters was observed (Figure 36 A). On the other hand, PCA of young trained samples showed two clearly separated and opposing clusters after cAMP stimulation (Figure 36 D). This indicates, that cAMP stimulation clearly influences both young untrained and trained soleus, but has a greater impact on the metabolome of young trained samples. Thus, young trained soleus might be more sensitive to cAMP induction.

cAMP stimulation of young untrained samples led to a significant increase in the levels of 36 metabolites, whereas 16 metabolites displayed a significant downregulation (Figure 36 B). The majority of significantly upregulated metabolites belonged to the class of “Lipids” (12/36), “Nucleotides” (7/36) and “Hormones” (6/36). The downregulated metabolites were mainly composed of “Lipids” (10/16) (Figure 36 C). Furthermore, cAMP stimulation of young trained samples led to a significant increase in the abundancy of 43 metabolites, and a significant decrease in the abundancy of 48 metabolites (Figure 36 E). The upregulated as well as the downregulated metabolites were mainly composed of “Lipids” (up: 20/48, down 17/43) (Figure 36 F). The higher number of significantly changed metabolites in young trained compared to young untrained samples further underlines the hypothesis, that training elevates the responsiveness to ex vivo exercise in soleus muscle from young participants.

Noteworthy, cAMP stimulation of both young untrained and trained samples, led to a significant increase in prostaglandins like 15-keto-PGE2, and PGE3 and hormones like 11-deoxycortisol. Strikingly, as described in sections 4.1.1.2, 4.1.2.2. and 4.1.3.2., cAMP stimulation increased levels of steroid hormones and prostaglandins in murine BAT, WATi and soleus SKM as well.

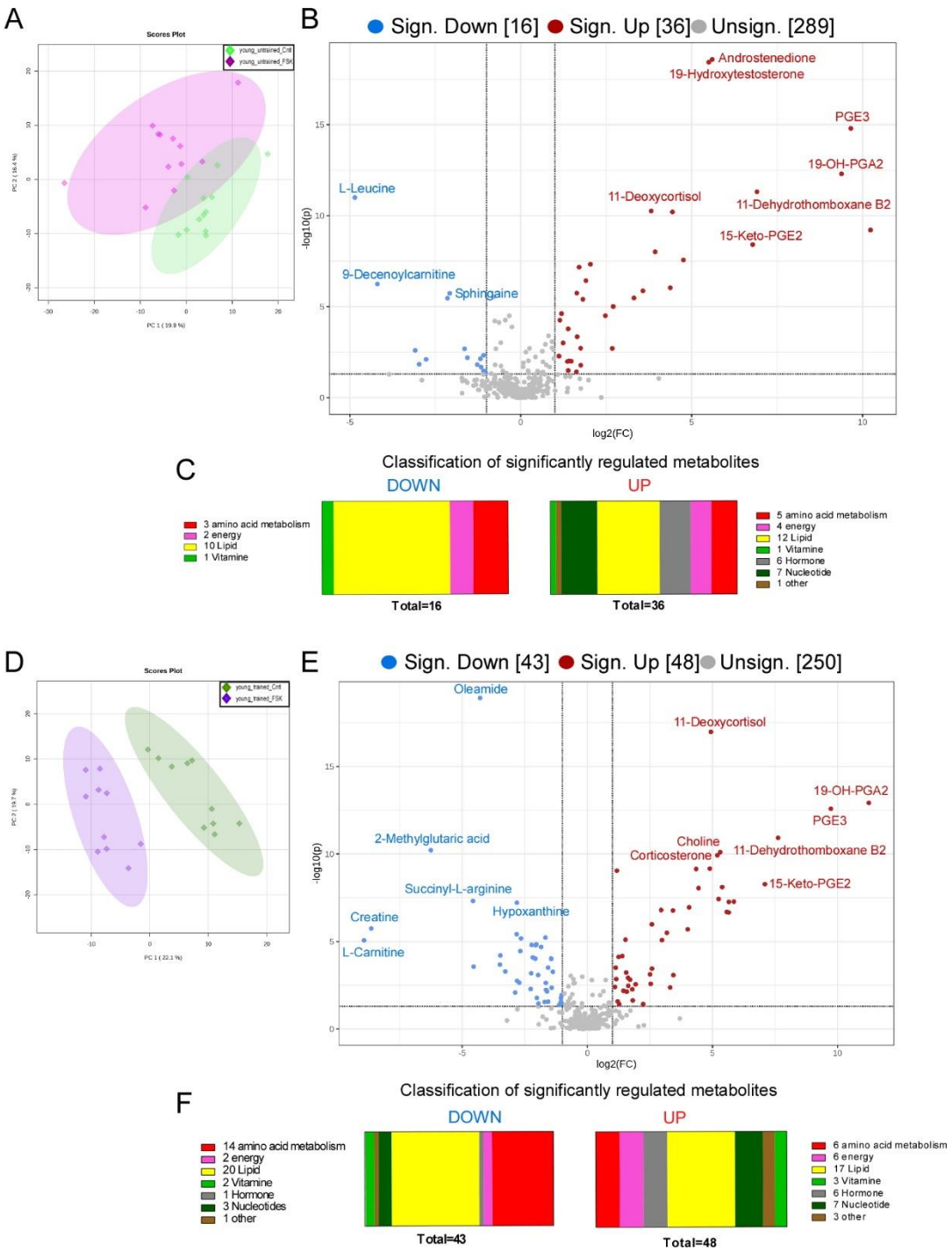

Figure 36: Effects of cAMP stimulation on the secretome of young untrained and trained soleus SKM. A: PCA and B: VP of young untrained soleus SKM after FSK treatment. C: Classification of significantly regulated metabolites from VP analysis(B). D: PCA and E: VP of young trained soleus SKM after FSK treatment. F: Classification of significantly regulated metabolites from VP analysis (E).

Next, the influence of cAMP stimulation on biological pathways in young untrained and trained samples was analysed. As already indicated by VP, QEA of young untrained samples showed highest changes in “Steroid hormone biosynthesis”, depicting 14 metabolites altered in this pathway due to cAMP induction. Moreover, 14 metabolites were altered in “Valine, leucine and Isoleucine

degradation", and 9 metabolites in "Pentose and glucuronate interconversions" (Figure 37 A). During exercise, SKM exerts amino acid pools for energy metabolism. Especially BCAAs (valine, leucine and isoleucine) undergo metabolic processes like oxidation or transamination to fuel citric acid cycle and gluconeogenesis (Gibala, 2001; Shimomura et al., 2004). Furthermore, pentose and glucuronate interconversions play important roles in the carbohydrate metabolic pathway and are involved in processes like gluconeogenesis, trans- and deamination and lipogenesis. As cAMP stimulation is a model for ex vivo exercise, the enrichment of BCAA metabolism after FSK stimulation highlights the importance of BCAAs in SKM metabolism during exercise.

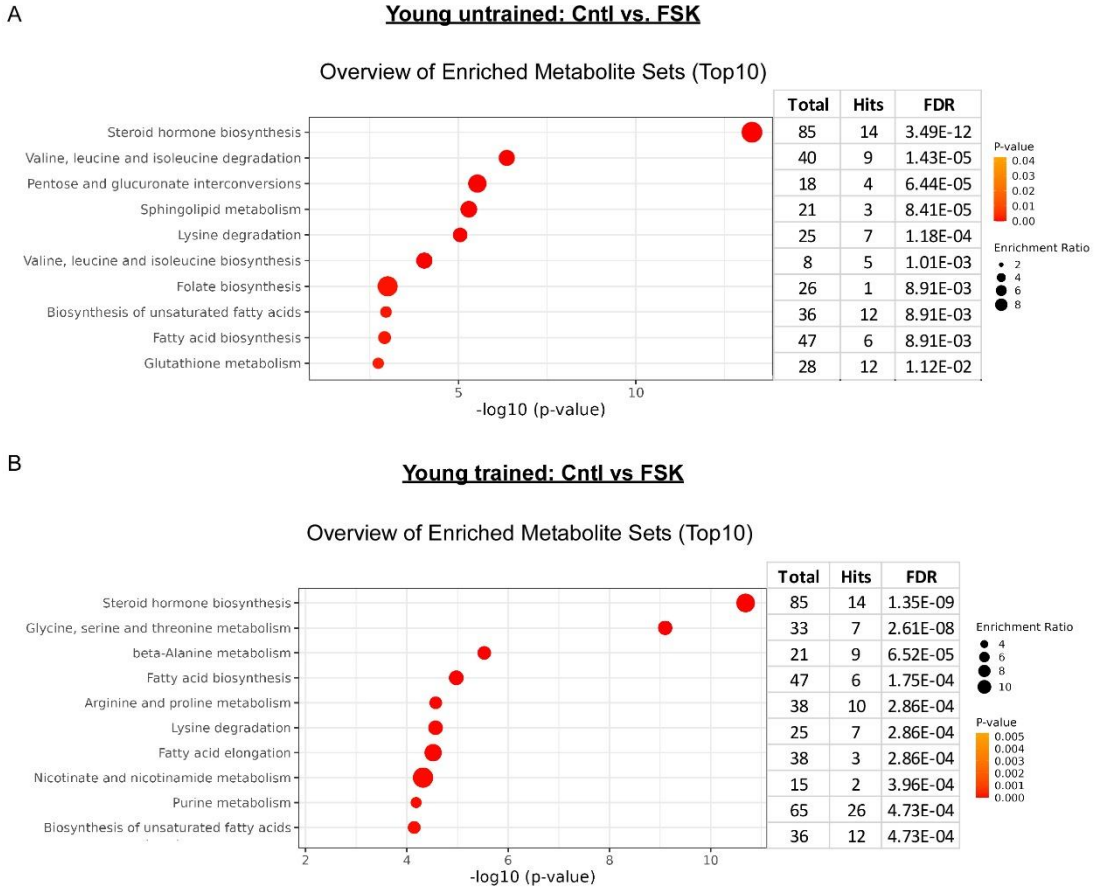

Figure 37: Quantitative Enrichment Analysis of young untrained (A) and trained (B) samples after cAMP stimulation

QEA of young trained samples showed the highest changes in "Steroid hormone biosynthesis" as well. Like in young untrained samples, 14 metabolites were significantly altered due to cAMP stimulation (Figure 37 B). The second most enriched pathway was "Glycine, serine and threonine metabolism", to which 7 metabolites were linked. Thirdly, "β-Alanine metabolism "was highly changed, with 9 metabolites which were altered in this pathway due to cAMP stimulation. Interestingly, glycine levels were found to be consistently lower in patients with obesity and diabetes compared to healthy controls. On the other hand, interventions like weight loss, exercise and improvement in insulin resistance elevates plasma glycine levels in obese and diabetic patients (Adeva-Andany et al., 2018).

Moreover, extracellular serine and glycine are vital for muscle stem cell expansion and reduced levels of serine and glycine can impair SKM regeneration (Gheller et al., 2021). Alanine is one predominant amino acid which is released by SKM and taken up by the liver to fuel gluconeogenesis. Intriguingly, the formation and release of alanine from rat SKM can be increased by many amino acids, amongst others glycine, serine and threonine (Garber et al., 1976). Additionally, alanine is known for its role in the synthesis of carnosine, of which a supplementation showed an improvement in anaerobic exercise capacity and performance (Matthews et al., 2019).

Overall, cAMP stimulation of young untrained vs. trained samples displayed a significant influence on the metabolic profile of both groups. Yet, cAMP induction showed a greater effect in young trained samples compared to untrained. Moreover, ex vivo exercise led a marked increase in steroid hormones and prostaglandins in both untrained and trained samples. Furthermore, amino acid metabolism was enriched in young untrained and trained samples, with the highest influence on BCAA and glycine, serine, threonine and alanine metabolism, respectively.

4.2.3. Influence of cAMP stimulation on the metabolome from old trained and untrained soleus muscle

Next, samples from old participants were analysed for the enrichment of biological processes due to cAMP induction (Figure 38). Unexpectedly, PCA from old untrained participants showed two clearly separated clusters after cAMP stimulation (Figure 38 A). This clear separation could not be observed for the old trained samples. Here the two groups showed a trend, but not completely separated clusters (Figure 38 C).

cAMP stimulation led to the significant upregulation of 39, and downregulation of 16 metabolites in the old untrained group (Figure 38 B). The majority (14) of the upregulated metabolites were classified as lipids, whereas the downregulated metabolites were mainly composed of lipids (6) and metabolites associated to amino acid metabolism (5). Among the top upregulated metabolites were androstenedione, 19-hydroxytestosterone, 11-dehydrothromboxane B2 and PGE3. Among the top downregulated metabolites were carnosine, 3-phenylpropionate and myristic acid. Interestingly, 3-phenylpropionate and myristic acid were already detected as significantly downregulated metabolites in old trained compared to old untrained samples without cAMP stimulation (c.f. Figure 35 D).

cAMP induction of old trained samples changed the levels of a comparable number of metabolites: 41 metabolites were significantly upregulated, and 12 significantly downregulated (Figure 38 D). The majority of up as well as downregulated metabolites were classified as lipids (19 up, 8 down). Under the top upregulated metabolites were again PGE3, androstenedione and 19-hydroxytestosterone. Strikingly, palmitic acid, stearic acid and heptadecanoic acid were among the most prominent

downregulated metabolites after cAMP stimulation. These three fatty acids were among the top upregulated in old trained compared to old untrained samples under basal conditions as well (c.f. Figure 35 D)

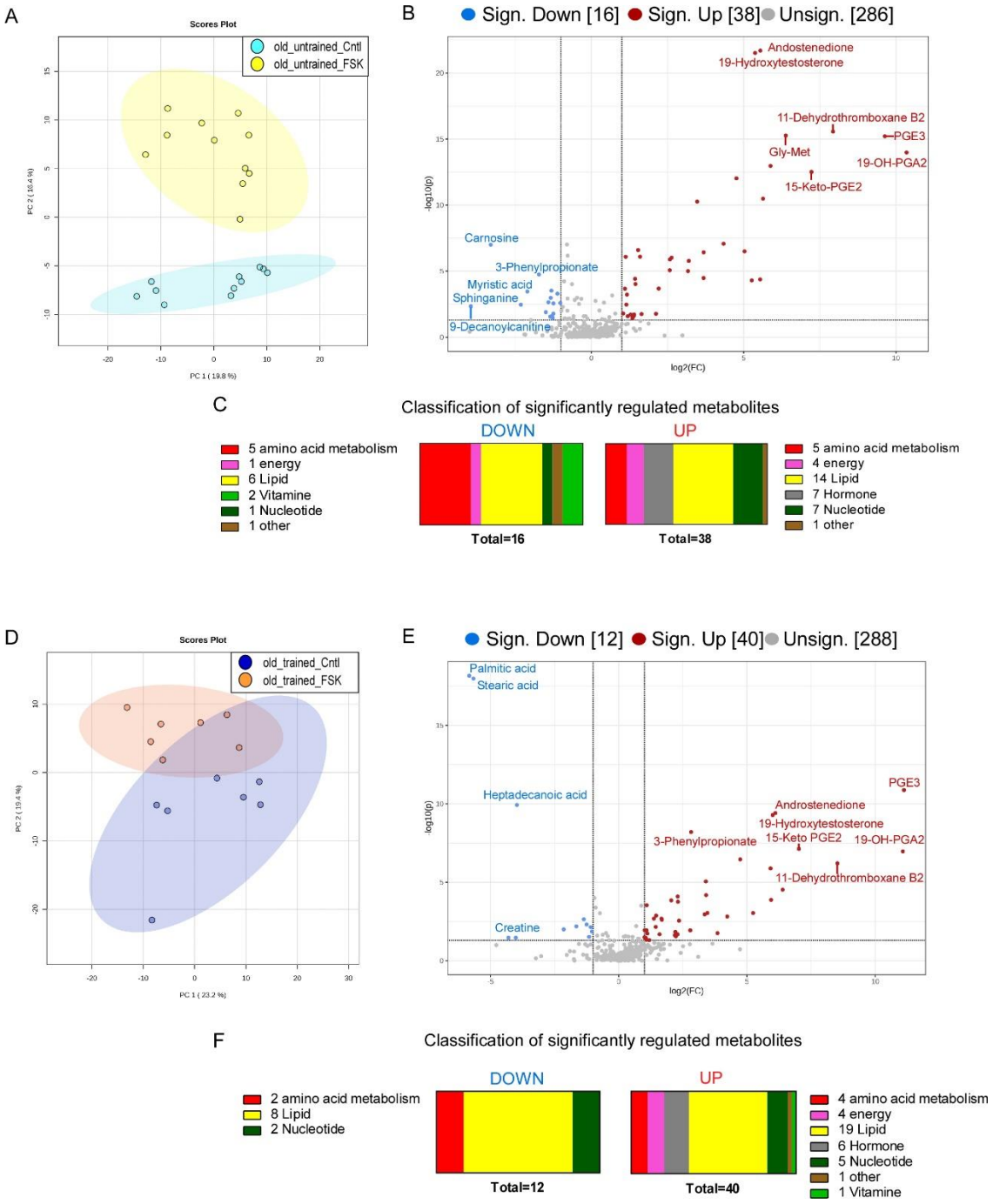

Figure 38: Effects of cAMP stimulation on the secretome of old untrained and trained soleus SKM. A: PCA and B: VP of old untrained soleus SKM after FSK treatment. C: Classification of significantly regulated metabolites from VP analysis(B). D: PCA and E: VP of old trained soleus SKM after FSK treatment. F: Classification of significantly regulated metabolites from VP analysis (E).

In the next step, the influence of ex vivo exercise on the enrichment of biological pathways was analysed in old soleus samples. Similar to young samples, QEA of old samples placed “Steroid hormone biosynthesis” pathway among the top three changed pathways, both in untrained and trained old samples (Figure 39 A,B). Furthermore, QEA of old untrained soleus revealed the enrichment of “Lysine degradation” and “Fatty acid degradation” due to cAMP stimulation.

QEA of old trained samples, showed “Fatty acid biosynthesis” and “Biosynthesis of unsaturated fatty acids” among the top enriched pathways due to cAMP induction (Figure 39 B). Strikingly, pathways related to fatty acid metabolism were highly enriched in both old untrained and trained sample groups upon cAMP induction. Additionally, lipids accounted for the majority of significantly regulated metabolites in both groups, as well. Furthermore, long chain fatty acids were among the top upregulated metabolites, and “Biosynthesis of unsaturated fatty acid” pathway was highly enriched in old murine soleus samples compared to young. On the contrary, lipid metabolism played a subordinate role in ex vivo exercise in human young untrained and trained samples. This underlines once more, that aging SKM is infiltrated with lipids, which on the one hand act as energy source during SKM stimulation and exercise, but on the other hand impair SKM strength and function. The observed enrichment in fatty acid metabolism in both untrained and trained old samples could hint at a general transition of SKM metabolism from amino acid metabolism to lipid metabolism due to aging.

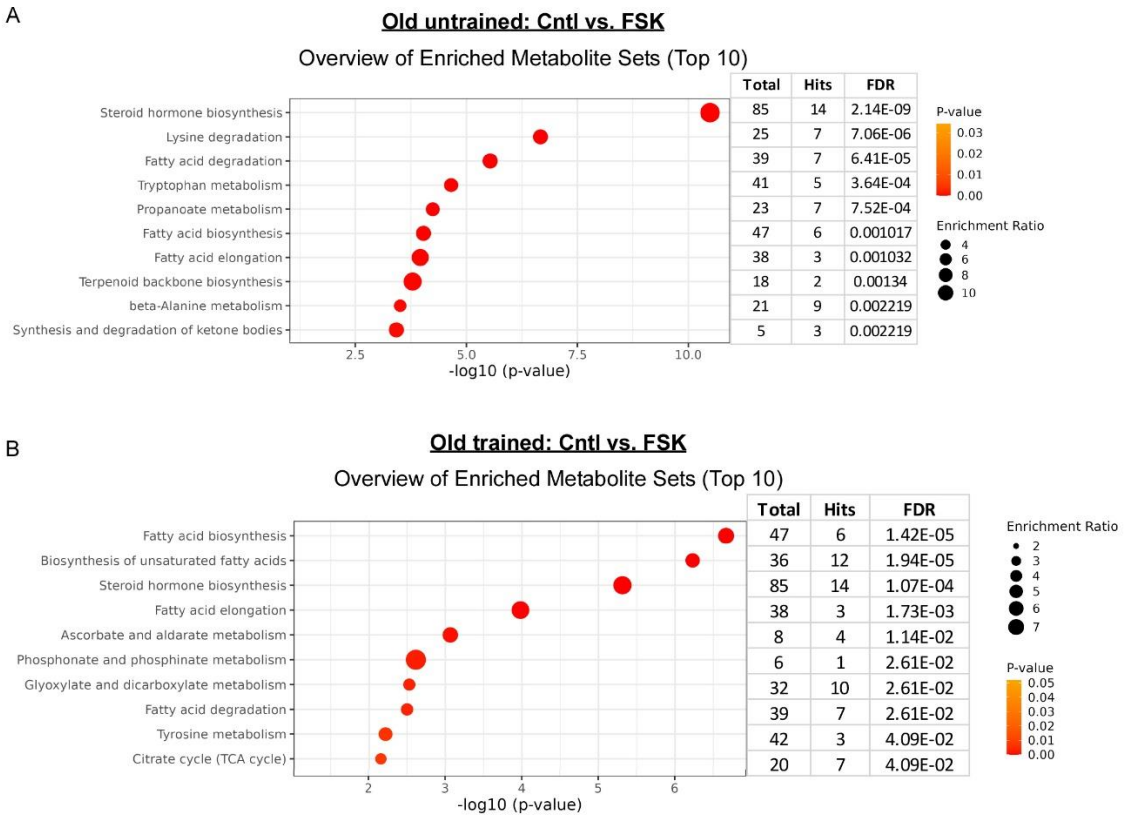

Figure 39: Quantitative Enrichment Analysis of old untrained (A) and old trained (B) samples after cAMP stimulation

4.2.4. Analysis of common and unique metabolome signatures between all sample groups

To examine the metabolomics data for interesting metabolite candidates, all significantly regulated metabolites after FSK treatment were analysed for matches. Due to cAMP stimulation 14 metabolites were upregulated in all groups (Figure 40 A). Heat Map Analysis of all groups and conditions showed that sample groups cluster according to experimental treatment (Cntl/FSK stimulation) rather than aging. Furthermore, heat map depicts the 14 commonly upregulated metabolites (Figure 40 B). Among these metabolites were the prostaglandins PGE3, 15-Keto-PGE2 and 19-hyroxyprostaglandin A2. Also steroid hormones were commonly upregulated: 19-hydroxytestosterone, androstenedione, corticosterone, estratetraenol. To analyse whether all 14 metabolites were regulated in the same manner, the relative peak intensities of all groups were compared to each other. In deed all 14 metabolites were upregulated in a comparable manner (Figure 40 C). A similar regulation pattern of prostaglandins and steroids was observed after the stimulation of young and old murine BAT, WATi and soleus, as well. This not only indicates that this cAMP-dependent upregulation is consistent throughout aging, but also throughout different species and different metabolically active tissues.

Venn diagram of the significantly regulated metabolites from all groups furthermore depicted the number of unique metabolites for each group (Figure 40 A). The greatest number of uniquely regulated

metabolites were detected in the young trained groups (39 metabolites), followed by the old trained group (28 metabolites). The young untrained group showed 13 and the old untrained group 10 unique metabolites. The high numbers of unique metabolites in young and old trained samples might indicate a distinct metabolome profile, which could result from training status.

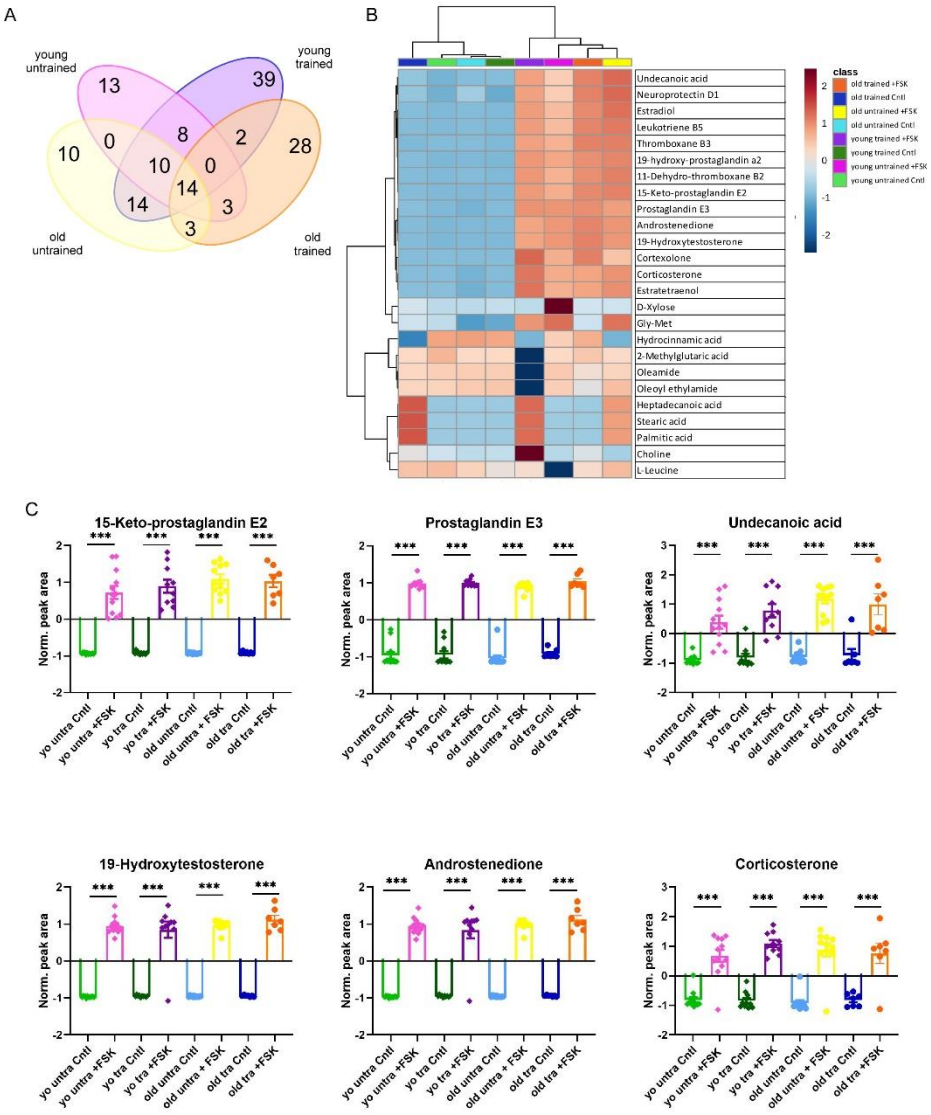

*Figure 40: Shared upregulated metabolites after cAMP stimulation. A: Venn diagramm showing shared metabolites between different groups. B: Heat Map showing top 25 regulated metabolites, depicting shared upregulated metabolites of all groups after FSK treatment. C: Bar graph showing 6 of the 14 commonly upregulated metabolites. Normalised peak areas are represented as mean ± SEM, one-way ANOVA, young soleus n=6, old soleus n=9, *p≤0.05, **p≤0.01, ***p≤0.001*

The young trained group showed the highest number of uniquely regulated metabolites: 39 metabolites were uniquely regulated after cAMP stimulation in young trained soleus samples. Of those, 16 were upregulated and 23 were downregulated (Figure 41 A). In a next step, these metabolites were analysed for enriched biological pathways by ORA. ORA of the unique metabolites showed the enrichment of “Arginine and proline metabolism” for which 4 hits were detected. Those metabolites

were: L-arginine, spermidine, L-proline and pyruvic acid. Also “β-Alanine metabolism” was enriched and 3 hits were associated with this pathway which were dihydrouracil, L-histidine and also spermidine. L-Arginine, spermidine and L-proline were uniquely upregulated in young trained samples after cAMP stimulation. Dihydrouracil, L-histidine and histamine were downregulated after the stimulation (Figure 41 C). The enrichment of amino acid metabolism in young trained samples furthermore indicates that young SKM utilises amino acids, either from protein degradation or from free amino acid pools, to fuel the elevated energy demand during stimulation.

Interestingly, the polyamine spermidine was found to be uniquely upregulated upon cAMP in young trained samples. Spermidine was recently shown to be downregulated in SKM of aged mice and a supplementation of spermidine in a combination with exercise was shown to ameliorate skeletal muscle atrophy (Fan et al., 2017; Uchitomi et al., 2019). Furthermore, L-histidine was uniquely downregulated due to ex vivo exercise in young trained soleus. L-histidine itself functions as a pH buffer, metal ion chelator and as an antioxidant. Additionally, it serves as a precursor in the synthesis of carnosine (β-Alanyl-L-histidine) and histamine. (Holeček, 2020). Carnosine is involved in SKM metabolic processes like excitation-contraction coupling and a supplementation of carnosine in senescence-accelerated mice can increase life span (Yuneva et al., 1999; Boldyrev et al., 2013). Histamine, on the other hand, is a driver of inflammation and usually originates from the degranulation of mast cells. In SKM, histamine levels are increased upon exercise, which leads to the degranulation of mast cells and de novo synthesis of histamine. This in turn leads to vasodilation in the exercised muscle (Romero et al., 2017). Furthermore, increased levels of histamine were detected in SKM of aged mice (Uchitomi et al., 2019). Both L-histidine and histamine levels were decreased after cAMP stimulation of young trained soleus. This could indicate that both metabolites are taken up by the muscle to fuel the synthesis of carnosine or to clear the muscle tissue from potentially harmful metabolites.

In total ORA linked 7 metabolites to two biological pathways. This in turn leaves 32 metabolites which could not be linked significantly to any pathways. Even though those metabolites might not indicate the enrichment of a specific process, they could still be of metabolic relevance.

In a next step these metabolites were analysed individually to check for interesting candidates. Indeed, six metabolites showed a strong regulation upon cAMP stimulation in young trained samples. Choline was highly upregulated after FSK stimulation. L-Carnitine, oleamide, hypoxanthine, taurine and methylnicotinamide showed a pronounced reduction after cAMP induction (Figure 41 D).

Choline is an essential micronutrient which belongs to the Vitamin B family. It has many important metabolic functions. For example, it serves as a methylgroup donor in the synthesis of S-

adenosylmethionine and it is a precursor in the synthesis of acetylcholine. Additionally, it influences cell membrane structure and function by its role in phospholipid synthesis (Zeisel et al., 2018; Moretti et al., 2020). In muscle metabolism, choline improves mitochondrial energy metabolism and lipid metabolism by decreasing FA synthesis. It can lower the intramuscular fat content and improve insulin signalling. Low concentrations of choline are associated with muscle impairment and wasting (Zeisel et al., 2018). The higher abundancy of choline in the supernatant from young trained muscle could be a result of the secretion of choline from the muscle itself to act in an auto- or paracrine effect. This secretion might be amplified by the training status.

L-Carnitine is a non-essential amino acid which plays a key role in lipid metabolism and beta-oxidation (Wächter et al., 2002). It forms long chain acetylcarnitine esters together with long chain fatty acids which allows their transport into the mitochondria. Carnitine is a key metabolite in skeletal muscle and its deficiency results in myopathy and impaired fatty acids oxidation. Especially in older patients this can in turn lead to exercise intolerance and rhabdomyolysis (Adeva-Andany et al., 2017). The young trained muscle might have a higher need for L-carnitine to induce fatty acid metabolism which could explain the lower levels of L-carnitine after cAMP stimulation.

Oleamide (9-Octadecenamide) is a long chain fatty amide of the fatty acid oleic acid. It has several biological functions like the induction of sleep, appetite and food intake, antianxiety and analgesic effects (Hiley and Hoi, 2007). Oleamide was found to be increased in the interstitial fluid of rats after exercise (Zhang et al., 2019) and a dietary intake of oleamide can have beneficial effects of skeletal muscle atrophy in mice (Kobayashi et al., 2021). The decreased levels of oleamide after FSK stimulation in young trained muscle might be explained with a higher demand of the fatty amide in comparison to the other samples groups.

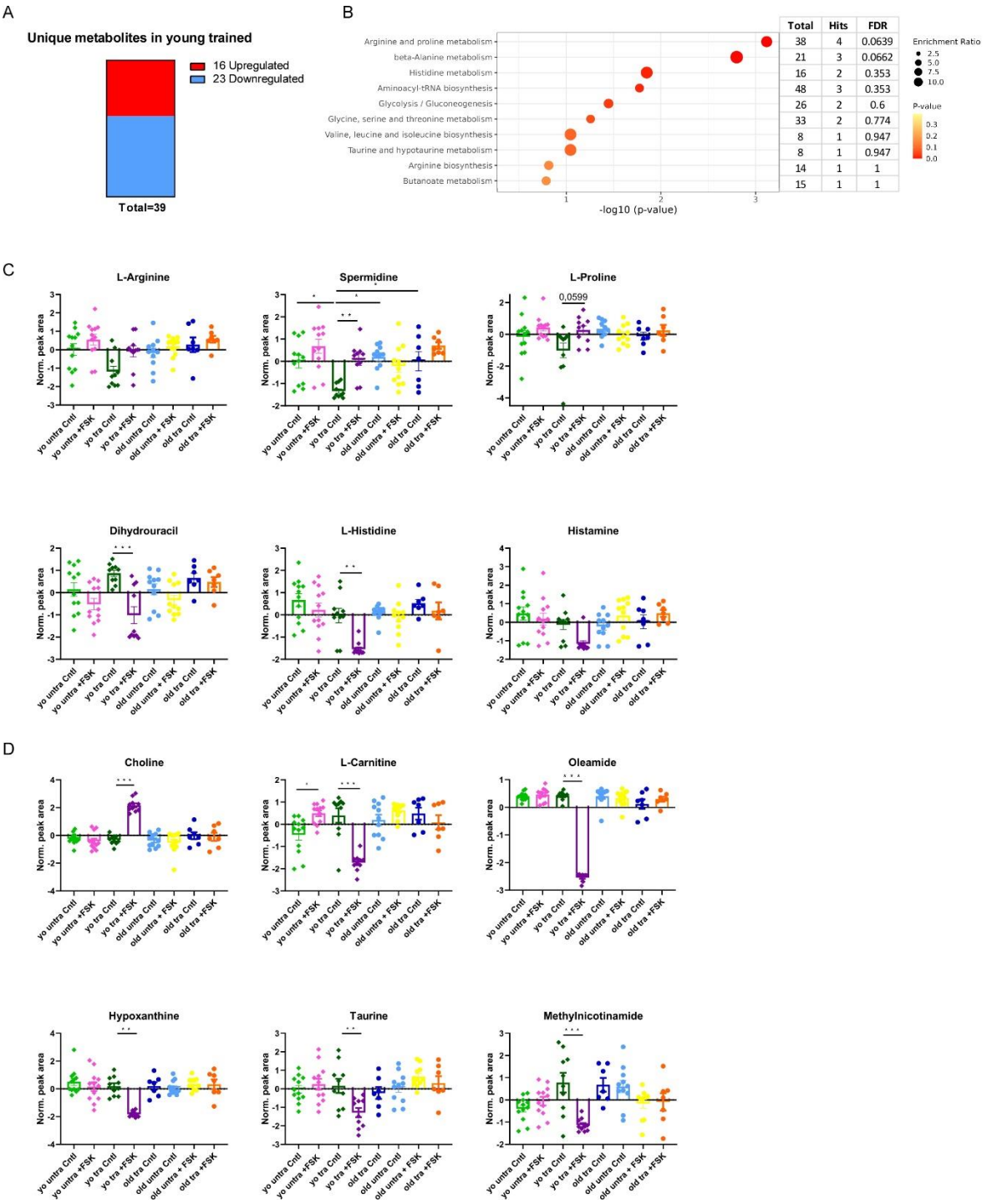

*Figure 41: Unique metabolites in young trained samples after FSK stimulation. A: Classification of the unique metabolites in up- or downregulated classes. B: ORA of unique metabolites from young trained samples. C: Normalised peak areas of detected hits from ORA. D: Normalised peak areas of special metabolites with pronounced unique effects in young trained samples. Normalised peak areas are represented as mean ± SEM, one-way ANOVA, young soleus n=6, old soleus n=9, *p≤0.05, **p≤0.01, ***p≤0.001*

Overall, untargeted metabolomics of human soleus muscle from young and old, untrained and trained participants revealed 14 commonly upregulated metabolites after cAMP induction. Like already observed in BAT, WATi and soleus from young and old mice, those metabolites contained steroid

hormones and prostaglandins. Moreover, the upregulation magnitude showed no influence of aging, since all metabolites were upregulated with similar fold change.

cAMP stimulation in young trained samples led to the greatest number of uniquely regulated metabolites, indicating that regular physical activity remodels SKM metabolism which in turns leads to a unique metabolic profile after ex vivo exercise.

4.3. Auto- and paracrine effects of muscle metabolites on the differentiation of skeletal muscle cells and brown adipocytes

4.3.1. Effects of muscle metabolites on the differentiation of murine C2C12 cells

The analysis of untargeted metabolomics of murine BAT, WATi, soleus muscle and human soleus muscle revealed several metabolites which were commonly upregulated in all sample groups after cAMP induction. Among those were eicosanoids like Prostaglandin E2 or E3, and hormones like corticosterone and desoxycortisol. Especially human soleus from young trained samples revealed a unique metabolic profile with a high number of uniquely changed metabolites upon cAMP stimulation. The metabolites with the most pronounced changes were histamine, L-carnitine, oleamide and choline. To study the effect of these metabolites on muscle cells, C2C12 cells were cultured *in vitro* and treated with these metabolites. Cells were treated either overnight for 16h to study the acute effect, or the metabolites were applied throughout the whole differentiation to study a long-term effect. Samples were examined for the effects on myogenesis, muscle differentiation, muscle formation and cell maintenance using a broad range of gene markers: *MyoD*, *Myf5* and *Myogenin* belong to the myogenic regulatory factors family (MRFs) and are crucial transcription factors for myogenesis. *MyoD* and *Myf5* ensure the fate of cell differentiation towards skeletal muscle lineage. A more downstream transcription factor is *Myogenin* but also *MyoD*, which activate myogenic differentiation (Zammit, 2017). *Pax3* is a stem cell marker for satellite cells. *Mef2c* is an important transcription factor in the maintenance of sarcomere integrity and postnatal maturation of skeletal muscle (Potthoff et al., 2007). *Myomaker* is a crucial factor for myoblast fusion during muscle development, differentiation and regeneration (Millay et al., 2014).

The acute metabolite treatment with PGE2, PGE3, corticosterone and desoxycortisol led to a significant decrease in the expression of *Myogenin* and *Myomaker*. Furthermore, the acute treatment with PGE2 and PGE3 also led to a significant reduction of *Mef2c.* PGE3 led to a significant increase in the expression of *MyoD.* Corticosterone and desoxycortisol increased the expression of *Myf5* (Figure 42 *A)*.

Additionally, a long-term treatment with desoxycortisol led to a significant increase in the expression of *Myf5*, whereas corticosterone was able to increase expression levels of *Myogenin.* PGE2 decreased levels of *Mef2c* significantly. *MyoD, Myomaker* and *Pax3* remained unchanged (Figure 42 B).

Together these data might indicate that the acute and chronic treatment with PGE2 could negatively influence muscle regeneration and repair. A treatment with steroid hormones on the other hand, might have a positive effect on muscle proliferation and differentiation.

C2C12 cells were also treated with metabolites, which were found to be specifically regulated in young trained samples. In an acute treatment with the four metabolites histamine, carnitine, oleamide and choline, no significant effect was observed on myogenesis (Figure 42 C).

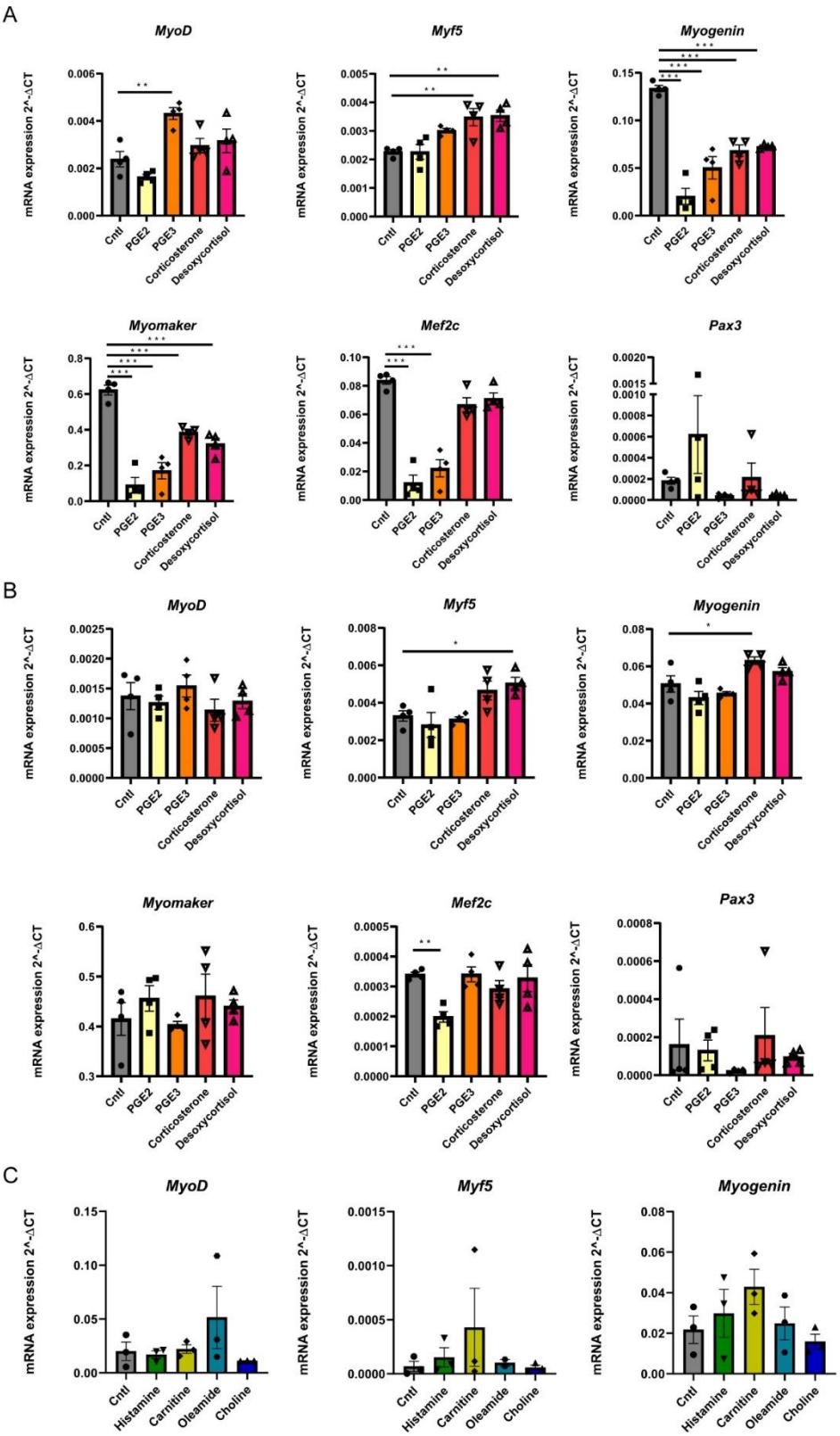

*Figure 42: Effects of secreted metabolites from skeletal muscle on C2C12 differentiation. A: Acute treatment (16h) of C2C12 skeletal muscle cells with shared metabolites. B: Chronic treatment (7 days) of C2C12 skeletal muscle cells with shared metabolites. C: Acute treatment (16h) of C2C12 skeletal muscle cells with unique metabolites from young trained samples. Metabolite concentrations: PGE2/ PGE3 c= 10ng/mL, Corticosterone/ Desoxycortisol c=50ng/mL. Histamine/Carnitine/Oleamide/Choline c=1µM. Expression data were normalised to GAPDH and are represented as mean ± SEM, One-way ANOVA, n=4, *p≤0.05, **p≤0.01***p≤0.001*

4.3.2. Effects of muscle metabolites on the differentiation of human skeletal muscle cells

Following up the treatment of murine skeletal muscle cells, the effect of particular metabolites on human skeletal muscle cells was studied. Therefore, hSKM cells were cultured *in vitro* and treated with the indicated metabolites for 16h overnight. The samples were analysed for effects on myocyte differentiation. No differences in the expressions levels of *MyoD* or *Mef2c* were observed after the metabolite treatment (Figure 43).

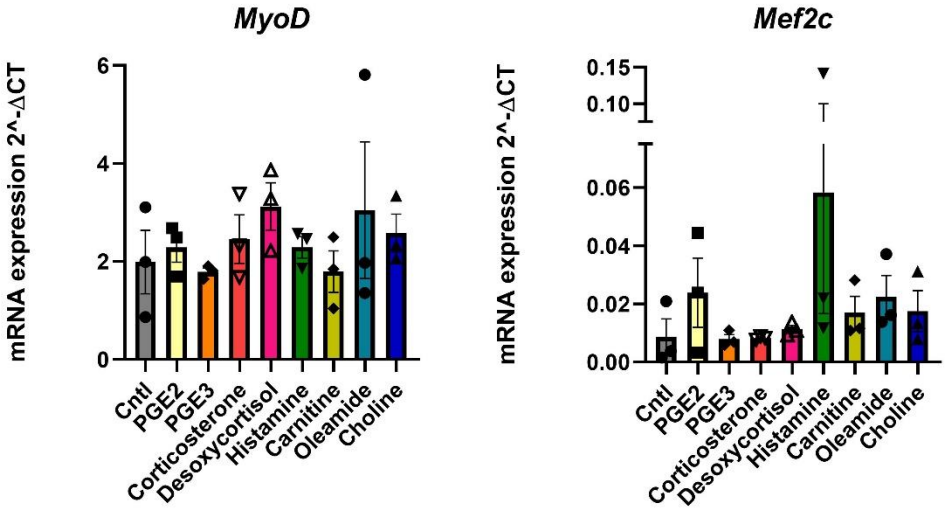

Figure 43: Acute effects (16h) of secreted metabolites from skeletal muscle on hSKM differentiation. Metabolite concentrations: PGE2/PGE3/Corticosterone/Desoxycortisol/Histamine/Carnitine/Oleamide c=100nM. Expression data were normalised to TBP and are represented as mean ± SEM, One-way ANOVA, n=3.

4.3.2. Effects of muscle metabolites on the differentiation of murine brown adipocytes

Factors which are secreted by the muscle during exercise or stimulation do not only have an effect on the muscle itself but can also influence other peripheral organs. Some myokines, like Irisin or β-aminoisobutyric acid, link skeletal muscle and adipose tissue and influence adipose tissue metabolism (Sanchez-Delgado et al., 2015; Stanford and Goodyear, 2018)

In a next step, it was analysed if the before mentioned metabolites might be potential factors which regulate BAT metabolism. Therefore, the effect of these metabolites on BAT differentiation and functionality was investigated. Murine BA were cultured in vitro and treated overnight (16h) with the selected metabolites. Again the samples were analysed for the metabolites' effect on the expression levels of cell specific genes.

Two metabolites could influence BA differentiation significantly: Carnitine significantly increased the expression levels of PPARg and AP2; whereas choline significantly increased the expression level of AP2. The remaining 6 metabolites showed no significant effect on gene expression levels (Figure 44).

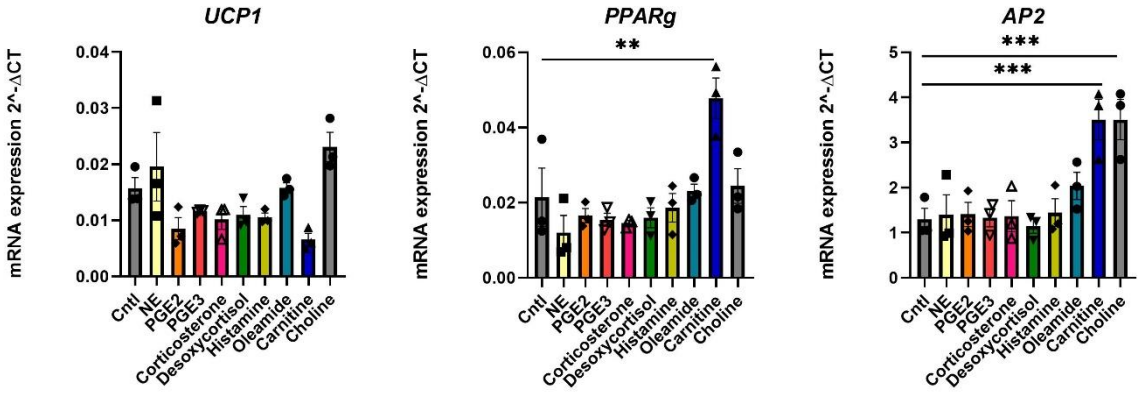

*Figure 44: Acute effects (16h) of secreted metabolites from skeletal muscle on murine BA differentiation. Metabolite concentrations: NE/PGE2/PGE3/Corticosterone/Desoxycortisol/Histamine/Carnitine/Oleamide c=1 µM. Expression data were normalised to GAPDH and are represented as mean ± SEM, One-way ANOVA, n=3, **p≤0.01***p≤0.001.*

5. Discussion

5.1. Influence of aging on the metabolome of young and old BAT

BAT is mainly known for its function as a thermogenic organ, which dissipates energy and thereby generates heat. Especially during activation by i.e. cold exposure, BAT serves as a metabolic sink for various metabolites like glucose, lactate and fatty acids (Park et al., 2023). Moreover, BAT has the ability to produce and secrete various autocrine or paracrine factors that influence metabolic pathways. The composition of this secretome influences BAT itself but furthermore regulates the communication with peripheral organs. BAT is highly affected by aging, including loss of BAT mass and function, a reduced sympathetic innervation and impaired endocrine function. Yet, the mechanisms involved in BAT aging are largely unknown. To study the influence of aging on the profile of metabolites secreted by young and old BAT, untargeted metabolomics was performed.

PCA of young and old BAT samples showed clustering within the sample groups, but a clear separation of the clusters according to age. This separation indicates significant differences of the metabolome between young vs. old BAT. However, although PCA clearly showed the variation between samples, it does not indicate in which direction (i.e. up- or downregulation of particular secreted factors) or with which magnitude the variations can be found.

VP analysis showed the significant upregulation of several amino acids and small peptides in old BAT. Among the strongest regulated metabolites were the peptide carnosine and its methylated form anserine. Moreover, precursors or breakdown products of these molecules like L-alanine or L-histidine were also significantly upregulated. Carnosine and anserine are mainly found in SKM, heart and brain of mammals and their levels were shown to decrease during aging (Cararo et al., 2015; Banerjee and Poddar, 2020). Carnosine was described to have a function as antioxidant and regulator of aged proteins which could be one among other reasons that they are also regarded as an anti-aging metabolite (Hipkiss et al., 2002). Nagasawa et al. showed that carnosine inhibits lipid peroxidation and oxidative modification of proteins in rat SKM *in vitro* and a reduction in muscle lipid peroxidation in SKM of rats fed a histidine supplemented diet (Nagasawa et al., 2001). Higher levels of carnosine and anserine might therefore be an indicator for compensatory mechanisms to counteract aging processes in BAT. Overall, the high abundancy of several amino acids, small peptides and linked metabolites, could indicate a higher demand of amino acid or peptide synthesis. The degrading enzyme serum carnosinase-1 can be found in brain, liver and serum of humans and the cytosolic form carnosinase-2 is ubiquitously epxressed in humans (Boldyrev et al., 2013). Elevated levels of carnosine, anserine, alanine and histidine could result from an increased secretion and degradation of carnosine and anserine. The resulting amino acids could then fuel the higher demand for amino acids during aging.

VP also showed the downregulation of lipids like OEA, LEA and S1P in old BAT. OEA and LEA both belong to the class of NEAs which are regarded as positive regulators of metabolic parameters and lipid metabolism (Brown et al., 2017; Tovar et al., 2023). The lower levels of OEA and LEA in older BAT might be linked to impaired metabolic function concomitant with increased body weight and body fat mass in older individuals. A lack of NEA could increase hunger and weight gain due to the reduced satiety promotion and have a negative impact on lipid metabolism. Furthermore, higher levels of short- and medium-chain n-acylglycines and n-acyl ethanolamides were found in the young group compared to the old group. In BAT, n-acylglycines are so far only poorly studied. Gujias et al. described that during BA differentiation, myristoylglycine can be synthesized de novo and secreted from BAs. Furthermore, they identified myristoylglycine as an inducer of adipocyte browning (Guijas et al., 2022). The significantly higher levels of n-acylethanolamides and n-acylglycines in the supernatant of young BAT compared to old BAT, make them interesting adipokine candidates, which could enhance BA differentiation. Reduced abundance of these metabolites in old BAT might contribute to reduced BAT mass and activity.

S1P is a lysosphingolipid and bioactive lipid mediator which is mostly characterized by its role in the vascular and immune system where it regulates i.e. angiogenesis and immune cell trafficking (Hla et al., 2008). S1P and its precursor metabolites, sphinganine and 3-ketosphingosine were downregulated in old BAT. In general, lower levels of S1P in old BAT might be contradictory to recent publications. As S1P was found to be elevated in serum of obese mice and humans (Kowalski et al., 2013), one could expect also higher levels in aged samples. Also sphingolipids were found to be elevated in murine aged BAT (Gohlke et al., 2019). The lower abundance of S1P in older samples might be the consequence of the lower abundance of its precursors. Furthermore, the activity of the synthesizing or degrading enzymes could influence S1P abundancies. S1P is synthesized by sphingomyelinases and ceramidases, which are ectoenzymes. Therefore, sphingosine can be generated in the extracellular space. S1P levels were so far only measured in serum samples or grinded BAT tissue but not in the supernatant or extracellular space. S1P might be taken up by aged BAT whereas young BAT might secrete S1P. Additionally, S1P was found to be highly regulated by cAMP stimulation in both young and old BAT, even though in opposing manner: high levels of S1P in young BAT were downregulated, and low levels of S1P in old BAT were upregulated after cAMP induction. In old BAT, the S1P precursors 3-dehydropshingosine and sphinganine were downregulated, albeit not significantly. This could indicate an increased synthesis of S1P from its precursors in old BAT due to cAMP.

cAMP stimulation of young and old BAT led to significant changes in the metabolome of both groups. However, PCA showed that FSK treatment led to the formation of two clearly separated clusters in young but not old BAT, indicating a higher sensitivity to cAMP in young tissue. This was furthermore

represented by VP analysis: in total, 28 metabolites were significantly changed in young BAT (22 up, 6 down), whereas only 15 were significantly changed in old BAT (12 up, 3 down). The higher sensitivity or response to cAMP stimulation in young BAT could result from higher expression of adenylyl cyclases. This in turn might result in higher cAMP levels, causing more pronounced downstream signalling. Alternatively, expression of cAMP degrading phosphodiesterases might be different between young and old BAT. Future work should be directed at analysing cAMP regulating enzyme expression in young an old BAT via RNA sequencing or proteomics.

cAMP induction led to the secretion of ten shared metabolites between young and old BAT, all of which were steroid hormones, prostaglandins and acylcarnitines. Additionally, "Steroid hormone biosynthesis" was the top enriched pathway in both sample groups after cAMP stimulation. Steroid hormones are mostly synthesized in and secreted from the gonads or adrenal gland, but also from the liver (Schiffer et al., 2019). In general, steroid hormone levels are regulated by the enzyme 11β-hydroxysteroid-dehydrogenase 1 (HSD1). Previous studies have shown that members of the C/EBP family control intracellular levels of glucocorticoids in preadipocytes via the regulation of cAMP dependent HSD1 expression (Gout et al., 2006). Hence, cAMP stimulation might generate the different steroid pattern observed in BAT via increased HSD1 expression or activity. Interestingly, Ramage et al. demonstrated that glucocorticoids can increase isoprenalin-stimulated respiration in murine BA in vitro (Ramage et al., 2016). Higher levels of corticohormones after cAMP stimulation could therefore be an amplification signal to induce BAT activity in an autocrine manner after stimulation by i.e. cold exposure. Moreover, Maushart and colleagues showed in a randomized and controlled clinical trial that high-dose glucocorticoids improved resting EE, but had no effect on cold-induced thermogenesis in humans (Maushart et al., 2023). Although overall steroid hormone levels are known to decrease during aging (Graja et al., 2019), the data presented here indicate, that aged BAT still preserves its capacity to produce or secrete steroids upon stimulation.

Prostaglandins are physiologically active lipids belonging to the class of eicosanoids, which are known regulators of BAT: PGE2 has been shown to promote murine BAT formation (Tao et al., 2022). Moreover, activation of murine and human BAT via cold exposure or pharmacological stimulation increases plasma levels of PGE1, PGE2 and other lipid mediators (Park et al., 2023; Walker et al., 2024). Here, cAMP stimulation of young and old BAT led to a significant increase in PGE3 levels. These data together with the previously published reports might indicate that lipid mediators such as PGE3 may serve as biomarkers of BAT.

Especially in reproductive tissues, prostaglandins and steroids are known to have mutual influences on each other's regulation and together regulate the tissue's functionality (Goff, 2004). Possibly, this could also be the case in BAT: under stimulatory conditions both steroids and prostaglandins are

formed and secreted and could influence BAT metabolism in a synergistic way. This stimulatory effect of cAMP on the metabolites' formation and secretion seems to be unaffected by aging, since the increase of metabolite abundance was of similar magnitude in both young and old tissue.

Besides steroids and prostaglandins, acylcarnitine levels were induced by cAMP stimulation in young and old BAT. Noteworthy, the production of acycarnitines has recently been linked to a subpopulation of lipogenic brown adipocytes important for thermogenic memory (Lundgren et al., 2023).

Metabolites uniquely regulated by cAMP stimulation of young BAT are of particular interest, as they might be potential mediators of self-renewal and sustained function. Lack of these metabolites in old BAT in turn might be involved in decline of metabolic capacity. Valine, leucine and isoleucine are amino acids which together form the group of branched-chain amino acids (BCAA). Lower levels of leucine and isoleucine, and higher levels of valine were detected in the supernatant of young BAT. Furthermore "Valine, leucine and isoleucine metabolism" was among the top regulated pathways in young compared to old BAT. cAMP stimulation slightly increased leucine and isoleucine and especially 3-ketoleucine levels, and decreased valine levels in young but not old BAT. Under stimulatory events like cold exposure, BCAAs are known to be taken up by BAT to fuel thermogenesis (Park et al., 2023). Impaired BAT activity can reduce BCAA clearance, while intact BAT takes up and filters circulating BCAAs (Yoneshiro et al., 2019). Moreover, BCAA catabolism in adipose tissues has been shown to promote age-associated metabolic derangement (Han et al., 2023). The elevated levels of leucine and isoleucine in old BAT could result from impaired BCAA catabolism and clearance. Instead of utilising BCAA for BAT metabolism, the amino acids might be secreted from the tissue. The elevated levels of valine, on the other hand, could indicate a shift between the different BCAA in their catabolism due to aging. In young BAT, cAMP could influence BCAA utilisation, a mechanism that might be lost in old BAT.

5.2. Influence of aging on the metabolome of young and old WATi

White adipose tissue is known for its role as energy storage and site of energy metabolism. Additionally, it functions as an endocrine organ which secretes various factors, termed adipokines, to regulate signalling of neighbouring cells, but also of peripheral organs (Fantuzzi, 2005). WAT is highly affected by aging which depicts in increased fat mass and an accumulation of inflammatory cytokines and lipids (Fülöp et al., 2019). The increased inflammatory state is mainly driven by gluco- and lipotoxicity, which describes the state of increased ROS production and inflammation due to accumulation of glucose and lipids (Prattichizzo et al., 2018). To analyse the influence of aging on the secretory capacity of WATi, untargeted metabolomics of young and old WATi was performed.

WAT aging is often described to be associated with elevated levels of adipokines like leptin or resistin, and proinflammatory cytokines like IL6 and TNFα (Mancuso and Bouchard, 2019; Peek et al., 2020).

Analysis of old compared to young WATi metabolomics showed a strong effect of aging on the secretome represented by distinct cluster formation in PCA, and a total of 55 differently regulated metabolites. The majority of the regulated metabolites (37) were downregulated in old compared to young WAT.

Aging leads to a hypertrophy of WAs due to excessive accumulation of lipids (Mancuso and Bouchard, 2019). Furthermore, aging can lead to an imbalance between fatty acid biosynthesis and uptake of FFAs from the circulation into the adipocytes (Picard and Guarente, 2005). Lipids represented the biggest class of metabolites, which were downregulated in old compared to young WATi. The balance between lipid storage and release is regulated by the activity and abundance of lipases, such as hormone-sensitive lipase (HSL) (Fredrikson et al., 1981), and proteins involved in lipid droplet formation/maintanance like perilipins (Conte et al., 2016). HSL can be activated by adrenergic stimulation (Shih and Taberner, 1995), which is known do be downregulated due to aging (Cannon and Nedergaard, 2004; Shin et al., 2017). Moreover, Perilipin2 was recently discussed to be involved in metabolic and age-related diseases (Conte et al., 2016). The data here indicated that old WAT has a "storage" phenotype, while young WAT is more active in secreting lipids, which might be important for the supply of peripheral organs.

On the other hand, QEA revealed an enrichment of lipid metabolism with an increase in saturated fatty acids (SFAs) and a decrease in polyunsaturated fatty acids (PUFAs) in old WAT. Stearic acid is a saturated long-chain fatty acid which is highly abundant in the adipose tissue and which is known to have proinflammatory potential (Jamar and Pisani, 2023). Polyunsaturated fatty acids like docosahexaenoic acid, on the other hand, can reduce levels of proinflammatory cytokines (Jamar and Pisani, 2023). The accumulation of proinflammatory lipids and a reduction of antiinflammtory lipids could account for the lipotoxicity found in old WAT. Therefore, future studies aiming to analyse expression and activity of lipid regulating enzymes might significantly enhance the understanding of the underlying cause shifting young WAT from a secreting phenotype to inflamed and lipotoxic old WAT with a storage phenotype.

Similar to the observation in young and old BAT, increased levels of steroid hormones and prostaglandins were found after cAMP stimulation of both young and old WATi. Prostaglandins were shown to be produced and secreted by adipose tissue and to have different and also opposing effects on adipocyte differentiation and function. While PGE2 and $PGF_{2\alpha}$ inhibit adipocyte differentiation, PGI2 and PGD2 have been shown to promote adipogenesis via PPARγ. Additionally, PGD2 suppresses lipolysis (Rahman, 2019). Furthermore, PGE2 and PGI2 were shown to be inducers of WAT browning (Vegiopoulos et al., 2010; Rahman, 2019). Here, PGE3 and PGA3 were found to be upregulated in both old and young WATi after cAMP stimulation. PGA3 is a dehydration product of PGE3 and so far barely

described in the literature, while PGE3 is mostly described in the context of cancer (Yang et al., 2014). Still, an administration of PGE3 in rats was shown to increase plasma levels of noradrenalin (Shimizu and Yokotani, 2009) and a simultaneous administration of PGE3 together with norepinephrine reduced plasma levels of free fatty acid levels in dogs (Bergstroem et al., 1964). Since both prostaglandins were increased after an acute stimulation of both young and old WAT an aging-independent role seems likely.

Steroid hormones are well known influencers of adipose tissue distribution and function (Meseguer et al., 2002). During aging, steroid hormone levels decline, which is thought to be partially responsible for the increase in adiposity. This effect seems to be regulated by estrogens rather by androgens since estrogen receptor knock out mice show increased amounts of WAT with advancing age in both male and female mice (Heine et al., 2000). 11β-HSD and aromatase cytochrome P450 (P450 arom) are the predominant enzymes catalysing the generation of active glucocorticoids in most tissues and also in WAT (Meseguer et al., 2002; Chapman et al., 2013). Testosterone is generated by 11β-HSD from androstenedione, whereas P450 arom generates estrogen from the same precursor. Metabolomics from young and old WAT showed an increase in androstenedione, 19-hydroxytestosterone and estradiolacetate levels after acute stimulation. cAMP induction might therefore lead to increased 11βHSD and P450 arom activity which eventually result in increased C18 and C19 steroid hormone levels. Interestingly, a proximal promoter of the human P450 arom gene (Cyp19) has been shown to be regulated by cAMP (Michael et al., 1997). Noteworthy, androgen and estrogen receptors, accounting for the downstream effects, are abundantly expressed in WAT (Mayes and Watson, 2004). Elevated levels of steroid hormones could then in turn lead to a pronounced autocrine signalling via stimulation of the corresponding receptors.

Young WATi showed a higher sensitivity to acute cAMP stimulation compared to old WATi, as specified in a clear PCA subclustering and a higher number of significantly changed metabolites in VP analysis. Even though the changes in the metabolome profile could not be linked to the enrichment of unique biological pathways in young WATi, some metabolite changes have to be highlighted: Increased levels of hydroxypalmitic acid and oxopalmitic acid were detected after cAMP stimulation of young WATi. This might indicate the presence of a class of lipids which only recently has been described: fatty acyl ester of hydroxyl fatty ester (FAHFA). FAHFAs are essential modulators of metabolic function and can have anti-diabetic and anti-inflammatory effects in mice and humans (Yore et al., 2014; Wood, 2020). Furthermore, Darcy et al. found decreased levels of FAHFAs in WAT lipidomics of extreme long living mice and attributed this lipid class to be potentially associated with lifespan and/or healthspan (Darcy et al., 2020). FAHFAs can be synthesized de novo in most organs and the biosynthesis is stimulated by increased glucose uptake into adipocytes (Yore et al., 2014). Together, this might indicate aged WATi

is ot capable of generating these metabolites after stimulation, which might contribute to the aging associated loss of metabolic capacity. Among the top downregulated metabolites in young WATi after cAMP stimulation were glucose and D-xylulose-5-phosphate, the latter is a metabolite linked to both glycolysis and lipogenesis, which might fuel the biosynthesis of FAHFA and account for the increased levels of hydroxyl-FA. As the changes in the metabolites' abundancies were only detected in young WATi but not old WATi, this mechanism might be age-related and uniquely found in young mice.

5.3. Influence of aging on the metabolome of young and old soleus muscle

Skeletal muscle serves as nutrient store of amino acids and carbohydrates, and is one of the major sites of energy turnover in mammals (Frontera and Ochala, 2015). Furthermore, SKM has the ability to secrete various factors (myokines as well as metabolites) which can influence SKM and peripheral organs in an auto- or paracrine manner. Aging highly affects skeletal muscle metabolism, leading to reduced muscle mass and function (Larsson et al., 2019). To understand changes in the metabolic profile of secreted factors by SKM, untargeted metabolomics was performed.

Metabolomic analyses of SKM have so far mainly been performed with murine *gastrocnemicus* whole tissue lysates. These previous studies show a strong influence of aging on the overall metabolite profile (Uchitomi et al., 2019; Tokarz et al., 2021). Tokarz et al. analysed the metabolome of 2-month and 21-month-old male mice and identified lipids, acylcarnitines, amino acids and polyamines to be altered due to increased age. Furthermore, they detected an accumulation of antioxidants like carnosine, anserine and ergothioneine in aged muscle (Tokarz et al., 2021). In another metabolome study from Uchitomi et al., 2-month and 28-month old murine SKM were analysed and showed significant changes in glucose metabolism and levels of phospholipids, polyamines and several amino acids (Uchitomi et al., 2019).

Untargeted metabolomics of the soleus muscle supernatant of young and old mice, showed significant changes in the overall metabolic profile as indicated by the distinct separation of the two groups in PCA and a large number of significantly regulated metabolites in VP. This supports previous data that aging highly affects the metabolic profile of SKM.

In line with data from Tokarz etl al., secretomics from aged soleus muscle showed increased levels of the antioxidant tocotrienol. Tocotrienol belongs to the Vitamin E family and cannot be synthesized in mammals but originates from the ingestion of plants or cereals (Chung et al., 2018). Therefore, the increased levels of tocotrienol found in old SKM cannot result from increased synthesis. Tocotrienol accumulates in tissues which are rich in lipids (Chung et al., 2018). As lipids accumulate in aged SKM (Cree et al., 2004), also tocotrienol might accumulate in soleus muscle, which in turn is leading to a higher secretion. Furthermore, tocotrienol acts as an antioxidant and the ingestion of Tocotrienol-rich fraction can have beneficial effects on myoblast proliferation and plasticity (Lim et al., 2013). Due to

higher ROS levels in aged tissue, higher levels of antioxidants could be a compensatory mechanism to prevent cell damage by ROS in SKM.

SKM aging is often accompanied by an infiltration of lipids into the muscle tissue which impairs muscle function and reduces muscle strength (Gueugneau et al., 2015). Especially, long chain SFA diminish insulin signalling and cause mitochondrial dysfunction in SKM cells (Hirabara et al., 2010). PUFAs, on the other hand, can have positive effects on muscle mass and physical function (Lipina and Hundal, 2017; Smith, 2019). Metabolomics of young and old mice, showed significant changes in lipid metabolism: SFAs, like stearic acid, arachidic acid and oleic acid, showed increased levels in old compared to young samples. On the other hand, PUFAs and fatty acid amides were downregulated in old compared to young soleus. Interestingly, Kim et al. showed decreased levels of fatty amides in serum and plasma levels of sarcopenic humans and mice (Kim et al., 2023). The data presented here might directly link these previous findings to muscle metabolomics: soleus secretes fatty amides in young mice, but the secretion is reduced in aged mice. Overall, old soleus muscle showed an imbalance in the levels of potentially harmful SFA and beneficial PUFAs. The observed changes in lipid metabolism are in line with previous data that lipid infiltration in the muscle is one driver of reduced muscle function and eventually sarcopenia.

cAMP stimulation with FSK is widely used as a model for in vitro exercise and can give insights into the underlying molecular mechanisms (Carter and Solomon, 2019). To mimic the influence of an acute exercise on the metabolome of young and old soleus, samples with and without FSK stimulation were analysed.

During exercise, the muscle demands energy in form of carbohydrates, lipids or, to a smaller extend, amino acids (Rivera-Brown and Frontera, 2012). Lipids are mostly stored in the form of TG in the adipose tissue, but SKM contains TG as well, which can be dissipated during exercise via lipolysis (Watt et al., 2002). Strikingly, cAMP stimulation of young soleus led to significant increases in long-chain FAs, and a decrease in medium chain FA. On the contrary, cAMP stimulation of old soleus led to significantly decreased levels of long chain FAs. SKM lipolysis is activated by the cAMP PKA pathway (Mason et al., 2012). Therefore, the release and detection of higher levels of free fatty acids in the supernatant of young soleus seems consequential. The reduced levels of long chain FA in old soleus after cAMP stimulation might suggest a higher demand of lipids which are used in β oxidation in the mitochondria, rather than being secreted. Another explanation might be reduced lipolyic capacity due to lower expression or activity of adenylylcyclases or lipases responsible for TG hydrolysis. In fact, adipose triglyceride lipase was shown to be downregulated in gastrognemicus of old mice which is accoompanied by impaired antioxidant response (Aquilano et al., 2016).

In addition to elevated levels of secreted lipids, an increase in free amino acids was observed in young but not old soleus samples after cAMP induction. This could indicate that young soleus uses free fatty acids as one source for energy during exercise. Amino acids could furthermore fuel the energy demand in young but not old soleus muscle during exercise. This might indicate, that aging leads to a shift in the energy sources and that amino acids are of higher importance for energy metabolism in young compared to old soleus SKM. Furthermore, amino acids can fuel TCA cycle and increased levels of TCA intermediates are observed, especially in the early state of exercise (Gibala, 2001). Together, these data indicate, that in young soleus free amino acids are used as energy source, either in direct oxidation or to fuel TCA.

Notably, similar to the observation in BAT and WATi, FSK treatment of young and old soleus SKM led to a marked increase in steroid hormones like 19-hydroxytestosterone, androstenedione or estradiol. Steroid hormones can be produced in SKM by the enzymes HSD and P450 arom, and an increased production is observed during exercise (Aizawa et al., 2010). Notably, steroid hormones like testosterone increase muscle protein anabolism, induce muscle hypertrophy and increase muscle strength (Ferrando et al., 2002; Sinha-Hikim et al., 2002). Furthermore, a dehydroepiandrosterone treatment was shown to potentiate weightlifting exercise and increase muscle strength and muscle mass in elderly women and men (Villareal and Holloszy, 2006). The increased levels of secreted steroids after cAMP stimulation of young and old soleus muscle indicates a mechanism which might contribute to the maintenance of muscle mass and function. As systemic steroid levels decline during aging (Sipilä et al., 2013), the data presented here indicate that reduced synthesis or secretion from SKM is likely o involved in this process.

Moreover, the prostaglandins PGE2, PGE3, 19-hydroxy PGE2 and PGE3-lactone were among the commonly upregulated metabolites after cAMP induction in young and old soleus. PG, especially PGE2 and $PGF_{2\alpha}$ are known regulators of muscle metabolism which are produced by exercising skeletal muscle and influence the muscle in auto- and paracrine ways (Trappe and Liu, 2013). PGE2 is the most abundant PG in skeletal muscle and regulates SKM protein turnover and exercise adaptations (Liu et al., 2016). Moreover, it has been identified as an inflammatory mediator of muscle stem cells, which is secreted in response to muscle injury and induces satellite cell proliferation and muscle repair. (Trappe and Liu, 2013; Ho et al., 2017). On the other hand, mice treated with a COX-2 inhibitor (which suppresses prostaglandin synthesis) showed impaired recovery after muscle injury (Bondesen et al., 2004). Although reduced muscle regeneration concomitant with reduced satellite cell number is well described in aging muscle (Sousa-Victor et al., 2022), the data presented here indicate that PGE2 or other PGs are not the underlying cause of this aging phenotype.

5.4. Influence of aging and regular physical exercise on the metabolome of human soleus muscle

Aging as well as physical inactivity greatly affect SKM, leading to loss of muscle mass, reduced muscle strength and impaired muscle metabolism. However, the molecular changes driving the metabolic decline are mainly unknown, especially in humans. So far, metabolic analysis of aged and exercised SKM have mainly been performed in *gastrocnemicus* or *quadriceps* muscle of mice or rats (Xiang et al., 2018; Uchitomi et al., 2019; Tokarz et al., 2021). Metabolomic analyses in humans are often performed with serum samples, owing to rather easy accessible sample material, or with *vastus lateralis* muscle (Huffman et al., 2014; Fazelzadeh et al., 2016; Zhang et al., 2019). So far, no metabolomics studies have been performed with human soleus muscle. Here, untargeted metabolomics of human soleus muscle was performed to evaluate the influence of aging and regular exercise on the muscle's secretome profile.

Unexpectedly, regular physical activity seemed to have only minor influences on the basal metabolic profile in both young and old groups. This was confirmed by PCA, depicting no cluster formation of , but an even distribution of all samples. Moreover, VP analysis of untrained compared to trained samples showed a rather small amount of significantly regulated metabolites (total of 19 in the young group, 25 in the old group). The lack of different metabolic profiles due to training status, most likely results from interindividual differences. The number of participants ranged from 7 to 12 participants per group, which is high given that muscle biopsies were analysed and subject aquistion is much more challenging with this invasive procedure compared to anaylsis of blood samples. Nevertheless, this group size might be too small to detect more common regulation patterns, which exceed the already high variance in the metabolic profile of humans.

Nevertheless, metabolomics data revealed an influence of training on the levels of L-carnitine and heptanoylcarnitine, which were upregulated in young trained compared to untrained samples. L-carnitine is essential for the shuttle of fatty acids into the mitochondria, where they are utilised for β-oxidation (Stephens et al., 2007). Endurance training increases overall fatty acid oxidation during rest and exercise (Tunstall et al., 2002). Additionally, regular exercise was shown to increase levels of the required enzyme for long-chain FA transport in the muscles of athletes (Lohninger et al., 2005). The observed upregulation of L-carnitine and heptanoylcarnitine are therefore likely a result from regular physical activity which elevates basal fatty acid metabolism and the mobilisation of lipids. As this increase was not observed in old samples, a lack of L-carnitine could on the other hand contribute to reduced metabolic capacity in old SKM.

Strikingly, the purine inosine was among the top downregulated metabolites in trained young soleus. Current data on purine metabolism in exercise is somewhat contradicting. On the one hand, exercise increases adenosine levels in human muscle, which is a direct precursor of inosine, and an activation of purinergic receptor A2B ameliorates aging effects in SKM (Hellsten et al., 1998; Gnad et al., 2020). On the other hand, purines and their metabolites were shown to be decreased due to exercise in diabetic mice (Xiang et al., 2018). Therefore, the decreased levels of inosine in the supernatant of trained young soleus could result from induced clearance of this metabolite in the course of exercise, but the regulation and its downstream effects cannot be explained completely.

Metabolomics of old SKM showed a significant upregulation of the long-chain FA stearic acid, palmitic acid and margaric acid, but a significant downregulation of 11-eicosenoic acid and myristic acid in trained compared to untrained samples. Palmitic acid is a C16, margaric acid a C17 and stearic acid a C18 saturated FA. On the other hand, 11-eicosenoic acid is a monounsaturated omega-9 FA and myrisitic acid a C14 saturated FA (Human Metabolome Database, 2023). The infiltration of SKM with lipids, is known to occur due to aging or sarcopenia. Especially saturated fatty acids are known to impair muscle mass und function (Gueugneau et al., 2015). Furthermore, aging is associated with a reduction of β-oxidation of fatty acids during rest and exercise. Still, aerobic exercise can increase fat oxidation and oxidative capacity in the elderly (Toth and Tchernof, 2000). Therefore, the elevated levels of long-chain, saturated FA in old trained samples appear rather conflicting. A possible explanation could be, that old trained SKM shows higher levels of basal lipolysis compared to untrained samples, which would increase the levels of free fatty acids in the supernatant. Moreover, training improves sympathetic nerve activity in exercising muscle (Ray and Hume, 1998), which in turn might increase activity of lipases. Yet, the observed changes in lipid abundancies raise the need for further analysis of the influence of exercise in the lipid profile in aged soleus muscle.

It is common sense, that exercise highly influences whole body metabolism and mobilizes metabolites which fuel the increased energy demand. So far, most studies that analyse the influence of acute exercise on the metabolic profile, are performed with blood or urine samples (Schranner et al., 2020; Khoramipour et al., 2022). Here, the influence of ex vivo exercise was directly analysed from human soleus biopsies.

In general, previous studies report an increase in free fatty acids and acylcarnitines in human blood samples early after exercise. Amino acid are known to fuel SKM energy demand during exercise as well, even though the magnitude and direction of the exercise-induced changes are inconsistent and vary among current publications (Schranner et al., 2020). Ex vivo exercise of human soleus muscle revealed a cAMP related enrichment of amino acid metabolism among the top regulated biological pathways in young untrained and trained sample groups. In young untrained soleus, cAMP induction

led to strong alterations in BCAA metabolism, whereas cAMP induction in young trained soleus induced the metabolism of glycine, serine, threonine and alanine. Ex vivo stimulation of old soleus turned out differently: in both untrained and trained samples, fatty acid metabolism was among the highly enriched pathways, showing an even more pronounced enrichment in old trained samples. This suggests, that aging of soleus muscle leads to a shift of metabolite utilisation from amino acid metabolism to fatty acid metabolism during stimulatory events. One explanation could be the general higher abundance of lipids in aged muscle, which can fuel energy demand to a greater extent. Nonetheless, the observed changes in the enrichment of amino acid and lipid metabolism will need further investigations comprising an analysis of the involved enzymes and an in depth and targeted analysis of the altered metabolites.

Intriguingly, cAMP stimulation of human soleus biopsies led to a marked increase in steroid hormone and prostaglandin levels in the supernatant of all groups. Furthermore, the 14 commonly regulated metabolites between all groups comprised steroids and PGs. The influence and effects of steroids and PGs in SKM metabolism were already described in section 5.3.. The finding, that cAMP induction elevates the levels of PGs and steroids similarly in young and old, human and murine metabolic tissues greatly demands further analysis and investigations to determine the specific role of the different metabolites in the tissues. Furthermore, these metabolites could likely function as circulating metabolites which influence the cross-talk between SKM and adipose tissues.

Interestingly, cAMP stimulation of young trained soleus showed the highest changes compared to all other groups. The stimulation led to a clear separation of the unstimulated and simulated young trained groups in PCA, indicating strong differences in the metabolic profiles. Furthermore, the highest number of significantly changed metabolites was detected in the young trained group compared to the other groups (in total 91). This implies, that regular physical exercise leads to a broad range of metabolic adaptations in the muscle which lead to a more profound response to an acute stimulation compared to individuals without regular exercise, but moreover also compared to older trained individuals. This might be due to a higher sensitivity to FSK stimulation mediated by a distinct cAMP/PKA/PDE signalosome. Furthermore, cAMP stimulation of young trained soleus samples revealed the highest number of uniquely regulated metabolites (39 up and down regulated metabolites). ORA of the uniquely regulated metabolites, once more indicated a distinctive utilisation of amino acids in young trained samples during ex vivo exercise. Additionally, metabolites like L-histidine, histamine, L-carnitine, oleamide, hypoxanthine, taurine and methylnicotinamide showed a significant downregulation of the metabolites' levels due to cAMP stimulation in young trained samples, whereas the levels did not change in all other groups. This could indicate that young trained

soleus has a higher demand of small metabolites during stimulation whereas the untrained and groups still secrete the metabolites to some extent.

In conclusion, untargeted metabolomics of human soleus biopsies from young and old, trained and untrained healthy participants showed that the analysis of the secretome under unstimulated conditions only revealed minor changes and made a discrimination of the different groups rather difficult. Yet, under stimulatory events like the treatment with FSK, the 4 groups show similar as well as distinct characteristics in their metabolic profile. Notably, young trained soleus seems to owe a unique SKM metabolism compared to the other groups.

5.5. Effects of shared and unique SKM secreted metabolites on the differentiation of myocytes and BA

Untargeted metabolomics of human SKM and murine BAT, WATi and SKM revealed metabolites which were commonly upregulated after cAMP stimulation. Furthermore, several metabolites were detected to be uniquely regulated in young trained samples. These secreted metabolites could be interesting candidates for the auto- and paracrine regulation of metabolic pathways and their influence on SKM energy expenditure and their ability to maintain muscle mass and quality. Therefore, the eicosanoids PGE2 and PGE3, the hormones corticosterone and desoxycortisol, and histamine, carnitine, oleamide and choline were analysed in vitro for their effects on the differentiation and proliferation of SKM cells as well as BAs.

The acute treatment of murine C2C12 SKM cells with the prostaglandins PGE2 and PGE3 significantly decreased the expression of the myogenic transcription factors *Myogenin*, *Myomaker* and *Mef2c*. On the other hand, PGE3 led a significant increase in the expression of *MyoD*. Moreover, a chronic treatment with PGE2 led to a significant decrease in *Mef2c* mRNA levels. *MyoD* and *Myogenin* are transcription factors regulating several processes like myogenesis, ensuring SKM lineage fate or myogenic differentiation (Zammit, 2017). *Myomaker* is an early marker for myoblast fusion whereas *Mef2c* is important for maturation and maintanence of SKM (Potthoff et al., 2007; Millay et al., 2014). This implies, that PGEs negatively influence myogenesis, myogenic differentiation and muscle cell maintenance and repair. The effect of several PGs have already been described, with inconsistent data. For example, PGD2 negatively influences C2C12 myogenesis specified by a reduction in *MyoD*, *Myogenin* and α-*actin* expression. (Veliça et al., 2010). On the other hand, PGE2 and $PGF_{2\alpha}$ were shown to induce cell proliferation and increase levels of myosin heavy chain 3, creatine kinase muscle and myomaker in primary bovine myoblasts (Mo et al., 2015; Leng and Jiang, 2019). Furthermore, PGE2 is vital for satellite cell function and an inhibition of PGE2 with nonsteroidal anti-inflammatory drugs (NSAID) diminishes muscle repair and regeneration (Ho et al., 2017). Knowing that, the decreased

levels of myogenic markers after the PGE2 and PGE3 treatment in C2C12 seems conflicting and not plausible. Future work should apply primary human SKM cells to understand th role of PGE2 and PGE3 in human muscle.

Corticosterone is the major glucocorticoid in rodents and regulates various metabolic pathways, especially in response to stress. Recently, the enzymes involved in the synthesis of corticosterone and desoxycortisol were shown to be expressed in C2C12 cells (Fujiki et al., 2018). An acute treatment of C2C12 cells with corticosterone and desoxycortisol significantly increased the mRNA levels of *Myf5*, which is an important transcription factor for myogenesis and myocyte cell line fate (Zammit, 2017). On the other hand, levels of *Myogenin* and *Myomaker* were significantly decreased. Furthermore, a long term administration of corticosterone elevated the expression levels of M*yogenin*, and a long term treatment with desoxycortisol increased the expression levels of *Myf5*. Together these data indicate, that a sudden exposure to stress, represented by an acute stimulation with endogenous glucocorticoids, could induce SKM cell proliferation but decrease cell differentiation and maintenance. On the other hand, the long-term exposure showed a positive influence on C2C12 myogenesis and SKM cell differentiation.

Finally, metabolites which were solely regulated in SKM from young trained participants after cAMP stimulation, were analysed for their autocrine (i.e. treatment of SKM cells) and paracrine effects (i.e. treatment of BAs). An acute treatment of C2C12 and hSKM cells with histamine, carnitine, oleamide and choline showed no significant changes in expression levels of myogenic markers. This might indicate that these metabolites do not exert autocrine effects on muscle cells. However, future analysis involving different time points of treatment and escalating doses of the metabolites might be needed to validate these findings

Notably, treatment of BAs with choline and carnitine increased the expression of adipogenic markers. Interestingly, a dietary intake of choline was shown to reduce body fat mass gain, adipocyte enlargement and adipose tissue inflammation in mice fed a western diet which suffered from lipoprotein and cardiometabolic diseases (Liu et al., 2023). Moreover, choline is taken up by BAT in humans during room temperature and cold exposure (Suchacki et al., 2022). Additionally, a genetic carnitine deficient mouse model showed increased lipid droplet size and decreased mitochondria size, as well as reduced UCP1 levels and lower body temperature (Ozaki et al., 2011). Notably, thermogenic markers such as UCP1 were not affected by choline and cornitine treatment. Nevertheless, both carnitine and choline are interesting candidates which could orchestrate the cross-talk between SKM and BAT. In a next step, the influence of exercise and aging on circulating levels of carnitine and choline should be analysed. Moreover, a combination of exercise with a genetic mouse model could be of high

relevance to investigate the choline- and creatinine-mediated cross-talk between SKM and adipose tissues.

5.6. Untargeted metabolomics as a powerful tool to study the metabolic fingerprint in biological samples

Metabolomics analysis belongs to the family of omics technologies which provide large scale and high-throughput analyses and generate great amounts of data and information on all levels of biological processes. With metabolomics, samples are systematically screened for a large number of known or unknown metabolites. The obtained data can give insights into regulation patterns and trends caused by biological or environmental factors (Idle and Gonzalez, 2007; Gargano et al., 2019).

Here untargeted metabolomics was performed using a state-of-the-art UHPL-MS/MS system. By this, the metabolites in one sample, are separated in the UHPLC system and further analysed with MS/MS. The separation of the various metabolites by UHPLC highly depends on the chemical structure of the metabolite and the applied conditions consisting of column, mobile phase, flow rate and sample preparation. A variation of one of the components can influence the metabolites separation and peak intensity. The metabolites are further analysed for their m/z values, chemical structure and fragmentation patterns by MS/MS. Especially the fragmentation process can vary due to the applied settings. The data obtained from the UHPLC-MS/MS are processed and metabolites are identified by assigning m/z values, molecular mass and fragmentation data to structures in various databases. These databases can be open-source or from metabolomics service providers. The selection of the metabolite databases influence and define the alignment and therefore the outcome of metabolome analysis (Gargano et al., 2019; Park et al., 2023). Here, three different open-source data bases and a selection for mammalian and endogenous metabolites were used for the identification of the metabolites to cover a broad range of information for data alignment.

In untargeted metabolomics, as many metabolites as possible shall be analysed and identified in one biological sample. In this approach no internal or external standards of references are used. This means, that the metabolite identification is based on matches in databases and not by the comparison of Rt and m/z values with definite reference values which would allow the reliable identification and quantification of the detected metabolites (Johnson et al., 2016; Gargano et al., 2019). Untargeted metabolomics data are therefore limited to qualitative identification and relative quantification.

Metabolomics is a fairly new technique which was formally introduced in the early 2000s and is ever since an emerging research field in regards of technology and implementation (Dettmer et al., 2007; Johnson et al., 2016). The complexity of metabolite diversity and concentration ranges, coupled with the dynamic nature of metabolic processes, makes comprehensive analysis difficult. However,

improvements in mass spectrometry, along with advancements in computational tools and bioinformatics, have enhanced sensitivity, resolution, and data interpretation capabilities (Johnson et al., 2016). These technological strides have pushed the field forward, yet metabolomics remains a constantly evolving discipline, requiring continual innovation to address its inherent complexities and to fully realize its potential. Taken together, untargeted metabolomics can give new insights on regulation patterns without pre-existing knowledge about the sample's composition. Yet, sample preparation, analytical methods and the use of certain databases directly impacts the results. With untargeted metabolomics, new hypothesis can be generated, but the absolute identification and quantification demands the application of internal and external standards.

6. References

Abelson, P., and Kennedy, D. (2004). The obesity epidemic. Science (New York, N.Y.) *304*, 1413. https://doi.org/10.1126/science.304.5676.1413.

Adeva-Andany, M., Souto-Adeva, G., Ameneiros-Rodríguez, E., Fernández-Fernández, C., Donapetry-García, C., and Domínguez-Montero, A. (2018). Insulin resistance and glycine metabolism in humans. Amino acids *50*, 11-27. https://doi.org/10.1007/s00726-017-2508-0.

Adeva-Andany, M.M., Calvo-Castro, I., Fernández-Fernández, C., Donapetry-García, C., and Pedre-Piñeiro, A.M. (2017). Significance of l-carnitine for human health. IUBMB life *69*, 578-594. https://doi.org/10.1002/iub.1646.

Aizawa, K., Iemitsu, M., Maeda, S., Otsuki, T., Sato, K., Ushida, T., Mesaki, N., and Akimoto, T. (2010). Acute exercise activates local bioactive androgen metabolism in skeletal muscle. Steroids *75*, 219-223. https://doi.org/10.1016/j.steroids.2009.12.002.

Aizawa, K., Iemitsu, M., Otsuki, T., Maeda, S., Miyauchi, T., and Mesaki, N. (2008). Sex differences in steroidogenesis in skeletal muscle following a single bout of exercise in rats. Journal of applied physiology (Bethesda, Md. : 1985) *104*, 67-74. https://doi.org/10.1152/japplphysiol.00558.2007.

Aksoy, S., Szumlanski, C.L., and Weinshilboum, R.M. (1994). Human liver nicotinamide N-methyltransferase. cDNA cloning, expression, and biochemical characterization. The Journal of biological chemistry *269*, 14835-14840.

Anderson, R.L., and Merkler, D.J. (2017). N-FATTY ACYLGLYCINES: UNDERAPPRECIATED ENDOCANNABINOID-LIKE FATTY ACID AMIDES? Journal of biology and nature *8*, 156-165.

Aquilano, K., Baldelli, S., La Barbera, L., Lettieri Barbato, D., Tatulli, G., and Ciriolo, M.R. (2016). Adipose triglyceride lipase decrement affects skeletal muscle homeostasis during aging through FAs-PPARα-PGC-1α antioxidant response. Oncotarget *7*, 23019-23032. https://doi.org/10.18632/oncotarget.8552.

Augusto, V., Padovani, C.R., and Campos, G.E.R. (2017). Skeletal muscle fibre types in C57BL6J mice. Journal of Morphological Sciences *21*, 0 - 0-0.

Banerjee, S., and Poddar, M.K. (2020). Carnosine research in relation to aging brain and neurodegeneration: A blessing for geriatrics and their neuronal disorders. Archives of gerontology and geriatrics *91*, 104239. https://doi.org/10.1016/j.archger.2020.104239.

Barnes, S., Benton, H.P., Casazza, K., Cooper, S.J., Cui, X., Du, X., Engler, J., Kabarowski, J.H., Li, S., and Pathmasiri, W., et al. (2016). Training in metabolomics research. I. Designing the experiment, collecting and extracting samples and generating metabolomics data. Journal of mass spectrometry : JMS *51*, 461-475. https://doi.org/10.1002/jms.3782.

Bartelt, A., and Heeren, J. (2014). Adipose tissue browning and metabolic health. Nature reviews. Endocrinology *10*, 24-36. https://doi.org/10.1038/nrendo.2013.204.

Becher, T., Palanisamy, S., Kramer, D.J., Eljalby, M., Marx, S.J., Wibmer, A.G., Butler, S.D., Jiang, C.S., Vaughan, R., and Schöder, H., et al. (2021). Brown adipose tissue is associated with cardiometabolic health. Nature medicine *27*, 58-65. https://doi.org/10.1038/s41591-020-1126-7.

Bełtowski, J. (2003). Adiponectin and resistin--new hormones of white adipose tissue. Medical science monitor : international medical journal of experimental and clinical research *9*, RA55-61.

Berdeaux, R., and Stewart, R. (2012). cAMP signaling in skeletal muscle adaptation: hypertrophy, metabolism, and regeneration. American journal of physiology. Endocrinology and metabolism *303*, E1-17. https://doi.org/10.1152/ajpendo.00555.2011.

Bergstroem, S., Carlson, L.A., and Oroe, L. (1964). Effect of Prostaglandids on Catecholamine induced changes in the free fatty acids of plasma and in blood pressure in the dog. PROSTAGLANDIN AND RELATED FACTORS 22. Acta physiologica Scandinavica *60*, 170-180. https://doi.org/10.1111/j.1748-1716.1964.tb02880.x.

Bingol, K. (2018). Recent Advances in Targeted and Untargeted Metabolomics by NMR and MS/NMR Methods. High-throughput *7*. https://doi.org/10.3390/ht7020009.

Blachnio-Zabielska, A.U., Koutsari, C., Tchkonia, T., and Jensen, M.D. (2012). Sphingolipid content of human adipose tissue: relationship to adiponectin and insulin resistance. Obesity (Silver Spring, Md.) *20*, 2341-2347. https://doi.org/10.1038/oby.2012.126.

Boldyrev, A.A., Aldini, G., and Derave, W. (2013). Physiology and pathophysiology of carnosine. Physiological reviews *93*, 1803-1845. https://doi.org/10.1152/physrev.00039.2012.

Bolsoni-Lopes, A., Festuccia, W.T., Farias, T.S.M., Chimin, P., Torres-Leal, F.L., Derogis, P.B.M., Andrade, P.B. de, Miyamoto, S., Lima, F.B., and Curi, R., et al. (2013). Palmitoleic acid (n-7) increases white adipocyte lipolysis and lipase content in a PPARα-dependent manner. American journal of physiology. Endocrinology and metabolism *305*, E1093-102. https://doi.org/10.1152/ajpendo.00082.2013.

Bondesen, B.A., Mills, S.T., Kegley, K.M., and Pavlath, G.K. (2004). The COX-2 pathway is essential during early stages of skeletal muscle regeneration. American journal of physiology. Cell physiology *287*, C475-83. https://doi.org/10.1152/ajpcell.00088.2004.

Borup, A., Donkin, I., Boon, M.R., Frydland, M., Martinez-Tellez, B., Loft, A., Keller, S.H., Kjaer, A., Kjaergaard, J., and Hassager, C., et al. (2022). Association of apolipoprotein M and sphingosine-1-phosphate with brown adipose tissue after cold exposure in humans. Scientific reports *12*, 18753. https://doi.org/10.1038/s41598-022-21938-2.

Boström, P., Wu, J., Jedrychowski, M.P., Korde, A., Ye, L., Lo, J.C., Rasbach, K.A., Boström, E.A., Choi, J.H., and Long, J.Z., et al. (2012). A PGC1-α-dependent myokine that drives brown-fat-like development of white fat and thermogenesis. Nature *481*, 463-468. https://doi.org/10.1038/nature10777.

Bradshaw, H.B., Rimmerman, N., Hu, S.S.-J., Burstein, S., and Walker, J.M. (2009). Chapter 8 Novel Endogenous N-Acyl Glycines. In Vitamins and Hormones (Elsevier), pp. 191–205.

Brass, E.P. (1995). Pharmacokinetic considerations for the therapeutic use of carnitine in hemodialysis patients. Clinical Therapeutics *17*, 176-85; discussion 175. https://doi.org/10.1016/0149-2918(95)80017-4.

Bray, G.A., Frühbeck, G., Ryan, D.H., and Wilding, J.P.H. (2016). Management of obesity. Lancet (London, England) *387*, 1947-1956. https://doi.org/10.1016/S0140-6736(16)00271-3.

Brett Sears, P.T. (2022). The Anatomy of the Soleus Muscle. The muscle of your lower leg that's essential for walking and running.

Broek, R.W. ten, Grefte, S., and den Hoff, J.W. von (2010). Regulatory factors and cell populations involved in skeletal muscle regeneration. Journal of cellular physiology *224*, 7-16. https://doi.org/10.1002/jcp.22127.

Brown, J.D., Karimian Azari, E., and Ayala, J.E. (2017). Oleoylethanolamide: A fat ally in the fight against obesity. Physiology & behavior *176*, 50-58. https://doi.org/10.1016/j.physbeh.2017.02.034.

Bruckbauer, A., and Zemel, M.B. (2011). Effects of dairy consumption on SIRT1 and mitochondrial biogenesis in adipocytes and muscle cells. Nutrition & metabolism *8*, 91. https://doi.org/10.1186/1743-7075-8-91.

Burton, E.G., Schoenhard, G.L., Hill, J.A., Schmidt, R.E., Hribar, J.D., Kotsonis, F.N., and Oppermann, J.A. (1989). Identification of N-beta-L-aspartyl-L-phenylalanine as a normal constituent of human plasma and urine. The Journal of nutrition *119*, 713-721. https://doi.org/10.1093/jn/119.5.713.

Cannon, B., and Nedergaard, J. (2004). Brown adipose tissue: function and physiological significance. Physiological reviews *84*, 277-359. https://doi.org/10.1152/physrev.00015.2003.

Cao, H., Gerhold, K., Mayers, J.R., Wiest, M.M., Watkins, S.M., and Hotamisligil, G.S. (2008). Identification of a lipokine, a lipid hormone linking adipose tissue to systemic metabolism. Cell *134*, 933-944. https://doi.org/10.1016/j.cell.2008.07.048.

Cappola, A.R., Xue, Q.-L., Ferrucci, L., Guralnik, J.M., Volpato, S., and Fried, L.P. (2003). Insulin-like growth factor I and interleukin-6 contribute synergistically to disability and mortality in older women. The Journal of clinical endocrinology and metabolism *88*, 2019-2025. https://doi.org/10.1210/jc.2002-021694.

Cararo, J.H., Streck, E.L., Schuck, P.F., and Da Ferreira, G.C. (2015). Carnosine and Related Peptides: Therapeutic Potential in Age-Related Disorders. Aging and disease *6*, 369-379. https://doi.org/10.14336/AD.2015.0616.

Cartee, G.D., Hepple, R.T., Bamman, M.M., and Zierath, J.R. (2016). Exercise Promotes Healthy Aging of Skeletal Muscle. Cell metabolism *23*, 1034-1047. https://doi.org/10.1016/j.cmet.2016.05.007.

Carter, S., and Solomon, T.P.J. (2019). In vitro experimental models for examining the skeletal muscle cell biology of exercise: the possibilities, challenges and future developments. Pflugers Archiv : European journal of physiology *471*, 413-429. https://doi.org/10.1007/s00424-018-2210-4.

Chapman, K., Holmes, M., and Seckl, J. (2013). 11β-hydroxysteroid dehydrogenases: intracellular gate-keepers of tissue glucocorticoid action. Physiological reviews *93*, 1139-1206. https://doi.org/10.1152/physrev.00020.2012.

Chłopicki, S., Kurdziel, M., Sternak, M., Szafarz, M., Szymura-Oleksiak, J., Kamiński, K., and Żołądź, J.A. (2012). Single bout of endurance exercise increases NNMT activity in the liver and MNA concentration in plasma; the role of IL-6. Pharmacological reports : PR *64*, 369-376. https://doi.org/10.1016/S1734-1140(12)70777-6.

Christoffersen, C., Federspiel, C.K., Borup, A., Christensen, P.M., Madsen, A.N., Heine, M., Nielsen, C.H., Kjaer, A., Holst, B., and Heeren, J., et al. (2018). The Apolipoprotein M/S1P Axis Controls Triglyceride

Metabolism and Brown Fat Activity. Cell reports *22*, 175-188. https://doi.org/10.1016/j.celrep.2017.12.029.

Chung, E., Mo, H., Wang, S., Zu, Y., Elfakhani, M., Rios, S.R., Chyu, M.-C., Yang, R.-S., and Shen, C.-L. (2018). Potential roles of vitamin E in age-related changes in skeletal muscle health. Nutrition research (New York, N.Y.) *49*, 23-36. https://doi.org/10.1016/j.nutres.2017.09.005.

Cinti, S. (2018). Obesity, Diabetes and the Adipose Organ. A Pictorial Atlas from Research to Clinical Applications (Cham: Springer).

Conte, M., Franceschi, C., Sandri, M., and Salvioli, S. (2016). Perilipin 2 and Age-Related Metabolic Diseases: A New Perspective. Trends in endocrinology and metabolism: TEM *27*, 893-903. https://doi.org/10.1016/j.tem.2016.09.001.

Cree, M.G., Newcomer, B.R., Katsanos, C.S., Sheffield-Moore, M., Chinkes, D., Aarsland, A., Urban, R., and Wolfe, R.R. (2004). Intramuscular and liver triglycerides are increased in the elderly. The Journal of clinical endocrinology and metabolism *89*, 3864-3871. https://doi.org/10.1210/jc.2003-031986.

Dambrova, M., Makrecka-Kuka, M., Kuka, J., Vilskersts, R., Nordberg, D., Attwood, M.M., Smesny, S., Sen, Z.D., Guo, A.C., and Oler, E., et al. (2022). Acylcarnitines: Nomenclature, Biomarkers, Therapeutic Potential, Drug Targets, and Clinical Trials. Pharmacological reviews *74*, 506-551. https://doi.org/10.1124/pharmrev.121.000408.

Darcy, J., Fang, Y., McFadden, S., Lynes, M.D., Leiria, L.O., Dreyfuss, J.M., Bussburg, V., Tolstikov, V., Greenwood, B., and Narain, N.R., et al. (2020). Integrated metabolomics reveals altered lipid metabolism in adipose tissue in a model of extreme longevity. GeroScience *42*, 1527-1546. https://doi.org/10.1007/s11357-020-00221-0.

Dettmer, K., Aronov, P.A., and Hammock, B.D. (2007). Mass spectrometry-based metabolomics. Mass spectrometry reviews *26*, 51-78. https://doi.org/10.1002/mas.20108.

Distefano, G., and Goodpaster, B.H. (2018). Effects of Exercise and Aging on Skeletal Muscle. Cold Spring Harbor perspectives in medicine *8*. https://doi.org/10.1101/cshperspect.a029785.

Elmquist, J.K. (2001). Hypothalamic pathways underlying the endocrine, autonomic, and behavioral effects of leptin. Physiology & behavior *74*, 703-708. https://doi.org/10.1016/S0031-9384(01)00613-8.

Fan, J., Yang, X., Li, J., Shu, Z., Dai, J., Liu, X., Li, B., Jia, S., Kou, X., and Yang, Y., et al. (2017). Spermidine coupled with exercise rescues skeletal muscle atrophy from D-gal-induced aging rats through enhanced autophagy and reduced apoptosis via AMPK-FOXO3a signal pathway. Oncotarget *8*, 17475-17490. https://doi.org/10.18632/oncotarget.15728.

Fang, Z., Pyne, S., and Pyne, N.J. (2019). Ceramide and sphingosine 1-phosphate in adipose dysfunction. Progress in lipid research *74*, 145-159. https://doi.org/10.1016/j.plipres.2019.04.001.

Fantuzzi, G. (2005). Adipose tissue, adipokines, and inflammation. The Journal of allergy and clinical immunology *115*, 911-9; quiz 920. https://doi.org/10.1016/j.jaci.2005.02.023.

Fazelzadeh, P., Hangelbroek, R.W.J., Tieland, M., Groot, L.C.P.G.M. de, Verdijk, L.B., van Loon, L.J.C., Smilde, A.K., Alves, R.D.A.M., Vervoort, J., and Müller, M., et al. (2016). The Muscle Metabolome Differs between Healthy and Frail Older Adults. Journal of proteome research *15*, 499-509. https://doi.org/10.1021/acs.jproteome.5b00840.

Felig, P., Marliss, E., and Cahill, G.F. (1969). Plasma amino acid levels and insulin secretion in obesity. The New England journal of medicine *281*, 811-816. https://doi.org/10.1056/NEJM196910092811503.

Ferrando, A.A., Sheffield-Moore, M., Yeckel, C.W., Gilkison, C., Jiang, J., Achacosa, A., Lieberman, S.A., Tipton, K., Wolfe, R.R., and Urban, R.J. (2002). Testosterone administration to older men improves muscle function: molecular and physiological mechanisms. American journal of physiology. Endocrinology and metabolism *282*, E601-7. https://doi.org/10.1152/ajpendo.00362.2001.

Foster, C.V., and Harris, R.C. (1992). Total carnitine content of the middle gluteal muscle of thoroughbred horses: normal values, variability and effect of acute exercise. Equine Veterinary Journal *24*, 52-57. https://doi.org/10.1111/j.2042-3306.1992.tb02779.x.

Fredrikson, G., Strålfors, P., Nilsson, N.O., and Belfrage, P. (1981). Hormone-sensitive lipase of rat adipose tissue. Purification and some properties. The Journal of biological chemistry *256*, 6311-6320.

Frontera, W.R., and Ochala, J. (2015). Skeletal muscle: a brief review of structure and function. Calcified tissue international *96*, 183-195. https://doi.org/10.1007/s00223-014-9915-y.

Fujiki, J., Maeda, N., Sato, M., Ieko, T., Inoue, H., Iwasaki, T., Iwano, H., and Yokota, H. (2018). Corticosterone biosynthesis in mouse clonal myoblastic C2C12 cells. Steroids *138*, 64-71. https://doi.org/10.1016/j.steroids.2018.07.001.

Fülöp, T., Larbi, A., and Witkowski, J.M. (2019). Human Inflammaging. Gerontology *65*, 495-504. https://doi.org/10.1159/000497375.

Garber, A.J., Karl, I.E., and Kipnis, D.M. (1976). Alanine and glutamine synthesis and release from skeletal muscle. II. The precursor role of amino acids in alanine and glutamine synthesis. The Journal of biological chemistry *251*, 836-843. https://doi.org/10.1016/S0021-9258(17)33860-7.

Gargano, A., Haselberg, R., Kohler, I., and Pirok, B.W. (2019). Clinical Metabolomics: Expanding the Metabolome Coverage Using Advanced Analytical Techniques. LCGC Eur., 465-480. https://doi.org/10.56530/lcgc.eu.ry4267t3.

Gheller, B.J., Blum, J.E., Lim, E.W., Handzlik, M.K., Hannah Fong, E.H., Ko, A.C., Khanna, S., Gheller, M.E., Bender, E.L., and Alexander, M.S., et al. (2021). Extracellular serine and glycine are required for mouse and human skeletal muscle stem and progenitor cell function. Molecular metabolism *43*, 101106. https://doi.org/10.1016/j.molmet.2020.101106.

Gibala, M.J. (2001). Regulation of skeletal muscle amino acid metabolism during exercise. International journal of sport nutrition and exercise metabolism *11*, 87-108. https://doi.org/10.1123/ijsnem.11.1.87.

Gnad, T., Navarro, G., Lahesmaa, M., Reverte-Salisa, L., Copperi, F., Cordomi, A., Naumann, J., Hochhäuser, A., Haufs-Brusberg, S., and Wenzel, D., et al. (2020). Adenosine/A2B Receptor Signaling Ameliorates the Effects of Aging and Counteracts Obesity. Cell metabolism *32*, 56-70.e7. https://doi.org/10.1016/j.cmet.2020.06.006.

Gnad, T., Scheibler, S., Kügelgen, I. von, Scheele, C., Kilić, A., Glöde, A., Hoffmann, L.S., Reverte-Salisa, L., Horn, P., and Mutlu, S., et al. (2014). Adenosine activates brown adipose tissue and recruits beige adipocytes via A2A receptors. Nature *516*, 395-399. https://doi.org/10.1038/nature13816.

Goff, A.K. (2004). Steroid hormone modulation of prostaglandin secretion in the ruminant endometrium during the estrous cycle. Biology of reproduction *71*, 11-16. https://doi.org/10.1095/biolreprod.103.025890.

Gohlke, S., Zagoriy, V., Cuadros Inostroza, A., Méret, M., Mancini, C., Japtok, L., Schumacher, F., Kuhlow, D., Graja, A., and Stephanowitz, H., et al. (2019). Identification of functional lipid metabolism biomarkers of brown adipose tissue aging. Molecular metabolism *24*, 1-17. https://doi.org/10.1016/j.molmet.2019.03.011.

Gollnick, P.D., Sjödin, B., Karlsson, J., Jansson, E., and Saltin, B. (1974). Human soleus muscle: a comparison of fiber composition and enzyme activities with other leg muscles. Pflugers Archiv : European journal of physiology *348*, 247-255. https://doi.org/10.1007/BF00587415.

Gout, J., Tirard, J., Thévenon, C., Riou, J.-P., Bégeot, M., and Naville, D. (2006). CCAAT/enhancer-binding proteins (C/EBPs) regulate the basal and cAMP-induced transcription of the human 11beta-hydroxysteroid dehydrogenase encoding gene in adipose cells. Biochimie *88*, 1115-1124. https://doi.org/10.1016/j.biochi.2006.05.020.

Graja, A., Gohlke, S., and Schulz, T.J. (2019). Aging of Brown and Beige/Brite Adipose Tissue. Handbook of experimental pharmacology *251*, 55-72. https://doi.org/10.1007/164_2018_151.

Greenacre, M., Groenen, P.J.F., Hastie, T., D'Enza, A.I., Markos, A., and Tuzhilina, E. (2022). Principal component analysis. Nat Rev Methods Primers *2*. https://doi.org/10.1038/s43586-022-00184-w.

Grootswagers, P., Mensink, M., Berendsen, A.A.M., Deen, C.P.J., Kema, I.P., Bakker, S.J.L., Santoro, A., Franceschi, C., Meunier, N., and Malpuech-Brugère, C., et al. (2021). Vitamin B-6 intake is related to physical performance in European older adults: results of the New Dietary Strategies Addressing the Specific Needs of the Elderly Population for Healthy Aging in Europe (NU-AGE) study. The American journal of clinical nutrition *113*, 781-789. https://doi.org/10.1093/ajcn/nqaa368.

Gueugneau, M., Coudy-Gandilhon, C., Théron, L., Meunier, B., Barboiron, C., Combaret, L., Taillandier, D., Polge, C., Attaix, D., and Picard, B., et al. (2015). Skeletal muscle lipid content and oxidative activity in relation to muscle fiber type in aging and metabolic syndrome. The journals of gerontology. Series A, Biological sciences and medical sciences *70*, 566-576. https://doi.org/10.1093/gerona/glu086.

Guijas, C., To, A., Montenegro-Burke, J.R., Domingo-Almenara, X., Alipio-Gloria, Z., Kok, B.P., Saez, E., Alvarez, N.H., Johnson, K.A., and Siuzdak, G. (2022). Drug-Initiated Activity Metabolomics Identifies Myristoylglycine as a Potent Endogenous Metabolite for Human Brown Fat Differentiation. Metabolites *12*. https://doi.org/10.3390/metabo12080749.

Guilherme, A., Rowland, L.A., Wang, H., and Czech, M.P. (2023). The adipocyte supersystem of insulin and cAMP signaling. Trends in cell biology *33*, 340-354. https://doi.org/10.1016/j.tcb.2022.07.009.

Hackney, A.C. (2017). Sex Hormones, Exercise and Women (Cham: Springer International Publishing).

Hamilton, M.T., Hamilton, D.G., and Zderic, T.W. (2022). A potent physiological method to magnify and sustain soleus oxidative metabolism improves glucose and lipid regulation. iScience *25*, 104869. https://doi.org/10.1016/j.isci.2022.104869.

Han, H.-S., Ahn, E., Park, E.S., Huh, T., Choi, S., Kwon, Y., Choi, B.H., Lee, J., Choi, Y.H., and Jeong, Y.L., et al. (2023). Impaired BCAA catabolism in adipose tissues promotes age-associated metabolic derangement. Nature aging *3*, 982-1000. https://doi.org/10.1038/s43587-023-00460-8.

Harteneck, C. (2013). Pregnenolone Sulfate: From Steroid Metabolite to TRP Channel Ligand. Molecules *18*, 12012-12028. https://doi.org/10.3390/molecules181012012.

Heidenreich, E., Pfeffer, T., Kracke, T., Mechtel, N., Nawroth, P., Hoffmann, G.F., Schmitt, C.P., Hell, R., Poschet, G., and Peters, V. (2021). A Novel UPLC-MS/MS Method Identifies Organ-Specific Dipeptide Profiles. International journal of molecular sciences *22*. https://doi.org/10.3390/ijms22189979.

Heine, P.A., Taylor, J.A., Iwamoto, G.A., Lubahn, D.B., and Cooke, P.S. (2000). Increased adipose tissue in male and female estrogen receptor-alpha knockout mice. Proceedings of the National Academy of Sciences of the United States of America *97*, 12729-12734. https://doi.org/10.1073/pnas.97.23.12729.

Hellsten, Y., Maclean, D., Rådegran, G., Saltin, B., and Bangsbo, J. (1998). Adenosine concentrations in the interstitium of resting and contracting human skeletal muscle. Circulation *98*, 6-8. https://doi.org/10.1161/01.cir.98.1.6.

Hiley, C.R., and Hoi, P.M. (2007). Oleamide: a fatty acid amide signaling molecule in the cardiovascular system? Cardiovascular drug reviews *25*, 46-60. https://doi.org/10.1111/j.1527-3466.2007.00004.x.

Hipkiss, A.R., Brownson, C., Bertani, M.F., Ruiz, E., and Ferro, A. (2002). Reaction of carnosine with aged proteins: another protective process? Annals of the New York Academy of Sciences *959*, 285-294. https://doi.org/10.1111/j.1749-6632.2002.tb02100.x.

Hirabara, S.M., Curi, R., and Maechler, P. (2010). Saturated fatty acid-induced insulin resistance is associated with mitochondrial dysfunction in skeletal muscle cells. Journal of cellular physiology *222*, 187-194. https://doi.org/10.1002/jcp.21936.

Hla, T., and Dannenberg, A.J. (2012). Sphingolipid signaling in metabolic disorders. Cell metabolism *16*, 420-434. https://doi.org/10.1016/j.cmet.2012.06.017.

Hla, T., Venkataraman, K., and Michaud, J. (2008). The vascular S1P gradient-cellular sources and biological significance. Biochimica et biophysica acta *1781*, 477-482. https://doi.org/10.1016/j.bbalip.2008.07.003.

Ho, A.T.V., Palla, A.R., Blake, M.R., Yucel, N.D., Wang, Y.X., Magnusson, K.E.G., Holbrook, C.A., Kraft, P.E., Delp, S.L., and Blau, H.M. (2017). Prostaglandin E2 is essential for efficacious skeletal muscle stem-cell function, augmenting regeneration and strength. Proceedings of the National Academy of Sciences of the United States of America *114*, 6675-6684. https://doi.org/10.1073/pnas.1705420114.

Holeček, M. (2020). Histidine in Health and Disease: Metabolism, Physiological Importance, and Use as a Supplement. Nutrients *12*. https://doi.org/10.3390/nu12030848.

Hopkins, P.M. (2006). Skeletal muscle physiology. Continuing Education in Anaesthesia Critical Care & Pain *6*, 1-6. https://doi.org/10.1093/bjaceaccp/mki062.

Hosseinkhani, S., Arjmand, B., Dilmaghani-Marand, A., Mohammadi Fateh, S., Dehghanbanadaki, H., Najjar, N., Alavi-Moghadam, S., Ghodssi-Ghassemabadi, R., Nasli-Esfahani, E., and Farzadfar, F., et al. (2022). Targeted metabolomics analysis of amino acids and acylcarnitines as risk markers for diabetes by LC-MS/MS technique. Scientific reports *12*, 8418. https://doi.org/10.1038/s41598-022-11970-7.

Huffman, K.M., Koves, T.R., Hubal, M.J., Abouassi, H., Beri, N., Bateman, L.A., Stevens, R.D., Ilkayeva, O.R., Hoffman, E.P., and Muoio, D.M., et al. (2014). Metabolite signatures of exercise training in human skeletal muscle relate to mitochondrial remodelling and cardiometabolic fitness. Diabetologia *57*, 2282-2295. https://doi.org/10.1007/s00125-014-3343-4.

Huh, J.Y. (2018). The role of exercise-induced myokines in regulating metabolism. Archives of pharmacal research *41*, 14-29. https://doi.org/10.1007/s12272-017-0994-y.

(2023). Human Metabolome Database. https://hmdb.ca/. 01/12/2023.

Idle, J.R., and Gonzalez, F.J. (2007). Metabolomics. Cell Metabolism *6*, 348-351. https://doi.org/10.1016/j.cmet.2007.10.005.

Jamar, G., and Pisani, L.P. (2023). Inflammatory crosstalk between saturated fatty acids and gut microbiota-white adipose tissue axis. European journal of nutrition *62*, 1077-1091. https://doi.org/10.1007/s00394-022-03062-z.

Johnson, C.H., Ivanisevic, J., and Siuzdak, G. (2016). Metabolomics: beyond biomarkers and towards mechanisms. Nature reviews. Molecular cell biology *17*, 451-459. https://doi.org/10.1038/nrm.2016.25.

Jungert, A., and Neuhäuser-Berthold, M. (2020). Determinants of Vitamin B6 Status in Community-Dwelling Older Adults: A Longitudinal Study Over a Period of 18 Years. The journals of gerontology. Series A, Biological sciences and medical sciences *75*, 374-379. https://doi.org/10.1093/gerona/glz010.

Junot, C., Fenaille, F., Colsch, B., and Bécher, F. (2014). High resolution mass spectrometry based techniques at the crossroads of metabolic pathways. Mass spectrometry reviews *33*, 471-500. https://doi.org/10.1002/mas.21401.

Kaikaew, K., Grefhorst, A., and Visser, J.A. (2021). Sex Differences in Brown Adipose Tissue Function: Sex Hormones, Glucocorticoids, and Their Crosstalk. Front. Endocrinol. *12*, 652444. https://doi.org/10.3389/fendo.2021.652444.

Kajimura, S., Spiegelman, B.M., and Seale, P. (2015). Brown and Beige Fat: Physiological Roles beyond Heat Generation. Cell metabolism *22*, 546-559. https://doi.org/10.1016/j.cmet.2015.09.007.

Kang, J.-S. (2012). Principles and Applications of LC-MS/MS for the Quantitative Bioanalysis of Analytes in Various Biological Samples. In Tandem Mass Spectrometry - Applications and Principles, J. Prasain, ed. (InTech).

Kelly, M., Gauthier, M.-S., Saha, A.K., and Ruderman, N.B. (2009). Activation of AMP-activated protein kinase by interleukin-6 in rat skeletal muscle: association with changes in cAMP, energy state, and endogenous fuel mobilization. Diabetes *58*, 1953-1960. https://doi.org/10.2337/db08-1293.

Kelly, R.S., Kelly, M.P., and Kelly, P. (2020). Metabolomics, physical activity, exercise and health: A review of the current evidence. Biochimica et biophysica acta. Molecular basis of disease *1866*, 165936. https://doi.org/10.1016/j.bbadis.2020.165936.

Kho, A.T., Kang, P.B., Kohane, I.S., and Kunkel, L.M. (2006). Transcriptome-scale similarities between mouse and human skeletal muscles with normal and myopathic phenotypes. BMC musculoskeletal disorders *7*, 23. https://doi.org/10.1186/1471-2474-7-23.

Khor, S.C., Razak, A.M., Wan Ngah, W.Z., Mohd Yusof, Y.A., Abdul Karim, N., and Makpol, S. (2016). The Tocotrienol-Rich Fraction Is Superior to Tocopherol in Promoting Myogenic Differentiation in the Prevention of Replicative Senescence of Myoblasts. PloS one *11*, e0149265. https://doi.org/10.1371/journal.pone.0149265.

Khoramipour, K., Sandbakk, Ø., Keshteli, A.H., Gaeini, A.A., Wishart, D.S., and Chamari, K. (2022). Metabolomics in Exercise and Sports: A Systematic Review. Sports medicine (Auckland, N.Z.) *52*, 547-583. https://doi.org/10.1007/s40279-021-01582-y.

Kim, Y. an, Lee, S.H., Koh, J.-M., Kwon, S.-H., Lee, Y., Cho, H.J., Kim, H., Kim, S.J., Lee, J.H., and Yoo, H.J., et al. (2023). Fatty acid amides as potential circulating biomarkers for sarcopenia. Journal of cachexia, sarcopenia and muscle *14*, 1558-1568. https://doi.org/10.1002/jcsm.13244.

Kim, Y.S., and Sainz, R.D. (1992). Beta-adrenergic agonists and hypertrophy of skeletal muscles. Life sciences *50*, 397-407. https://doi.org/10.1016/0024-3205(92)90374-x.

Kobayashi, H., Matsuda, M., Fukuhara, A., Komuro, R., and Shimomura, I. (2009). Dysregulated glutathione metabolism links to impaired insulin action in adipocytes. American journal of physiology. Endocrinology and metabolism *296*, E1326-34. https://doi.org/10.1152/ajpendo.90921.2008.

Kobayashi, Y., Watanabe, N., Kitakaze, T., Sugimoto, K., Izawa, T., Kai, K., Harada, N., and Yamaji, R. (2021). Oleamide rescues tibialis anterior muscle atrophy of mice housed in small cages. The British journal of nutrition *126*, 481-491. https://doi.org/10.1017/S0007114520004304.

Kowalski, G.M., Carey, A.L., Selathurai, A., Kingwell, B.A., and Bruce, C.R. (2013). Plasma Sphingosine-1-Phosphate Is Elevated in Obesity. PloS one *8*, e72449. https://doi.org/10.1371/journal.pone.0072449.

Kumar, A., Kumar, Y., Sevak, J.K., Kumar, S., Kumar, N., and Gopinath, S.D. (2020). Metabolomic analysis of primary human skeletal muscle cells during myogenic progression. Scientific reports *10*, 11824. https://doi.org/10.1038/s41598-020-68796-4.

Kuo, I.Y., and Ehrlich, B.E. (2015). Signaling in muscle contraction. Cold Spring Harbor perspectives in biology *7*, a006023. https://doi.org/10.1101/cshperspect.a006023.

Kuroiwa, M., Hamaoka-Fuse, S., Sugimoto, M., Kurosawa, Y., Aita, Y., Tomita, A., Anjo, M., Tanaka, R., Endo, T., and Kime, R., et al. (2021). Correlation of Plasma Amino Acid and Anthropometric Profiles

with Brown Adipose Tissue Density in Humans. Journal of clinical medicine *10*. https://doi.org/10.3390/jcm10112339.

Larson, C.J. (2019). Translational Pharmacology and Physiology of Brown Adipose Tissue in Human Disease and Treatment. Handbook of experimental pharmacology *251*, 381-424. https://doi.org/10.1007/164_2018_184.

Larsson, L., Degens, H., Li, M., Salviati, L., Lee, Y.I., Thompson, W., Kirkland, J.L., and Sandri, M. (2019). Sarcopenia: Aging-Related Loss of Muscle Mass and Function. Physiological reviews *99*, 427-511. https://doi.org/10.1152/physrev.00061.2017.

Law, J., Bloor, I., Budge, H., and Symonds, M.E. (2014). The influence of sex steroids on adipose tissue growth and function. Hormone molecular biology and clinical investigation *19*, 13-24. https://doi.org/10.1515/hmbci-2014-0015.

Lawton, K.A., Berger, A., Mitchell, M., Milgram, K.E., Evans, A.M., Guo, L., Hanson, R.W., Kalhan, S.C., Ryals, J.A., and Milburn, M.V. (2008). Analysis of the adult human plasma metabolome. Pharmacogenomics *9*, 383-397. https://doi.org/10.2217/14622416.9.4.383.

Lecturio (2022). Overview of Skeletal Muscle Tissue. https://www.lecturio.com/concepts/skeletal-muscle-contraction/. 24.07.2023.

Lee, H., and Lim, Y. (2018). Tocotrienol-rich fraction supplementation reduces hyperglycemia-induced skeletal muscle damage through regulation of insulin signaling and oxidative stress in type 2 diabetic mice. The Journal of nutritional biochemistry *57*, 77-85. https://doi.org/10.1016/j.jnutbio.2018.03.016.

Lefkimmiatis, K., and Zaccolo, M. (2014). cAMP signaling in subcellular compartments. Pharmacology & therapeutics *143*, 295-304. https://doi.org/10.1016/j.pharmthera.2014.03.008.

Leng, X., and Jiang, H. (2019). Effects of arachidonic acid and its major prostaglandin derivatives on bovine myoblast proliferation, differentiation, and fusion. Domestic animal endocrinology *67*, 28-36. https://doi.org/10.1016/j.domaniend.2018.12.006.

Lennon, D.L., Stratman, F.W., Shrago, E., Nagle, F.J., Madden, M., Hanson, P., and Carter, A.L. (1983). Effects of acute moderate-intensity exercise on carnitine metabolism in men and women. Journal of applied physiology: respiratory, environmental and exercise physiology *55*, 489-495. https://doi.org/10.1152/jappl.1983.55.2.489.

Lim, J.J., Ngah, W.Z.W., Mouly, V., and Abdul Karim, N. (2013). Reversal of myoblast aging by tocotrienol rich fraction posttreatment. Oxidative medicine and cellular longevity *2013*, 978101. https://doi.org/10.1155/2013/978101.

Lipina, C., and Hundal, H.S. (2017). Lipid modulation of skeletal muscle mass and function. Journal of cachexia, sarcopenia and muscle *8*, 190-201. https://doi.org/10.1002/jcsm.12144.

Liu, C., Song, Z., Li, Z., Boon, M.R., Schönke, M., Rensen, P.C.N., and Wang, Y. (2023). Dietary choline increases brown adipose tissue activation markers and improves cholesterol metabolism in female APOE*3-Leiden.CETP mice. International journal of obesity (2005) *47*, 236-243. https://doi.org/10.1038/s41366-023-01269-6.

Liu, S.Z., Jemiolo, B., Lavin, K.M., Lester, B.E., Trappe, S.W., and Trappe, T.A. (2016). Prostaglandin E2/cyclooxygenase pathway in human skeletal muscle: influence of muscle fiber type and age. Journal of applied physiology (Bethesda, Md. : 1985) *120*, 546-551. https://doi.org/10.1152/japplphysiol.00396.2015.

Lohninger, A., Sendic, A., Litzlbauer, E., Hofbauer, R., Staniek, H., Blesky, D., Schwieglhofer, C., Eder, M., Bergmüler, H., and Mascher, D., et al. (2005). Endurance Exercise Training and L-Carnitine Supplementation Stimulates Gene Expression in the Blood and Muscle Cells in Young Athletes and Middle Aged Subjects. Monatsh. Chem. *136*, 1425-1442. https://doi.org/10.1007/s00706-005-0335-6.

Lopez, M.J., and Mohiuddin, S.S. (2023). StatPearls [Internet] (StatPearls Publishing).

Luijten, I.H.N., Cannon, B., and Nedergaard, J. (2019). Glucocorticoids and Brown Adipose Tissue: Do glucocorticoids really inhibit thermogenesis? Molecular aspects of medicine *68*, 42-59. https://doi.org/10.1016/j.mam.2019.07.002.

Lundgren, P., Sharma, P.V., Dohnalová, L., Coleman, K., Uhr, G.T., Kircher, S., Litichevskiy, L., Bahnsen, K., Descamps, H.C., and Demetriadou, C., et al. (2023). A subpopulation of lipogenic brown adipocytes drives thermogenic memory. Nature metabolism *5*, 1691-1705. https://doi.org/10.1038/s42255-023-00893-w.

Luzak, A., Heier, M., Thorand, B., Laxy, M., Nowak, D., Peters, A., and Schulz, H. (2017). Physical activity levels, duration pattern and adherence to WHO recommendations in German adults. PloS one *12*, e0172503. https://doi.org/10.1371/journal.pone.0172503.

Lynch, C.J., Gern, B., Lloyd, C., Hutson, S.M., Eicher, R., and Vary, T.C. (2006). Leucine in food mediates some of the postprandial rise in plasma leptin concentrations. American journal of physiology. Endocrinology and metabolism *291*, E621-30. https://doi.org/10.1152/ajpendo.00462.2005.

Macfarlane, D.P., Forbes, S., and Walker, B.R. (2008). Glucocorticoids and fatty acid metabolism in humans: fuelling fat redistribution in the metabolic syndrome. The Journal of endocrinology *197*, 189-204. https://doi.org/10.1677/JOE-08-0054.

Mancuso, P., and Bouchard, B. (2019). The Impact of Aging on Adipose Function and Adipokine Synthesis. Front. Endocrinol. *10*, 137. https://doi.org/10.3389/fendo.2019.00137.

Marshall, A.G., and Hendrickson, C.L. (2008). High-resolution mass spectrometers. Annual review of analytical chemistry (Palo Alto, Calif.) *1*, 579-599. https://doi.org/10.1146/annurev.anchem.1.031207.112945.

Mason, R.R., Meex, R.C.R., Lee-Young, R., Canny, B.J., and Watt, M.J. (2012). Phosphorylation of adipose triglyceride lipase Ser(404) is not related to 5'-AMPK activation during moderate-intensity exercise in humans. American journal of physiology. Endocrinology and metabolism *303*, E534-41. https://doi.org/10.1152/ajpendo.00082.2012.

Matthews, J.J., Artioli, G.G., Turner, M.D., and Sale, C. (2019). The Physiological Roles of Carnosine and β-Alanine in Exercising Human Skeletal Muscle. Medicine and science in sports and exercise *51*, 2098-2108. https://doi.org/10.1249/MSS.0000000000002033.

Maurer, S.F., Dieckmann, S., Kleigrewe, K., Colson, C., Amri, E.-Z., and Klingenspor, M. (2019). Fatty Acid Metabolites as Novel Regulators of Non-shivering Thermogenesis. Handbook of experimental pharmacology *251*, 183-214. https://doi.org/10.1007/164_2018_150.

Maushart, C.I., Sun, W., Othman, A., Ghosh, A., Senn, J.R., Fischer, J.G.W., Madoerin, P., Loeliger, R.C., Benz, R.M., and Takes, M., et al. (2023). Effect of high-dose glucocorticoid treatment on human brown adipose tissue activity: a randomised, double-blinded, placebo-controlled cross-over trial in healthy men. eBioMedicine *96*, 104771. https://doi.org/10.1016/j.ebiom.2023.104771.

Mayes, J.S., and Watson, G.H. (2004). Direct effects of sex steroid hormones on adipose tissues and obesity. Obesity reviews : an official journal of the International Association for the Study of Obesity *5*, 197-216. https://doi.org/10.1111/j.1467-789X.2004.00152.x.

McCoin, C.S., Knotts, T.A., and Adams, S.H. (2015). Acylcarnitines--old actors auditioning for new roles in metabolic physiology. Nature reviews. Endocrinology *11*, 617-625. https://doi.org/10.1038/nrendo.2015.129.

McKnight, G.S. (1991). Cyclic AMP second messenger systems. Current opinion in cell biology *3*, 213-217. https://doi.org/10.1016/0955-0674(91)90141-K.

Melzig, M.F., and Alasbahi, R.H. (2012). Forskolin and derivatives as tools for studying the role of cAMP. 0031-7144, 5-13. https://doi.org/10.1691/ph.2012.1642.

Méndez-Lara, K.A., Rodríguez-Millán, E., Sebastián, D., Blanco-Soto, R., Camacho, M., Nan, M.N., Diarte-Añazco, E.M.G., Mato, E., Lope-Piedrafita, S., and Roglans, N., et al. (2021). Nicotinamide Protects Against Diet-Induced Body Weight Gain, Increases Energy Expenditure, and Induces White

Adipose Tissue Beiging. Molecular nutrition & food research *65*, e2100111. https://doi.org/10.1002/mnfr.202100111.

Meseguer, A., Puche, C., and Cabero, A. (2002). Sex steroid biosynthesis in white adipose tissue. Hormone and metabolic research = Hormon- und Stoffwechselforschung = Hormones et metabolisme *34*, 731-736. https://doi.org/10.1055/s-2002-38249.

Michael, M.D., Michael, L.F., and Simpson, E.R. (1997). A CRE-like sequence that binds CREB and contributes to cAMP-dependent regulation of the proximal promoter of the human aromatase P450 (CYP19) gene. Molecular and cellular endocrinology *134*, 147-156. https://doi.org/10.1016/s0303-7207(97)00178-0.

Millay, D.P., Sutherland, L.B., Bassel-Duby, R., and Olson, E.N. (2014). Myomaker is essential for muscle regeneration. Genes & development *28*, 1641-1646. https://doi.org/10.1101/gad.247205.114.

Miller, S.B. (2006). Prostaglandins in health and disease: an overview. Seminars in arthritis and rheumatism *36*, 37-49. https://doi.org/10.1016/j.semarthrit.2006.03.005.

Mills, E.L., Harmon, C., Jedrychowski, M.P., Xiao, H., Garrity, R., Tran, N.V., Bradshaw, G.A., Fu, A., Szpyt, J., and Reddy, A., et al. (2021). UCP1 governs liver extracellular succinate and inflammatory pathogenesis. Nature metabolism *3*, 604-617. https://doi.org/10.1038/s42255-021-00389-5.

Mitchell, W.K., Williams, J., Atherton, P., Larvin, M., Lund, J., and Narici, M. (2012). Sarcopenia, dynapenia, and the impact of advancing age on human skeletal muscle size and strength; a quantitative review. Frontiers in physiology *3*, 260. https://doi.org/10.3389/fphys.2012.00260.

Mitterberger, M.C., Lechner, S., Mattesich, M., and Zwerschke, W. (2014). Adipogenic differentiation is impaired in replicative senescent human subcutaneous adipose-derived stromal/progenitor cells. The journals of gerontology. Series A, Biological sciences and medical sciences *69*, 13-24. https://doi.org/10.1093/gerona/glt043.

Mo, C., Zhao, R., Vallejo, J., Igwe, O., Bonewald, L., Wetmore, L., and Brotto, M. (2015). Prostaglandin E2 promotes proliferation of skeletal muscle myoblasts via EP4 receptor activation. Cell cycle (Georgetown, Tex.) *14*, 1507-1516. https://doi.org/10.1080/15384101.2015.1026520.

Moretti, A., Paoletta, M., Liguori, S., Bertone, M., Toro, G., and Iolascon, G. (2020). Choline: An Essential Nutrient for Skeletal Muscle. Nutrients *12*. https://doi.org/10.3390/nu12072144.

Mukherjee, T., Hanes, J., Tews, I., Ealick, S.E., and Begley, T.P. (2011). Pyridoxal phosphate: biosynthesis and catabolism. Biochimica et biophysica acta *1814*, 1585-1596. https://doi.org/10.1016/j.bbapap.2011.06.018.

Nagai, M., Tuchiya, K., and Kojima, H. (1996). Prostaglandin E2 increases the calcium concentration in rat brown adipocytes and their consumption of oxygen. Prostaglandins *51*, 377-386. https://doi.org/10.1016/0090-6980(96)00044-5.

Nagasawa, T., Yonekura, T., Nishizawa, N., and Kitts, D.D. (2001). In vitro and in vivo inhibition of muscle lipid and protein oxidation by carnosine. Mol Cell Biochem *225*, 29-34. https://doi.org/10.1023/A:1012256521840.

Niemann, B., Haufs-Brusberg, S., Puetz, L., Feickert, M., Jaeckstein, M.Y., Hoffmann, A., Zurkovic, J., Heine, M., Trautmann, E.-M., and Müller, C.E., et al. (2022). Apoptotic brown adipocytes enhance energy expenditure via extracellular inosine. Nature *609*, 361-368. https://doi.org/10.1038/s41586-022-05041-0.

Okajima, K., Inoue, M., and Morino, Y. (1985). Studies on the mechanism for renal elimination of N-acetylphenylalanine: its pathophysiologic significance in phenylketonuria. The Journal of laboratory and clinical medicine *105*, 132-138.

Ou, M.-Y., Zhang, H., Tan, P.-C., Zhou, S.-B., and Li, Q.-F. (2022). Adipose tissue aging: mechanisms and therapeutic implications. Cell death & disease *13*, 300. https://doi.org/10.1038/s41419-022-04752-6.

(2023). Overweight & Obesity Statistics. NIDDK - National Institute of Diabetes and Digestive and Kidney Diseases.

Ozaki, K., Sano, T., Tsuji, N., Matsuura, T., and Narama, I. (2011). Carnitine is necessary to maintain the phenotype and function of brown adipose tissue. Laboratory investigation; a journal of technical methods and pathology *91*, 704-710. https://doi.org/10.1038/labinvest.2011.6.

Park, G., Haley, J.A., Le, J., Jung, S.M., Fitzgibbons, T.P., Korobkina, E.D., Li, H., Fluharty, S.M., Chen, Q., and Spinelli, J.B., et al. (2023). Quantitative analysis of metabolic fluxes in brown fat and skeletal muscle during thermogenesis. Nature metabolism *5*, 1204-1220. https://doi.org/10.1038/s42255-023-00825-8.

Patti, G.J. (2011). Separation strategies for untargeted metabolomics. Journal of separation science *34*, 3460-3469. https://doi.org/10.1002/jssc.201100532.

Pedersen, B.K., and Febbraio, M.A. (2008). Muscle as an endocrine organ: focus on muscle-derived interleukin-6. Physiological reviews *88*, 1379-1406. https://doi.org/10.1152/physrev.90100.2007.

Peek, V., Neumann, E., Inoue, T., Koenig, S., Pflieger, F.J., Gerstberger, R., Roth, J., Matsumura, K., and Rummel, C. (2020). Age-Dependent Changes of Adipokine and Cytokine Secretion From Rat Adipose Tissue by Endogenous and Exogenous Toll-Like Receptor Agonists. Frontiers in immunology *11*, 1800. https://doi.org/10.3389/fimmu.2020.01800.

Picard, F., and Guarente, L. (2005). Molecular links between aging and adipose tissue. International journal of obesity (2005) *29 Suppl 1*, S36-9. https://doi.org/10.1038/sj.ijo.0802912.

Potthoff, M.J., Arnold, M.A., McAnally, J., Richardson, J.A., Bassel-Duby, R., and Olson, E.N. (2007). Regulation of Skeletal Muscle Sarcomere Integrity and Postnatal Muscle Function by Mef2c. Molecular and cellular biology *27*, 8143-8151. https://doi.org/10.1128/MCB.01187-07.

Prattichizzo, F., Nigris, V. de, Spiga, R., Mancuso, E., La Sala, L., Antonicelli, R., Testa, R., Procopio, A.D., Olivieri, F., and Ceriello, A. (2018). Inflammageing and metaflammation: The yin and yang of type 2 diabetes. Ageing research reviews *41*, 1-17. https://doi.org/10.1016/j.arr.2017.10.003.

Proia, R.L., and Hla, T. (2015). Emerging biology of sphingosine-1-phosphate: its role in pathogenesis and therapy. J Clin Invest *125*, 1379-1387. https://doi.org/10.1172/JCI76369.

Przyborowski, K., Wojewoda, M., Sitek, B., Zakrzewska, A., Kij, A., Wandzel, K., Zoladz, J.A., and Chlopicki, S. (2015). Effects of 1-Methylnicotinamide (MNA) on Exercise Capacity and Endothelial Response in Diabetic Mice. PloS one *10*, e0130908. https://doi.org/10.1371/journal.pone.0130908.

Quevedo, S., Roca, P., Picó, C., and Palou, A. (1998). Sex-associated differences in cold-induced UCP1 synthesis in rodent brown adipose tissue. Pflugers Archiv : European journal of physiology *436*, 689-695. https://doi.org/10.1007/s004240050690.

Rafecas, I., Esteve, M., Remesar, X., and Alemany, M. (1991). Plasma amino acids of lean and obese Zucker rats subjected to a cafeteria diet after weaning. Biochemistry international *25*, 797-806.

Rahman, M.S. (2019). Prostacyclin: A major prostaglandin in the regulation of adipose tissue development. Journal of cellular physiology *234*, 3254-3262. https://doi.org/10.1002/jcp.26932.

Ramage, L.E., Akyol, M., Fletcher, A.M., Forsythe, J., Nixon, M., Carter, R.N., van Beek, E.J.R., Morton, N.M., Walker, B.R., and Stimson, R.H. (2016). Glucocorticoids Acutely Increase Brown Adipose Tissue Activity in Humans, Revealing Species-Specific Differences in UCP-1 Regulation. Cell metabolism *24*, 130-141. https://doi.org/10.1016/j.cmet.2016.06.011.

Rathod, R.H., Chaudhari, S.R., Patil, A.S., and Shirkhedkar, A.A. (2019). Ultra-high performance liquid chromatography-MS/MS (UHPLC-MS/MS) in practice: analysis of drugs and pharmaceutical formulations. Futur J Pharm Sci *5*. https://doi.org/10.1186/s43094-019-0007-8.

Ray, C.A., and Hume, K.M. (1998). Sympathetic neural adaptations to exercise training in humans: insights from microneurography. Medicine and science in sports and exercise *30*, 387-391. https://doi.org/10.1097/00005768-199803000-00008.

Reverte-Salisa, L., Sanyal, A., and Pfeifer, A. (2019). Role of cAMP and cGMP Signaling in Brown Fat. Handbook of experimental pharmacology *251*, 161-182. https://doi.org/10.1007/164_2018_117.

Reverte-Salisa, L., Siddig, S., Hildebrand, S., Yao, X., Zurkovic, J., Jaeckstein, M.Y., Heeren, J., Lezoualc'h, F., Krahmer, N., and Pfeifer, A. (2024). EPAC1 enhances brown fat growth and beige adipogenesis. Nature cell biology *26*, 113-123. https://doi.org/10.1038/s41556-023-01311-9.

Richter, E.A., Garetto, L.P., Goodman, M.N., and Ruderman, N.B. (1982). Muscle glucose metabolism following exercise in the rat: increased sensitivity to insulin. J Clin Invest *69*, 785-793. https://doi.org/10.1172/JCI110517.

Richter, E.A., Mikines, K.J., Galbo, H., and Kiens, B. (1989). Effect of exercise on insulin action in human skeletal muscle. Journal of applied physiology (Bethesda, Md. : 1985) *66*, 876-885. https://doi.org/10.1152/jappl.1989.66.2.876.

Ringnér, M. (2008). What is principal component analysis? Nature biotechnology *26*, 303-304. https://doi.org/10.1038/nbt0308-303.

Rivera-Brown, A.M., and Frontera, W.R. (2012). Principles of exercise physiology: responses to acute exercise and long-term adaptations to training. PM & R : the journal of injury, function, and rehabilitation *4*, 797-804. https://doi.org/10.1016/j.pmrj.2012.10.007.

Rogers, N.H. (2015). Brown adipose tissue during puberty and with aging. Annals of medicine *47*, 142-149. https://doi.org/10.3109/07853890.2014.914807.

Roh, C., Han, J., Tzatsos, A., and Kandror, K.V. (2003). Nutrient-sensing mTOR-mediated pathway regulates leptin production in isolated rat adipocytes. American journal of physiology. Endocrinology and metabolism *284*, E322-30. https://doi.org/10.1152/ajpendo.00230.2002.

Romero, S.A., McCord, J.L., Ely, M.R., Sieck, D.C., Buck, T.M., Luttrell, M.J., MacLean, D.A., and Halliwill, J.R. (2017). Mast cell degranulation and de novo histamine formation contribute to sustained postexercise vasodilation in humans. Journal of applied physiology (Bethesda, Md. : 1985) *122*, 603-610. https://doi.org/10.1152/japplphysiol.00633.2016.

Roth, J., Qiang, X., Marbán, S.L., Redelt, H., and Lowell, B.C. (2004). The obesity pandemic: where have we been and where are we going? Obesity research *12 Suppl 2*, 88S-101S. https://doi.org/10.1038/oby.2004.273.

Rudolf, R., Magalhães, P.J., and Pozzan, T. (2006). Direct in vivo monitoring of sarcoplasmic reticulum Ca2+ and cytosolic cAMP dynamics in mouse skeletal muscle. The Journal of cell biology *173*, 187-193. https://doi.org/10.1083/jcb.200601160.

Rui, L. (2017). Brown and Beige Adipose Tissues in Health and Disease. Comprehensive Physiology *7*, 1281-1306. https://doi.org/10.1002/cphy.c170001.

Rutledge, J., Oh, H., and Wyss-Coray, T. (2022). Measuring biological age using omics data. Nature reviews. Genetics. https://doi.org/10.1038/s41576-022-00511-7.

Saely, C.H., Geiger, K., and Drexel, H. (2012). Brown versus white adipose tissue: a mini-review. Gerontology *58*, 15-23. https://doi.org/10.1159/000321319.

Saito, M. (2013). Brown adipose tissue as a regulator of energy expenditure and body fat in humans. Diabetes & metabolism journal *37*, 22-29. https://doi.org/10.4093/dmj.2013.37.1.22.

Sanchez-Delgado, G., Martinez-Tellez, B., Olza, J., Aguilera, C.M., Gil, Á., and Ruiz, J.R. (2015). Role of Exercise in the Activation of Brown Adipose Tissue. Annals of nutrition & metabolism *67*, 21-32. https://doi.org/10.1159/000437173.

Sato, K., and Iemitsu, M. (2015). Exercise and sex steroid hormones in skeletal muscle. The Journal of steroid biochemistry and molecular biology *145*, 200-205. https://doi.org/10.1016/j.jsbmb.2014.03.009.

Sato, K., Iemitsu, M., Aizawa, K., and Ajisaka, R. (2008). Testosterone and DHEA activate the glucose metabolism-related signaling pathway in skeletal muscle. American journal of physiology. Endocrinology and metabolism *294*, E961-8. https://doi.org/10.1152/ajpendo.00678.2007.

Schiaffino, S., and Reggiani, C. (2011). Fiber types in mammalian skeletal muscles. Physiological reviews *91*, 1447-1531. https://doi.org/10.1152/physrev.00031.2010.

Schiffer, L., Barnard, L., Baranowski, E.S., Gilligan, L.C., Taylor, A.E., Arlt, W., Shackleton, C.H.L., and Storbeck, K.-H. (2019). Human steroid biosynthesis, metabolism and excretion are differentially reflected by serum and urine steroid metabolomes: A comprehensive review. The Journal of steroid biochemistry and molecular biology *194*, 105439. https://doi.org/10.1016/j.jsbmb.2019.105439.

Schosserer, M., Grillari, J., Wolfrum, C., and Scheideler, M. (2018). Age-Induced Changes in White, Brite, and Brown Adipose Depots: A Mini-Review. Gerontology *64*, 229-236. https://doi.org/10.1159/000485183.

Schranner, D., Kastenmüller, G., Schönfelder, M., Römisch-Margl, W., and Wackerhage, H. (2020). Metabolite Concentration Changes in Humans After a Bout of Exercise: a Systematic Review of Exercise Metabolomics Studies. Sports medicine - open *6*, 11. https://doi.org/10.1186/s40798-020-0238-4.

Sharma, P., and Agnihotri, N. (2020). Fish oil and corn oil induced differential effect on beiging of visceral and subcutaneous white adipose tissue in high-fat-diet-induced obesity. The Journal of nutritional biochemistry *84*, 108458. https://doi.org/10.1016/j.jnutbio.2020.108458.

Shih, M.F., and Taberner, P.V. (1995). Selective activation of brown adipocyte hormone-sensitive lipase and cAMP production in the mouse by beta 3-adrenoceptor agonists. Biochemical pharmacology *50*, 601-608. https://doi.org/10.1016/0006-2952(95)00185-3.

Shimizu, T., and Yokotani, K. (2009). Effects of centrally administered prostaglandin E(3) and thromboxane A(3) on plasma noradrenaline and adrenaline in rats: comparison with prostaglandin E(2) and thromboxane A(2). European journal of pharmacology *611*, 30-34. https://doi.org/10.1016/j.ejphar.2009.03.057.

Shimomura, Y., Murakami, T., Nakai, N., Nagasaki, M., and Harris, R.A. (2004). Exercise promotes BCAA catabolism: effects of BCAA supplementation on skeletal muscle during exercise. The Journal of nutrition *134*, 1583S-1587S. https://doi.org/10.1093/jn/134.6.1583S.

Shin, W., Okamatsu-Ogura, Y., Machida, K., Tsubota, A., Nio-Kobayashi, J., and Kimura, K. (2017). Impaired adrenergic agonist-dependent beige adipocyte induction in aged mice. Obesity (Silver Spring, Md.) *25*, 417-423. https://doi.org/10.1002/oby.21727.

Sigal, R.J., Kenny, G.P., Wasserman, D.H., and Castaneda-Sceppa, C. (2004). Physical activity/exercise and type 2 diabetes. Diabetes care *27*, 2518-2539. https://doi.org/10.2337/diacare.27.10.2518.

Silveira, W.A., Gonçalves, D.A., Graça, F.A., Andrade-Lopes, A.L., Bergantin, L.B., Zanon, N.M., Godinho, R.O., Kettelhut, I.C., and Navegantes, L.C.C. (2014). Activating cAMP/PKA signaling in skeletal muscle suppresses the ubiquitin-proteasome-dependent proteolysis: implications for sympathetic regulation. Journal of applied physiology (Bethesda, Md. : 1985) *117*, 11-19. https://doi.org/10.1152/japplphysiol.01055.2013.

Singh, P., Gollapalli, K., Mangiola, S., Schranner, D., Yusuf, M.A., Chamoli, M., Shi, S.L., Lopes Bastos, B., Nair, T., and Riermeier, A., et al. (2023). Taurine deficiency as a driver of aging. Science (New York, N.Y.) *380*, eabn9257. https://doi.org/10.1126/science.abn9257.

Sinha-Hikim, I., Artaza, J., Woodhouse, L., Gonzalez-Cadavid, N., Singh, A.B., Lee, M.I., Storer, T.W., Casaburi, R., Shen, R., and Bhasin, S. (2002). Testosterone-induced increase in muscle size in healthy young men is associated with muscle fiber hypertrophy. American journal of physiology. Endocrinology and metabolism *283*, E154-64. https://doi.org/10.1152/ajpendo.00502.2001.

Sipilä, S., Narici, M., Kjaer, M., Pöllänen, E., Atkinson, R.A., Hansen, M., and Kovanen, V. (2013). Sex hormones and skeletal muscle weakness. Biogerontology *14*, 231-245. https://doi.org/10.1007/s10522-013-9425-8.

Smith, G.I. (2019). Polyunsaturated Omega-3 Fatty Acids and Skeletal Muscle. In Nutrition and Skeletal Muscle (Elsevier), pp. 379–392.

Sousa-Victor, P., García-Prat, L., and Muñoz-Cánoves, P. (2022). Control of satellite cell function in muscle regeneration and its disruption in ageing. Nature reviews. Molecular cell biology *23*, 204-226. https://doi.org/10.1038/s41580-021-00421-2.

Stanford, K.I., and Goodyear, L.J. (2018). Muscle-Adipose Tissue Cross Talk. Cold Spring Harbor perspectives in medicine *8*. https://doi.org/10.1101/cshperspect.a029801.

Stanford, K.I., Middelbeek, R.J.W., and Goodyear, L.J. (2015). Exercise Effects on White Adipose Tissue: Beiging and Metabolic Adaptations. Diabetes *64*, 2361-2368. https://doi.org/10.2337/db15-0227.

Stanford, K.I., Middelbeek, R.J.W., Townsend, K.L., An, D., Nygaard, E.B., Hitchcox, K.M., Markan, K.R., Nakano, K., Hirshman, M.F., and Tseng, Y.-H., et al. (2013). Brown adipose tissue regulates glucose homeostasis and insulin sensitivity. The Journal of clinical investigation *123*, 215-223. https://doi.org/10.1172/JCI62308.

Stephens, F.B., Constantin-Teodosiu, D., and Greenhaff, P.L. (2007). New insights concerning the role of carnitine in the regulation of fuel metabolism in skeletal muscle. The Journal of physiology *581*, 431-444. https://doi.org/10.1113/jphysiol.2006.125799.

Stincone, A., Prigione, A., Cramer, T., Wamelink, M.M.C., Campbell, K., Cheung, E., Olin-Sandoval, V., Grüning, N.-M., Krüger, A., and Tauqeer Alam, M., et al. (2015). The return of metabolism: biochemistry and physiology of the pentose phosphate pathway. Biological reviews of the Cambridge Philosophical Society *90*, 927-963. https://doi.org/10.1111/brv.12140.

Suchacki, K., Ramage, L., Gray, C., Rodrguez, B.G., Choong, K.T., Boyle, L., MacNaught, G., Gregoriades, M., Wakelin, S., and von, K.A., et al. (2022). Human brown adipose tissue demonstrates substantial choline uptake for incorporation into phosphatidylcholines. EJEA. https://doi.org/10.1530/endoabs.86.OC5.1.

Suchacki, K.J., and Stimson, R.H. (2021). Nutritional Regulation of Human Brown Adipose Tissue. Nutrients *13*. https://doi.org/10.3390/nu13061748.

Tanida, M., Gotoh, H., Taniguchi, H., Otani, H., Shen, J., Nakamura, T., Tsuruoka, N., Kiso, Y., Okumura, N., and Nagai, K. (2007). Effects of central injection of L-carnosine on sympathetic nerve activity innervating brown adipose tissue and body temperature in rats. Regulatory Peptides *144*, 62-71. https://doi.org/10.1016/j.regpep.2007.06.001.

Tao, X., Du, R., Guo, S., Feng, X., Yu, T., OuYang, Q., Chen, Q., Fan, X., Wang, X., and Guo, C., et al. (2022). PGE2 -EP3 axis promotes brown adipose tissue formation through stabilization of WTAP RNA methyltransferase. The EMBO journal *41*, e110439. https://doi.org/10.15252/embj.2021110439.

Teruya, T., Sunagawa, S., Mori, A., Masuzaki, H., and Yanagida, M. (2023). Markers for obese and non-obese Type 2 diabetes identified using whole blood metabolomics. Sci Rep *13*, 2460. https://doi.org/10.1038/s41598-023-29619-4.

Theriault, A., Chao, J.T., Wang, Q., Gapor, A., and Adeli, K. (1999). Tocotrienol: a review of its therapeutic potential. Clinical biochemistry *32*, 309-319. https://doi.org/10.1016/S0009-9120(99)00027-2.

Thompson, L.V., and Brown, M. (1999). Age-related changes in contractile properties of single skeletal fibers from the soleus muscle. Journal of applied physiology (Bethesda, Md. : 1985) *86*, 881-886. https://doi.org/10.1152/jappl.1999.86.3.881.

Tokarz, J., Möller, G., Artati, A., Huber, S., Zeigerer, A., Blaauw, B., Adamski, J., and Dyar, K.A. (2021). Common Muscle Metabolic Signatures Highlight Arginine and Lysine Metabolism as Potential Therapeutic Targets to Combat Unhealthy Aging. International journal of molecular sciences *22*. https://doi.org/10.3390/ijms22157958.

Tong, Q., and Hotamisligil, G.S. (2001). Molecular mechanisms of adipocyte differentiation. Reviews in endocrine & metabolic disorders *2*, 349-355. https://doi.org/10.1023/a:1011863414321.

Torres Irizarry, V.C., Jiang, Y., He, Y., and Xu, P. (2022). Hypothalamic Estrogen Signaling and Adipose Tissue Metabolism in Energy Homeostasis. Front. Endocrinol. *13*, 898139. https://doi.org/10.3389/fendo.2022.898139.

Toth, M.J., and Tchernof, A. (2000). Lipid metabolism in the elderly. European journal of clinical nutrition *54 Suppl 3*, S121-5. https://doi.org/10.1038/sj.ejcn.1601033.

Tovar, R., Ceglia, M. de, Ubaldi, M., Rodríguez-Pozo, M., Soverchia, L., Cifani, C., Rojo, G., Gavito, A., Hernandez-Folgado, L., and Jagerovic, N., et al. (2023). Administration of Linoleoylethanolamide Reduced Weight Gain, Dyslipidemia, and Inflammation Associated with High-Fat-Diet-Induced Obesity. Nutrients *15*. https://doi.org/10.3390/nu15204448.

Trappe, T.A., and Liu, S.Z. (2013). Effects of prostaglandins and COX-inhibiting drugs on skeletal muscle adaptations to exercise. Journal of applied physiology (Bethesda, Md. : 1985) *115*, 909-919. https://doi.org/10.1152/japplphysiol.00061.2013.

Tresguerres, M., Levin, L.R., and Buck, J. (2011). Intracellular cAMP signaling by soluble adenylyl cyclase. Kidney international *79*, 1277-1288. https://doi.org/10.1038/ki.2011.95.

Tunstall, R.J., Mehan, K.A., Wadley, G.D., Collier, G.R., Bonen, A., Hargreaves, M., and Cameron-Smith, D. (2002). Exercise training increases lipid metabolism gene expression in human skeletal muscle.

American journal of physiology. Endocrinology and metabolism *283*, E66-72. https://doi.org/10.1152/ajpendo.00475.2001.

Turcotte, L.P., and Fisher, J.S. (2008). Skeletal muscle insulin resistance: roles of fatty acid metabolism and exercise. Physical therapy *88*, 1279-1296. https://doi.org/10.2522/ptj.20080018.

Uchitomi, R., Hatazawa, Y., Senoo, N., Yoshioka, K., Fujita, M., Shimizu, T., Miura, S., Ono, Y., and Kamei, Y. (2019). Metabolomic Analysis of Skeletal Muscle in Aged Mice. Scientific reports *9*, 10425. https://doi.org/10.1038/s41598-019-46929-8.

Valdes, A.M., Glass, D., and Spector, T.D. (2013). Omics technologies and the study of human ageing. Nature reviews. Genetics *14*, 601-607. https://doi.org/10.1038/nrg3553.

Valle, A., Guevara, R., García-Palmer, F.J., Roca, P., and Oliver, J. (2008). Caloric restriction retards the age-related decline in mitochondrial function of brown adipose tissue. Rejuvenation research *11*, 597-604. https://doi.org/10.1089/rej.2007.0626.

van Loon, L.J.C. (2004). Use of intramuscular triacylglycerol as a substrate source during exercise in humans. Journal of applied physiology (Bethesda, Md. : 1985) *97*, 1170-1187. https://doi.org/10.1152/japplphysiol.00368.2004.

Vegiopoulos, A., Müller-Decker, K., Strzoda, D., Schmitt, I., Chichelnitskiy, E., Ostertag, A., Berriel Diaz, M., Rozman, J., Hrabe de Angelis, M., and Nüsing, R.M., et al. (2010). Cyclooxygenase-2 controls energy homeostasis in mice by de novo recruitment of brown adipocytes. Science (New York, N.Y.) *328*, 1158-1161. https://doi.org/10.1126/science.1186034.

Veliça, P., Khanim, F.L., and Bunce, C.M. (2010). Prostaglandin D2 inhibits C2C12 myogenesis. Molecular and cellular endocrinology *319*, 71-78. https://doi.org/10.1016/j.mce.2010.01.023.

Villareal, D.T., and Holloszy, J.O. (2006). DHEA enhances effects of weight training on muscle mass and strength in elderly women and men. American journal of physiology. Endocrinology and metabolism *291*, E1003-8. https://doi.org/10.1152/ajpendo.00100.2006.

Villarroya, F., Cereijo, R., Villarroya, J., and Giralt, M. (2017). Brown adipose tissue as a secretory organ. Nature reviews. Endocrinology *13*, 26-35. https://doi.org/10.1038/nrendo.2016.136.

Visser, M., Kritchevsky, S.B., Goodpaster, B.H., Newman, A.B., Nevitt, M., Stamm, E., and Harris, T.B. (2002). Leg muscle mass and composition in relation to lower extremity performance in men and women aged 70 to 79: the health, aging and body composition study. Journal of the American Geriatrics Society *50*, 897-904. https://doi.org/10.1046/j.1532-5415.2002.50217.x.

Wächter, S., Vogt, M., Kreis, R., Boesch, C., Bigler, P., Hoppeler, H., and Krähenbühl, S. (2002). Long-term administration of L-carnitine to humans: effect on skeletal muscle carnitine content and physical

performance. Clinica chimica acta; international journal of clinical chemistry *318*, 51-61. https://doi.org/10.1016/s0009-8981(01)00804-x.

Walker, M.E., Kodani, S.D., Mena, H.A., Tseng, Y.-H., Cypess, A.M., and Spite, M. (2024). Brown adipose tissue activation in humans increases plasma levels of lipid mediators. The Journal of clinical endocrinology and metabolism. https://doi.org/10.1210/clinem/dgae016.

Wang, T.J., Larson, M.G., Vasan, R.S., Cheng, S., Rhee, E.P., McCabe, E., Lewis, G.D., Fox, C.S., Jacques, P.F., and Fernandez, C., et al. (2011). Metabolite profiles and the risk of developing diabetes. Nature medicine *17*, 448-453. https://doi.org/10.1038/nm.2307.

Watt, M.J., Heigenhauser, G.J.F., Dyck, D.J., and Spriet, L.L. (2002). Intramuscular triacylglycerol, glycogen and acetyl group metabolism during 4 h of moderate exercise in man. The Journal of physiology *541*, 969-978. https://doi.org/10.1113/jphysiol.2002.018820.

westcoastsci (2018a). Soleus, the forgotten muscle for runners. Anatomy, Exercises, Health and Wellness, Injuries. https://westcoastsci.com/blog/soleus-the-forgotten-muscle-for-runners/.

westcoastsci (2018b). Soleus, the forgotten muscle for runners.

Whitehead, A., Krause, F.N., Moran, A., MacCannell, A.D.V., Scragg, J.L., McNally, B.D., Boateng, E., Murfitt, S.A., Virtue, S., and Wright, J., et al. (2021). Brown and beige adipose tissue regulate systemic metabolism through a metabolite interorgan signaling axis. Nature communications *12*, 1905. https://doi.org/10.1038/s41467-021-22272-3.

WHO (2004). Global strategy on diet, physical activity and health (Geneva).

Wierman, M.E. (2007). Sex steroid effects at target tissues: mechanisms of action. Advances in physiology education *31*, 26-33. https://doi.org/10.1152/advan.00086.2006.

Williams, G.N., Higgins, M.J., and Lewek, M.D. (2002). Aging skeletal muscle: physiologic changes and the effects of training. Physical therapy *82*, 62-68. https://doi.org/10.1093/ptj/82.1.62.

Wood, P.L. (2020). Fatty Acyl Esters of Hydroxy Fatty Acid (FAHFA) Lipid Families. Metabolites *10*. https://doi.org/10.3390/metabo10120512.

World Health Organization (2021). Obesity and overweight. https://www.who.int/news-room/fact-sheets/detail/obesity-and-overweight.

World Health Organization (2022a). Ageing and Health. https://www.who.int/news-room/fact-sheets/detail/ageing-and-health. 23.03.2024.

World Health Organization (2022b). Health topics: Physical activity. https://www.who.int/health-topics/physical-activity#tab=tab_1.

Wronska, A., and Kmiec, Z. (2012). Structural and biochemical characteristics of various white adipose tissue depots. Acta physiologica (Oxford, England) *205*, 194-208. https://doi.org/10.1111/j.1748-1716.2012.02409.x.

Xiang, L., Zhang, H., Wei, J., Tian, X.Y., Luan, H., Li, S., Zhao, H., Cao, G., Chung, A.C.K., and Yang, C., et al. (2018). Metabolomics studies on db/db diabetic mice in skeletal muscle reveal effective clearance of overloaded intermediates by exercise. Analytica chimica acta *1037*, 130-139. https://doi.org/10.1016/j.aca.2017.11.082.

Xu, R.N., Fan, L., Rieser, M.J., and El-Shourbagy, T.A. (2007). Recent advances in high-throughput quantitative bioanalysis by LC-MS/MS. Journal of pharmaceutical and biomedical analysis *44*, 342-355. https://doi.org/10.1016/j.jpba.2007.02.006.

Yamashita, H., Yamamoto, M., Ookawara, T., Sato, Y., Ueno, N., and Ohno, H. (1994). Discordance between thermogenic activity and expression of uncoupling protein in brown adipose tissue of old rats. Journal of gerontology *49*, B54-9. https://doi.org/10.1093/geronj/49.2.b54.

Yan, X.-T., Zhang, Y., Zhou, Y., Li, G.-H., and Feng, X.-S. (2022). Technical Overview of Orbitrap High Resolution Mass Spectrometry and Its Application to the Detection of Small Molecules in Food (Update Since 2012). Critical reviews in analytical chemistry *52*, 593-626. https://doi.org/10.1080/10408347.2020.1815168.

Yang, F.T., and Stanford, K.I. (2022). Batokines: Mediators of Inter-Tissue Communication (a Mini-Review). Current obesity reports *11*, 1-9. https://doi.org/10.1007/s13679-021-00465-7.

Yang, P., Jiang, Y., and Fischer, S.M. (2014). Prostaglandin E3 metabolism and cancer. Cancer letters *348*, 1-11. https://doi.org/10.1016/j.canlet.2014.03.010.

Yasui, M., Tamura, Y., Minami, M., Higuchi, S., Fujikawa, R., Ikedo, T., Nagata, M., Arai, H., Murayama, T., and Yokode, M. (2015). The Prostaglandin E2 Receptor EP4 Regulates Obesity-Related Inflammation and Insulin Sensitivity. PloS one *10*, e0136304. https://doi.org/10.1371/journal.pone.0136304.

Yoneshiro, T., Wang, Q., Tajima, K., Matsushita, M., Maki, H., Igarashi, K., Dai, Z., White, P.J., McGarrah, R.W., and Ilkayeva, O.R., et al. (2019). BCAA catabolism in brown fat controls energy homeostasis through SLC25A44. Nature *572*, 614-619. https://doi.org/10.1038/s41586-019-1503-x.

Yore, M.M., Syed, I., Moraes-Vieira, P.M., Zhang, T., Herman, M.A., Homan, E.A., Patel, R.T., Lee, J., Chen, S., and Peroni, O.D., et al. (2014). Discovery of a class of endogenous mammalian lipids with anti-diabetic and anti-inflammatory effects. Cell *159*, 318-332. https://doi.org/10.1016/j.cell.2014.09.035.

Yu, Z., Zhai, G., Singmann, P., He, Y., Xu, T., Prehn, C., Römisch-Margl, W., Lattka, E., Gieger, C., and Soranzo, N., et al. (2012). Human serum metabolic profiles are age dependent. Aging cell *11*, 960-967. https://doi.org/10.1111/j.1474-9726.2012.00865.x.

Yuneva, M.O., Bulygina, E.R., Gallant, S.C., Kramarenko, G.G., Stvolinsky, S.L., Semyonova, M.L., and Boldyrev, A.A. (1999). Effect of Carnosine on Age-Induced Changes in Senescence-Accelerated Mice. Journal of Anti-Aging Medicine *2*, 337-342. https://doi.org/10.1089/rej.1.1999.2.337.

Zalin, R.J., and Leaver, R. (1975). The effect of a transient increase in intracellular cyclic AMP upon muscle cell fusion. FEBS letters *53*, 33-36. https://doi.org/10.1016/0014-5793(75)80675-2.

Zammit, P.S. (2017). Function of the myogenic regulatory factors Myf5, MyoD, Myogenin and MRF4 in skeletal muscle, satellite cells and regenerative myogenesis. Seminars in cell & developmental biology *72*, 19-32. https://doi.org/10.1016/j.semcdb.2017.11.011.

Zeisel, S.H., Klatt, K.C., and Caudill, M.A. (2018). Choline. Advances in nutrition (Bethesda, Md.) *9*, 58-60. https://doi.org/10.1093/advances/nmx004.

Zhang, A., Sun, H., Wang, P., Han, Y., and Wang, X. (2012). Modern analytical techniques in metabolomics analysis. The Analyst *137*, 293-300. https://doi.org/10.1039/C1AN15605E.

Zhang, J., Bhattacharyya, S., Hickner, R.C., Light, A.R., Lambert, C.J., Gale, B.K., Fiehn, O., and Adams, S.H. (2019). Skeletal muscle interstitial fluid metabolomics at rest and associated with an exercise bout: application in rats and humans. American journal of physiology. Endocrinology and metabolism *316*, E43-E53. https://doi.org/10.1152/ajpendo.00156.2018.

Zhang, J.-M., and An, J. (2007). Cytokines, inflammation, and pain. International anesthesiology clinics *45*, 27-37. https://doi.org/10.1097/AIA.0b013e318034194e.

Zhao, Y.-Y., and Lin, R.-C. (2014). UPLC-MS(E) application in disease biomarker discovery: the discoveries in proteomics to metabolomics. Chemico-biological interactions *215*, 7-16. https://doi.org/10.1016/j.cbi.2014.02.014.

Zheng, J., Wang, R., Zambraski, E., Wu, D., Jacobson, K.A., and Liang, B.T. (2007). Protective roles of adenosine A1, A2A, and A3 receptors in skeletal muscle ischemia and reperfusion injury. American journal of physiology. Heart and circulatory physiology *293*, H3685-91. https://doi.org/10.1152/ajpheart.00819.2007.

Zoico, E., Rubele, S., Caro, A. de, Nori, N., Mazzali, G., Fantin, F., Rossi, A., and Zamboni, M. (2019). Brown and Beige Adipose Tissue and Aging. Frontiers in endocrinology *10*, 368. https://doi.org/10.3389/fendo.2019.00368.

7. Abstract

Aging, obesity and physical inactivity are three major risk factors leading to non-communicable diseases, like coronary heart disease or type 2 diabetes, resulting in reduced health and quality of life. As the number of obese, aged and multimorbid patients continuously rise worldwide, the treatment of the associated diseases are major burdens for the healthcare systems. Research in aging and exercise is crucial to uncover the physiological and molecular mechanisms involved, aiming at identifying biomarkers and pathways that improve health outcomes in the elderly. Metabolomics technology is a powerful tool to analyse dynamic changes in small molecules and the associated metabolic finger-print, to elucidate pathways and patterns associated with aging or exercise.

In this thesis, the influence of aging on the profile of secreted metabolites of the highly metabolic active tissues brown adipose tissue (BAT), inguinal white adipose tissue (WATi) and soleus skeletal muscle (SKM) was analysed from young and old mice. Furthermore, the influence of aging and exercise on human soleus SKM was investigated. For this, state-of-the-art untargeted metabolomics was performed to elucidate the changes in the metabolic profile under basal and cAMP-stimulated conditions.

Secretomic analysis of BAT, WATi, and soleus tissues demonstrated that supernatants can serve as specimen material, revealing a broad spectrum of metabolites, including lipids, amino acids, and carbohydrates. Overall, metabolomic analyses of young compared to old murine BAT, WATi and soleus SKM revealed a strong influence of aging on the metabolic profile in all three tissues. Furthermore, cAMP stimulation could induce the secretion of various metabolites in all tissues. Nevertheless, cAMP stimulation showed greater alterations in young compared to old tissues. This shows that aging not only influences the intracellular metabolism, but furthermore, impacts the tissues' responsiveness to stimuli and the endocrine function. Among the three tissues, BAT and soleus showed a higher impact of aging than WATi.

In human studies, untargeted metabolomics of soleus biopsies from young and old, trained and untrained participants highlighted significant interindividual differences, complicating the identification of common regulatory patterns. Nevertheless, regular physical activity in young participants seems to result in distinct metabolic adaptations and different responses to acute stimulation compared to young untrained but furthermore compared to old untrained and trained soleus muscle.

This thesis underscores the value of untargeted metabolomics in uncovering metabolic adaptations to aging and exercise. This collection of data greatly demands further in-depth analysis including linking metabolomics data to RNA sequencing or proteomics, and in-depth in vitro and in vivo studies of key candidates, are needed to fully understand these adaptations.